

**THE FUNCTION OF SUBDISTAL**  
**APPENDAGES IN THE SPATIAL CONTROL**  
**OF CILIA**

By

Gregory Mazo

A Dissertation

Presented to the Faculty of the Louis V. Gerstner, Jr.

Gerstner Sloan-Kettering Graduate School

Memorial Sloan-Kettering Cancer Center

in Partial Fulfillment of the Requirements for the Degree of

Doctor of Philosophy

Bryan Tsou  
Dissertation Mentor  
New York, NY  
2017

Copyright by Gregory Mazo 2017

## **Acknowledgements**

I would like to thank everyone who made this made my thesis possible. I would like to thank Dr. Bryan Tsou for the privilege of working in his lab. His passion for research, scientific insights and patience has been essential for this project. Without his guidance and ambition, I would not have produced work of this quality. I would also like to thank my thesis committee, which has included Dr. Prasad Jallepalli, Dr. Kathryn Anderson, Dr. Marylyn Resh and the late Dr. Allen Hall.

I would like to thank all current and former members of the Tsou Lab. At various times, each member of the lab has either taught me techniques, troubleshot experiments, contributed protocols, and/or guided me in some way. Although the form and magnitude of assistance that each lab member has given me varies, I list them in no particular order: Hui-Ju Yang, Minhee Kim, Chii Shyang Fong, Won-Jing Wang, Barbera Tanos, Denisse Izquierdo, Brian O'Rourke, Tuhin Das, Shagurika Pachal, and Rageesh Soni. Hui-Ju Yang began the preliminary work that led to this project.

I would also like to thank Nadine Soplop and Kunihiro Uryu at the Electron Microscopy Resource Center in Rockefeller University. They performed the tedious and difficult steps within the electron microscopy. This critical contribution massively helped my research. A few EM images were also provided to me by the work of Won-Jing Wang. Won-Jing's instruction and advice was especially helpful to me during the several years she spent in the lab.

I would also like to thank the Gerstner Sloan Kettering Graduate School. GSK has provided an excellent learning environment.

I must also thank my parents who have provided emotional support during my years of graduate study. They have been indispensable.

# **The function of subdistal appendages in the spatial control of cilia**

## **Thesis Abstract**

Many vertebrate cells maintain centrioles at the cell center, near the Golgi, forming primary cilia that are confined or submerged in a deep narrow pit. We refer to these cilia as “submerged cilia”. The position of submerged cilia appears incompatible with or suboptimal for the known functions of the primary cilium. Furthermore, the mechanisms controlling cilia position and the purpose of submerged cilia have long been a mystery. Vertebrate centrioles contain several accessory structures. The distal and subdistal appendages project radially from the mother centriole. By characterizing the subdistal appendages (sDAP), we have gained novel insights into the mechanisms by which cilia position is controlled. We first studied the localization of centriolar proteins in detail to understand the sDAP and identify novel sDAP components. We identified three new components of the sDAP (Cep128, Kif2a and the dynein complex). This work included construction of an assembly hierarchy of sDAP proteins. A group of sDAP components (ninein, Cep170, Kif2a, dynein complex) localize to the centriole proximal ends via activity of the centrosome cohesion factor C-Nap1. In order to localize to the sDAP, ninein, Cep170, Kif2a and dynein require another group of proteins (ODF2, Cep128, centriolin) that are exclusive to the sDAP. We found that the sDAP functions redundantly with C-Nap1 for submerged cilia maintenance. Simultaneous loss of sDAP and C-Nap1 disrupts stable Golgi-cilia association and allows normally submerged cilia to fully surface, losing the deep

pit. This phenotype correlated with distant separation between the two centrosomes. Unlike the stationary submerged cilia, surfaced cilia respond to mechanical stimuli with motion. Surfaced cilia can also ectopically recruit hedgehog-signaling components in the absence of ligand.

# Table of contents

## Chapter 1: Introduction and Background

List of Figures and List of Tables	xi
<u>1.1 Overview</u>	1
<u>1.2 The Centriole/Basal Body and Cilia</u>	3
<u>1.3 The centrosome</u>	4
<u>1.3.1 Historical Overview</u>	4
<u>1.3.2 The pericentriolar material (PCM)</u>	5
<u>1.3.3 The Centrosome as a mitotic MTOC</u>	6
<u>1.3.4 Are Mitotic Centrosomes critical for cell division?</u>	9
<u>1.3.5 The centrosome as an Interphase MTOC</u>	10
<u>1.3.5.1 The microtubule organization of the interphase centrosome</u>	10
<u>1.3.5.2 Ciliation of the Interphase centrosome</u>	13
<u>1.4 The Structural modifications of ciliated centrosomes</u>	13
<u>1.4.1 The Distal Appendages</u>	13
<u>1.4.2 The subdistal appendages (sDAP)</u>	14
<u>1.4.2.1 Overview of the sDAP</u>	14
<u>1.4.2.2 Natural History of appendages</u>	15
<u>1.4.2.3 Reported functions of subdistal appendage components</u>	16
<u>1.4.3 The Centrosome cohesion; intercentrosomal linker, ciliary rootlet and other structures</u>	19
<u>1.4.4 The Centriolar Satellites</u>	22
<u>1.4.5 Centrosome Cycle</u>	22

<b><u>14.4.6 Summary of structural modifications on Centrosomes</u></b>	<b>26</b>
<b><u>1.5 Centrosome, Cilia and Golgi position</u></b>	<b>27</b>
<b><u>1.5.1 Control of Centrosome and Cilia position</u></b>	<b>27</b>
<b><u>1.5.2 Golgi Position, Centrosome position and cell polarity</u></b>	<b>29</b>
<b><u>1.5.3 The position of the cilia on the edge of the plasma membrane</u></b>	<b>31</b>
<b><u>1.5.4 The ciliary membrane and periciliary membranes</u></b>	<b>36</b>
<b><u>1.6 Cilia signaling</u></b>	<b>37</b>
<b><u>1.6.1 Several signaling pathways are linked to the primary cilia</u></b>	<b>37</b>
<b><u>1.6.2 Hedgehog signaling</u></b>	<b>39</b>
<b><u>1.7 Centrosomes, Cilia and human disease</u></b>	<b>41</b>
<b><u>1.7.1 Centrosome Amplification and Clustering</u></b>	<b>41</b>
<b><u>1.7.2 Ciliopathies</u></b>	<b>42</b>
<b><u>1.7.3 Cilia, hedgehog and Cancer</u></b>	<b>43</b>

**Chapter 2: Spatial Control of Primary Ciliogenesis by Subdistal  
Appendages Alters Sensation-Associated Properties of Cilia**

<b><u>2.1 Introduction</u></b>	<b>44</b>
<b><u>2.2 Results</u></b>	<b>47</b>
<b><u>2.2.1 Initial Approach</u></b>	<b>47</b>
<b><u>2.2.2 The assembly hierarchy of sDAP components</u></b>	<b>48</b>
<b><u>2.2.3 sDAP associated proteins are independently targeted to centriole proximal ends through C-Nap1</u></b>	<b>55</b>



<b><u>2.2.4 sDAP at mother centrioles are not essential for cilia assembly nor microtubule aster formation</u></b>	<b>56</b>
<b><u>2.2.5 sDAP and C-Nap1 work together to establish intact centrosome cohesion</u></b>	<b>61</b>
<b><u>2.2.6 C-Nap1 and sDAP are required for stable association of ciliated centrosomes with the Golgi.</u></b>	<b>62</b>
<b><u>2.2.7 The Golgi does not contribute to centrosome cohesion.</u></b>	<b>66</b>
<b><u>2.2.8 The sDAP does not function to maintain the linker.</u></b>	<b>66</b>
<b><u>2.2.9 Simultaneous mutation of Rootletin linker and sDAP does not produce the phenotypes characteristic of C-Nap1-sDAP mutants.</u></b>	<b>67</b>
<b><u>2.2.10 C-Nap1<sup>-/-</sup>; CEP128<sup>-/-</sup> double mutant cells grow surfaced cilia capable of responding to fluid flow with motion.</u></b>	<b>69</b>
<b><u>2.2.11 C-Nap1<sup>-/-</sup>; CEP128<sup>-/-</sup> double mutant cells grow cilia not trapped in a deep membrane invagination</u></b>	<b>71</b>
<b><u>2.2.12 Loss of deep ciliary pit allows multiple intact cilia to form individually in the same cell</u></b>	<b>74</b>
<b><u>2.2.13 Abnormally positioned cilia at the apical cell surface results in ectopic accumulation of Hedgehog signaling components.</u></b>	<b>77</b>
<b><u>2.3 Brief summary and discussion of results</u></b>	<b>82</b>
<b><u>2.4 Experimental Procedures</u></b>	
<b><u>2.4.1 Cloning and Plasmids</u></b>	<b>83</b>
<b><u>2.4.2 CRISPR</u></b>	<b>84</b>
<b><u>2.4.3 Cell culture.</u></b>	<b>85</b>

<b><u>2.4.4 Antibodies</u></b>	<b>85</b>
<b><u>2.4.5 Immunofluorescence</u></b>	<b>86</b>
<b><u>2.4.6 Arl13b level and Smoothened-GFP quantification</u></b>	<b>87</b>
<b><u>2.4.7 Time-lapse microscopy and generation of fluid flow</u></b>	<b>88</b>
<b><u>2.4.8 Correlated light and Electron Microscopy.</u></b>	<b>89</b>
<b><u>2.4.9 siRNA for knockdown</u></b>	<b>90</b>
<b><u>Chapter 3: Findings, Conclusions, Discussion and Future work:</u></b>	
<b><u>3.1 Subdistal appendages</u></b>	<b>91</b>
<b><u>3.1.1 The role of sDAP in microtubule organization</u></b>	<b>91</b>
<b><u>3.1.2 The assembly of the sDAP</u></b>	<b>93</b>
<b><u>3.1.3 The limitations of the assembly hierarchy and future directions</u></b>	<b>95</b>
<b><u>3.2 Centrosome Positioning</u></b>	<b>96</b>
<b><u>3.2.1 Models of centrosome position control</u></b>	<b>96</b>
<b><u>3.2.2 Testing models of Centrosome positioning</u></b>	<b>99</b>
<b><u>3.3 Golgi and cilia positioning</u></b>	<b>99</b>
<b><u>3.3.1 Scoring of surfaced cilia phenotypes</u></b>	<b>99</b>
<b><u>3.3.2 Cilia position and Hedgehog Signaling</u></b>	<b>101</b>
<b><u>3.3.2.1 Mystery of PKA at the centrosome</u></b>	<b>103</b>
<b><u>3.3.2.2 Important questions regarding HH signaling</u></b>	<b>104</b>
<b><u>3.4 Submerged cilia</u></b>	<b>104</b>
<b><u>3.4.1 What are the roles of submerged cilia?</u></b>	<b>105</b>
<b><u>3.4.2 Characterize the ciliary pit that traps submerged cilia</u></b>	<b>106</b>

## **List of Tables**

**Table 1: Sequence Analysis of the mutation in each CRISPR knockout cell**

**line generated in this study 54**

## **List of Figures**

**Figure 1.1 The structural complexity of the vertebrate centriole 2**

**Figure 1.2 The structure of the Basal Body 3**

**Figure 1.3 The ciliated centriole 3**

**Figure 1.4 The Centrosomes 5**

**Figure 1.5 The Distal Appendages 13**

**Figure 1.6 Microtubules attach to subdistal appendages 14**

**Figure 1.7 The subdistal appendage and basal foot 15**

**Figure 1.8 The Ciliary Rootlet and Intercentrosomal linker 19**

**Figure 1.9 The Centrosome during the Cell Cycle 23**

**Figure 1.10 Structural modifications of the Vertebrate Centrosome 26**

**Figure 1.11 The tug-of-war model 27**

**Figure 1.12 The Golgi Centrosome link 29**

**Figure 1.13 The ciliary membranes 31**

**Figure 1.14 Surfaced and submerged cilia 33**

**Figure 1.15 Non-Emergent cilia 35**

**Figure 1.16 The Cilia's role in the Hedgehog pathway 40**

**Figure 2.1 Different types of sDAP protein localization are distinguishable**

**through immune fluorescent staining 48**

<b>Figure 2.2 The assembly hierarchy of subdistal appendage components</b>	<b>51</b>
<b>Figure 2.3 Depletion of sDAP associated proteins by RNAi phenocopies depletion by CRISPR</b>	<b>53</b>
<b>Figure 2.4 Removal of sDAP-associated components from both ends of the centrioles</b>	<b>57</b>
<b>Figure 2.5 C-Nap1 and sDAP depletion do not affect cilia formation or MTOC activity</b>	<b>59</b>
<b>Figure 2.6 C-Nap1 and sDAP depletion disrupts centrosome cohesion and Golgi-Cilia association</b>	<b>61</b>
<b>Figure 2.7 AKAP450 localizes normally to the Golgi in C-Nap1<sup>-/-</sup>;CEP128<sup>-/-</sup> double mutant cells</b>	<b>65</b>
<b>Figure 2.8 Neither intercentrosomal linker loss alone nor Golgi detachment alone can help recapitulate the centrosome cohesion defects in C-Nap1 and sDAP mutants</b>	<b>68</b>
<b>Figure 2.9 Cilia mobility and position are altered upon depletion of sDAP and C-Nap1</b>	<b>70</b>
<b>Figure 2.10 Loss of the deep ciliary pit in C-Nap1<sup>-/-</sup>;CEP128<sup>-/-</sup> double knockout cells</b>	<b>73</b>
<b>Figure 2.11 Dilution of Arl13b in cells with two clustered cilia</b>	<b>75</b>
<b>Figure 2.12 Loss of the deep ciliary pit allows multiple intact cilia to form with undiluted membrane composition in one cell</b>	<b>76</b>
<b>Figure 2.13 Apically surfaced cilia can be identified with light microscopy based on the focal plane of the cilia</b>	<b>78</b>

<b>Figure 2.14 Apically surfaced cilia can ectopically recruit Smoothened and Gli2 in the absence of agonist</b>	<b>80</b>
<b>Figure 2.15 Accumulation of Smoothened at surfaced cilia is robustly seen in multiple cell lines and staining conditions</b>	<b>81</b>
<b>Figure 3.1 Assembly hierarchy of centriolar proteins</b>	<b>93</b>
<b>Figure 3.2 The forces pulling on the centrosome</b>	<b>97</b>
<b>Figure 3.3 Apex-Smo construct selectively biotinlyates submerged cilia</b>	<b>106</b>

# Chapter 1: Introduction

## 1.1 Overview

The vertebrate centriole/centrosome has three main functions that are known: (1) A template function for growing the cilia, (2) A Mitotic MTOC (microtubule organizing center) function that incorporates centrosomes into the spindle pole and (3) an interphase MTOC function. The most evolutionarily ancient and conserved function of centrioles is their role as the cilia's '**basal bodies**' that template cilia formation. The cilia appeared at the beginning of eukaryote evolution. The centriole as mitotic MTOC, however, is associated with animals while the interphase MTOC activity is only present in some animal lineages including vertebrates. The multiple activities of vertebrate centrioles are reflected by their structural complexity. Electron microscopy (EM) analyses showed that mature vertebrate centrioles have accessory structures called the distal appendages and subdistal appendages [4, 5] (See [Figure 1.1](#)). The subdistal appendages (sDAPs) project radially from the centriole wall and attach cytoskeletal microtubules at their tips [5]. It is not clear why vertebrates evolved special structures that attach cytoskeletal microtubules. Published literature implicates individual sDAP associated proteins in functions as diverse as cytoskeletal organization, cilia formation, centrosome cohesion and the assembly of the distal appendage (DAP) that mediates membrane docking [6-10]. Although much has been published, gaps and inconsistencies in the research leave a lot still unknown about the subdistal appendages. My thesis work addresses the composition and function of the subdistal appendages. On the composition end, I

have identified novel components and determined their assembly hierarchy. For functional studies, although we could not reproduce published results regarding the role of sDAP proteins in distal appendage assembly, cilia formation and cytoskeletal organization, we found interesting novel functions of the sDAP.

Many vertebrate cells maintain the centrosomes at the center of the cell near the Golgi, forming cilia that are confined in a deep pit within the membrane. We refer to the cilia in these deep pits as submerged cilia. Prior to my work, the mechanisms and the purpose behind cilia-Golgi attachment and submerged cilia formation have been a mystery. My work revealed a functional redundancy involving sDAP components and other associated molecules at both distal and proximal end of centrioles in maintaining submerged cilia. When all redundant pathways are removed, cilia separate from the Golgi and can move to the surface of the cell. The results of my work contribute to the understanding of sDAP composition, cilia position control, cilia-Golgi attachment, signaling, cytoskeleton structure and cellular organization.

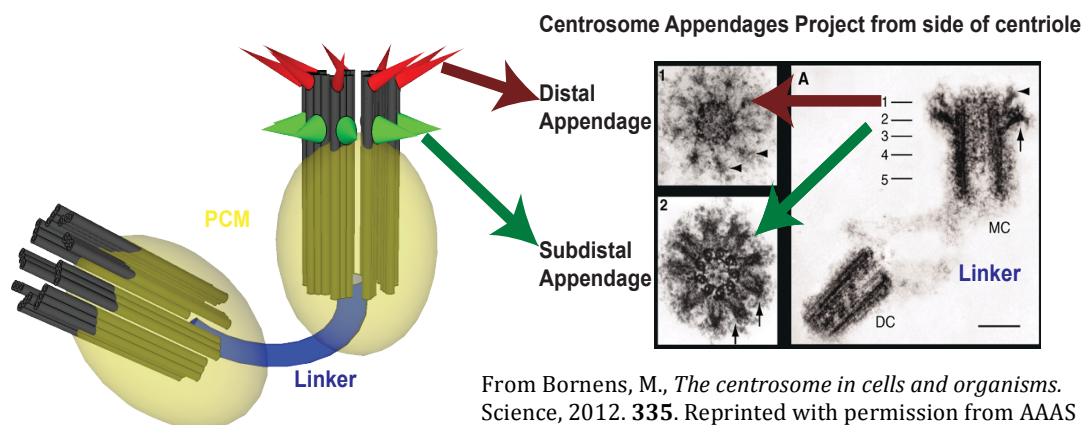


Figure 1.1 The Structural complexity of the vertebrate centrioles  
Diagram and EM of centrioles

From Bornens, M., *The centrosome in cells and organisms*. Science, 2012. 335. Reprinted with permission from AAAS [1].

## 1.2 The Centriole/Basal Body and Cilia

Centrioles are cylindrical structures composed of 9 triplet microtubules arranged to form a cylinder. These are referred to as the A, B and C tubules respectively (see [Figure 1.2](#)). Like microtubules, the centrioles are polarized structures. The centriole ends are termed proximal/distal ([Figure 1.2](#)). The minus

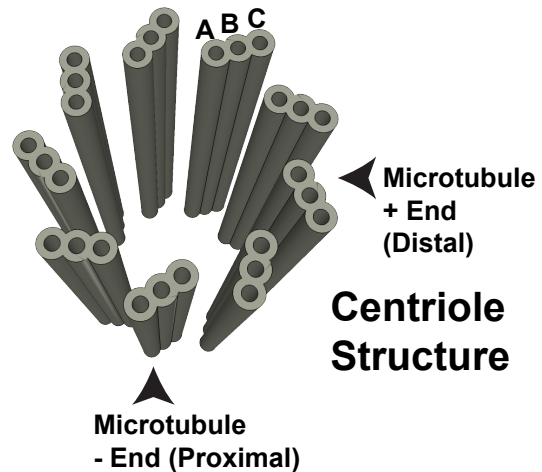


Figure 1.2 The Structure of the Basal Body

ends of the 9 triplet microtubules are at the proximal end of the centriole while the plus ends of microtubules are at the distal end of the centriole. Different proteins and accessory structures that localize to each end of the centriole can be used as markers. Furthermore the term subdistal refers to an area on the lateral sites of the centrioles that is near the distal end but not beyond it. The A and B tubules of the nine triplets can extend to form a long structure called the ciliary axoneme. The axoneme is surrounded by membrane to form a vital organelle called the cilium ([Figure 1.3](#)).

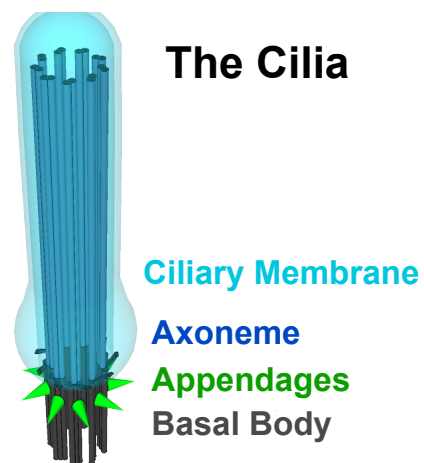


Figure 1.3 The ciliated centriole



Cilia and centrioles are found in organisms from most major branches of the eukaryotic family tree including plants, animals, and many protozoa. Therefore both structures were likely present in the last eukaryotic common ancestor [11]. Cilia are observed in unicellular protozoa of many taxonomic groups, some fungi clades, algae, several multicellular plant lineages and nearly all animals [11]. The cilia mediate cell motility and act as sensory antenna in diverse lineages [11], suggesting that both these functions are ancient/ancestral. Transport of cilia components along the microtubules of the axoneme maintains the cilia structure in a process called intraflagellar transport (IFT). In IFT, an IFTB complex containing kinesin transports proteins from the base of the cilia to the tip. After reaching the tip, an IFTA complex containing a dynein heavy chain motor transports material back [12]. Both ciliary membrane components and axoneme components associate with IFT for transport [12, 13]. IFT is required for cilia formation and stability. Cilia function as ‘cellular antennas’ to sense a variety of chemical and mechanical signals [14, 15]. Additional details regarding cilia function, structure and membrane composition will be described later.

### **1.3 The Centrosome**

#### **1.3.1 Historical overview**

Over 100 years ago, Theodore Boveri named the centrosome, a permanent organelle that was found at the spindle poles of animal cells during mitosis [16]. Despite the limits of light microscopy in 1900, Boveri was able to accurately describe two basic features of the centrosomes (now confirmed by electron microscopy). Boveri saw that centrosomes consist of two parts: A dense

structure called the centriole and a more diffuse 'centroplasm' that organized microtubules. The 'centroplasm' is currently called the pericentriolar material (PCM) (See [Figure 1.4](#)). Boveri proposed that the centrosome is a cell division organelle. However, this conventional view is currently challenged by the idea that the centrosome is simply a passenger rather than a driver of cell division.

### 1.3.2 The pericentriolar material (PCM)

The centrioles are surrounded by a matrix of proteins called the

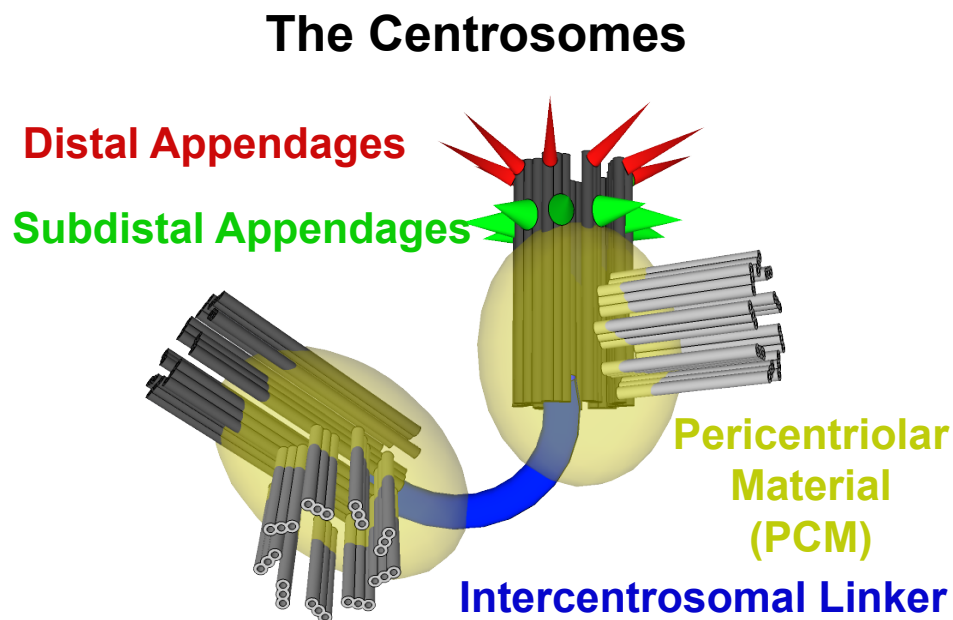


Figure 1.4 The Centrosomes

pericentriolar material (PCM). The PCM is found on the centrioles of animals, and some fungi but not in most other branches of the eukaryotic family tree [11]. Consistent with the lack of PCM, most protozoa have centrioles that function only as basal bodies and not MTOCs [11]. The PCM is therefore a later evolutionary innovation. In vertebrates, the PCM forms around a new centriole at the start of

G1. Two fibrous proteins, Pericentrin and cep152, form the foundation of the PCM by attaching to the microtubule walls of the centriole. Subsequently, pericentrin and cep152 recruit other proteins like CDK5rap2 and cep192 which form a second layer of PCM called the “PCM matrix” [17]. The CDK5rap2 and cep192 can facilitate the recruitment of more pericentrin to complete the formation of PCM [17, 18]. With more pericentrin, multiple additional “PCM matrix” layers can assemble. Pericentriolar material components recruit the gamma tubulin ring complex ( $\gamma$ -TuRC) to the centrosome [18-21]. The PCM functions primarily as the platform for the microtubule nucleation from the  $\gamma$ -TuRC. PCM proteins are also required for formation of new centrioles adjacent to preexisting mothers [17, 22].

### **1.3.3 The Centrosome as a mitotic MTOC**

During mitosis, centrosomes determine the sites of spindle pole formation by acting as MTOCs (microtubule organizing centers). The MTOC function of centrosome is primarily defined by centrosomal enrichment of the gamma tubulin ring complex ( $\gamma$ -TuRC). The gamma tubulin ring complex ( $\gamma$ -TuRC) promotes nucleation of microtubules.  $\gamma$ -TuRCs consists of gamma tubulin, GCP2, GCP3, GCP4, GCP5 GCP6, GCP-WD/NEDD1/GCP7 and GCP8 [23-25]. These complexes act as nuclei for tubulin polymers to grow from. The  $\gamma$ -TuRCs also prevent polymerization/depolymerization from the minus of microtubules by capping the ends [26]. As a consequence, a radial aster of microtubules surrounds the centrosome. CDK5rap2, NEDD1, and pericentrin contribute to

targeting  $\gamma$ -TuRC localization to the PCM [19, 21, 27] by binding  $\gamma$ -TuRC components [21, 28]. Simultaneous binding of different centrosomal proteins to distinct  $\gamma$ -TuRC components is believed to help secure the  $\gamma$ -TuRC to centrosomes. Interestingly, distinct gamma tubulin containing complexes specialize in nucleation or anchorage [29].

During mitosis, the centrosome gains a greater microtubule nucleation capacity to function as a mitotic MTOC rather than an interphase MTOC. Termed “centrosome maturation”, this shift involves the removal of many interphase components, posttranslational modifications and recruitment of additional pericentriolar material from the cytoplasm [17]. The size of the PCM increases and mitosis specific proteins are recruited to the PCM [30]. The molecular details of this process are partly understood. At this time, the kinase plk1 causes the phosphorylation of pericentrin, NEDD1, CDK5rap2, gamma tubulin and numerous spindle pole proteins [17, 18, 30] directly or via activation of other kinases [31, 32]. This transformation of the PCM includes an increase in the amount of  $\gamma$ -TuRC complex to help facilitate attachment to spindle microtubules. Interestingly the mechanisms of microtubule organization appear to be different between interphase and mitosis. For example the interaction of pericentrin with the  $\gamma$ -TuRC contributes to gamma tubulin localization during mitosis but not during interphase [19]. Similarly, cep192 is far more important for microtubule nucleation during mitosis than interphase [20]. Interphase microtubule organization around centrosomes is a distinct process from mitotic aster organization.

Although microtubule nucleation at centrosomes defines the sites of spindle pole formation, the capacity to nucleate microtubules is not sufficient for centrosomes to stably attach to spindle poles. Centrosome to spindle pole attachment depends on the functions of CDK5rap2, GC-NAP, CENP-32 at the centrosomes/PCM [33, 34] as well as WD62, NuMa and dynactin at the spindle poles [35, 36]. Spindle formation and centrosome attachment are likely separate processes. In certain mutants (of CDK5rap2 and CENP-32), centrosomes can detach from spindle poles after participating in successful spindle formation [33, 34]. However, the centrosomes of these mutants are not guaranteed to segregate to the appropriate daughter cells. Wang et al showed that centrioles will only attach to spindle poles if they have acquired pericentriolar material (and hence became part of a centrosome) [37]. Without attachment to the spindle pole, centrioles segregate to random daughter cells after mitosis. It follows that the link between centrioles and spindle poles evolved to facilitate equal segregation of centrioles to each daughter cell [37, 38]. Consistent with this hypothesis, many protozoa have spindles poles form/function without centriole involvement [39, 40] regardless of whether the species has centrioles. The centrioles of many protozoan taxa neither nucleate microtubules nor have PCM nor associate directly with spindle poles during mitosis. These organisms do not use the spindle to segregate their centrioles but have alternate mechanisms of segregating centrioles to daughter cell via cortical inheritance [41-44]. This indicates that both centrosome-to-spindle attachment and the centriole to centrosome/MTOC transformation evolved later than the basal body function.

### **1.3.4 Are Mitotic Centrosomes critical for cell division?**

The idea of centrosome as passengers of the mitotic spindle is not consistent with conventional views of centrioles being important drivers of spindle assembly and cell division. While centrosomes contain both centrioles and PCM, recent evidence indicates that only some components of the PCM contribute to mitosis. Although depletion of these PCM proteins causes severe spindle defects [19, 24, 45], the loss of the centrioles (and consequently the centrosomes) surprisingly causes only a delay in an otherwise successful mitosis [46-49]. *Drosophila* can develop into nearly normal adults without centrioles in spite of that delay [46]. Although the mitotic delay can cause p53 dependent cell cycle arrest/apoptosis in mammals, p53 mutation or suppression of the delay results in normal cell growth in absence of centrioles [48, 49]. These results indicate that absence of centrioles is a minor issue for dividing cells. Furthermore, centrioles are normally absent from mouse cells during meiosis [50] and the first several divisions of the early zygote [51]. During mitosis without centrioles, PCM components like pericentrin and cep152 still localize to spindle poles and function [47, 51, 52]. Organisms like flatworms and land plants entirely lack centrioles in dividing cells but form *de novo* centrioles after division in only the few cells that need cilia [53, 54]. When all facts about PCM in mitosis are taken together, three implications become apparent 1) PCM components play a critical role in mitosis 2) PCM components can function separately from the centrioles/centrosomes and 3) centrioles play a dispensable role in mitosis.

### **1.3.5 The centrosome as an Interphase MTOC**

The centrosomes of vertebrates organize microtubules not only during mitosis during interphase as well. A single interphase MTOC is believed to be important for cell polarization, directional movements and secretion [55, 56]. Consistent with this view, cells that form multiple centrosomes in opposite parts of the cell have defects in directional migration [57]. Furthermore the array of interphase microtubules attached to centrosome is necessary for regulating the position of centrioles within cells [58-60]. Unlike the centrosomes of vertebrates, the interphase centrosomes of *Drosophila* do not maintain radial microtubule arrays [61-63]. Therefore, the interphase centrosome/MTOC must have evolved to perform specific functions that are only needed in certain animal lineages including vertebrates. My thesis work sheds light on this (See submerged cilia section).

#### **1.3.5.1 The microtubule organization of the interphase centrosome**

A balance of four processes control microtubule organization: 1) Nucleation of microtubules, 2) Detachment of the nucleated microtubules from PCM, 3) Anchorage of microtubules to more permanent sites and 4) the polymerization/depolymerization of microtubules. Most microtubule nucleation occurs at centrosomes or Golgi [25]. Centrosomes nucleate microtubules in most vertebrate cell types, even in cell types like neurons that normally do not organize radial microtubule [64]. In certain contexts, the nuclear envelopes and

chromatin also have microtubule nucleating capacity [24, 26, 65]. Microtubule severing enzymes, like katanin and spastin localize to the centrosome and can cut the nucleated microtubules from the PCM [64, 66, 67]. Without katanin's severing activity abnormally large numbers of microtubules remain attached to the PCM [64]. Microtubules are also believed to simply detach from the PCM independent of severing enzymes even though the relative contributions of passive detachment versus active severing has not been explored [26]. Stable attachment of microtubule minus ends to a structure is referred to as microtubule "anchoring". The steady state organization of cytoplasmic microtubules is believed to depend largely on where minus ends are anchored. The older mother centrosome (with appendages) harbors greater microtubule anchoring activity than the daughter [68]. Because microtubules are seen attached to the subdistal appendages (sDAPs) under EM [2, 69], the sDAPs are believed to be responsible for anchoring microtubules to the mother centriole. The apparent link between ninein, a subdistal appendage protein and microtubule organization supports this model [70-72]. However, multiple results suggest microtubule anchorage is certainly a much more complex process than simple ninein-to-microtubule attachment. Several centrosomal proteins including FOP, Msd1, EB1, Cap350, NEDD1 and PCM-1 function in microtubule anchorage despite having no link to the sDAP [29, 70, 71, 73]. Models of microtubule anchorage at centrosomes postulate that either these proteins act as intermediates before microtubule minus ends are delivered to the sDAPs or (more likely) that the pericentriolar material has microtubule anchorage activity separate from the



sDAP [29, 71]. Anchorage of microtubules to the centrosome maintains a radial cytoskeletal structure [17, 68, 71, 72, 74, 75]. However, microtubules can also anchor to the Golgi or cell cortex among other organelles [25, 26, 76-78]. Importantly, non-centrosomal microtubule anchorage and stabilization determines the equilibrium microtubule organization in some tissues. Epithelial tissues have microtubule proximal ends anchored at the apical cortex of the cell. In skeletal muscle fibers, microtubule minus ends are anchored at nuclei to form arrays along the long axis of the cell [76]. In neuronal cells, microtubules will polymerize at the centrosome, get released and subsequently be actively transported into the axons and dendrites where they are stabilized/anchored [64, 76]. Microtubules can be much more dynamic in migrating or undifferentiated cells. In any cells with a very high rate of microtubule turnover, the equilibrium microtubule organization would not be exclusively dependent on anchorage. If the rate of microtubule detachment from nucleation sites were low in a cell, the sites of nucleation activity would determine the final microtubule organization. However, the balance of nucleation, severing, anchorage and growth of microtubules has not been studied quantitatively and certainly varies greatly between tissues. Due to the complications of the processes involved, interphase microtubule organization remains imperfectly understood.

#### **1.3.5.2 Ciliation of the Interphase centrosome**

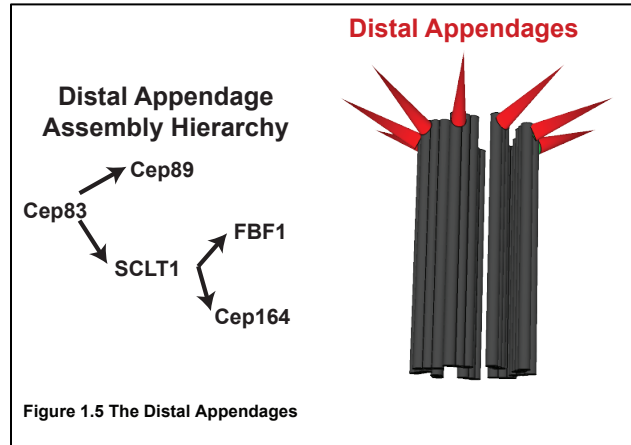
In many vertebrate cell types, the same centrosome that acts as an Interphase MTOC also grows cilia during interphase. The result is a complex

organelle in which cilia functions are wired together with the cell's MTOC function in vertebrates. It is not yet clear how this new fusion of multiple functions into a single complex organelle contributes to vertebrate physiology. The major goal of my thesis is to characterize the assembly and function of the centrosome-cilia complex.

## **1.4 The Structural modifications of ciliated centrosomes**

### **1.4.1 The Distal Appendages**

The distal appendages (DAPs) are structures attached at the distal end of centrioles that are required for cilia assembly. Distal appendages facilitate the attachment of the centriole to vesicle or plasma



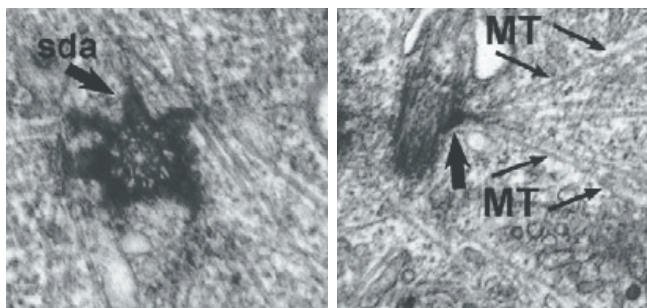
membranes, an early and essential step in cilia formation [79-81]. The DAPs are known to contain 5 proteins (SCLT1, CEP83/CCDC41, CEP89/CCDC123, FBF1, and CEP164). Several distal appendage proteins function to facilitate the localization other DAP proteins [80, 82] (see assembly Hierarchy [Figure 1.5](#)). Consistent with a role in cilia formation, mutations in DAP proteins occur in patients with ciliopathies [83]. Despite similar names, the distal appendages are distinct structures with separate molecular composition from the subdistal appendages (sDAP)

## **1.4.2 The subdistal appendages (sDAP)**

### **1.4.2.1 Overview of the sDAP**

The sDAPs are electron dense structures that are attached laterally to the centriole wall [5, 84] (Figures 1.6, 1.7). Other EM studies have identified a similarly dense structure called the basal foot at the same location

### **Microtubules attached to subdistal appendages**



Reproduced and adapted with permission from Journal of Cell Science [2].

Figure 1.6 Microtubules attach to subdistal appendages

as the sDAP in many ciliated cells [84]. Based on many similarities, the basal foot is speculated to be a specialized sDAP [84]. Various EM studies have observed cytoskeletal microtubules attached to the subdistal appendages and basal feet [5, 69, 85, 86] suggesting a role in microtubule organization. Since the sDAP/basal feet disappear during mitosis [87], the structures must serve interphase specific roles. Between my thesis work and work by others, several protein components of the subdistal appendages are known: ODF2, ninein, Cep170, centriolin, epsilon tubulin, the dynactin complex, Kif2a and Cep128 [6, 88, 89]. Functions attributed to the sDAP components include centrosome cohesion, cilia formation, microtubule-array organization, asymmetric cell division, bipolar spindle formation and neuron migration [6, 9, 10, 72, 77, 90-95]. Some sDAP components also have localizations and functions at non-

centrosomal sites, complicating interpretation of these results [77, 96]. Furthermore, inconsistencies between different published results suggest our understanding of the sDAP is incomplete and confused. Clearly, a detailed

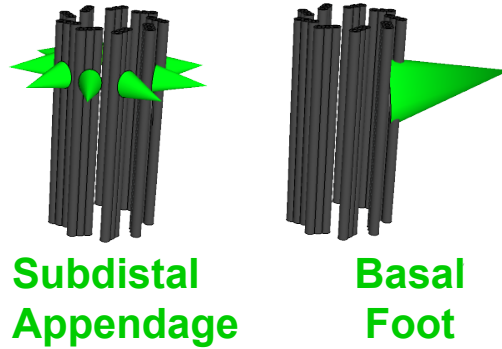


Figure 1.7 The subdistal appendage and basal foot

component-by-component analysis of the subdistal appendages is needed to clarify our understanding of the sDAP.

#### **1.4.2.2 Natural History of appendages**

Subdistal appendages are clearly seen in electron micrographs of mouse, zebrafish, *Xenopus* and human centrioles [5, 97-100] but have not been observed in invertebrate models like *Drosophila* and *C. elegans* [101-103]. Among core subdistal appendage proteins, only ninein has a documented *Drosophila* homolog which localizes to pericentriolar material rather than the subdistal part of the centriole [104]. Although few animals have had their centriole ultrastructure studied by EM, sequence homology between known subdistal appendage components can provide clues about how widespread the structure might be. For example, echinoderms have homologs for every core subdistal appendage component (pBlast of ODF2, Cep128, Cep170, Ninein, & Centriolin) so might have subdistal appendages. Basal feet are seen not only in the same vertebrate lineages as the sDAP but also in some mollusks (which have a close homologs of nearly all core sDAP components) [84]. Although a

comprehensive survey of centriole ultrastructure and sequence homology across the animal kingdom has not been done, it appears that subdistal appendages are conserved in most phyla within the deuterostome lineage and some protostome lineages like mollusks. Under EM, a variety of other accessory structures have been observed attached to centrioles in various protozoa [105-107]. This includes structures that attach to microtubules but otherwise do not resemble subdistal appendages [108-110]. These structures are most likely not related to subdistal appendages.

#### **1.4.2.3 Reported functions of subdistal appendage components**

Ninein localizes to the proximal ends of centrioles in addition to the subdistal appendages [6, 111, 112]. The earliest analyses of ninein function were done by overexpression of ninein fragments [113-115]. These studies all agree that overexpressed ninein fragments form aggregates that contain gamma tubulin and prevent anchorage of microtubules at the centrosome. Ninein knockdown causes comparable defects in microtubule organization [70, 71, 91] while ninein overexpression can also prevent microtubule release from centrosomes [116]. Furthermore, ninein co-localizes with microtubule minus ends [117-119]. This is consistent with reports of cytoskeletal microtubules attached to the subdistal appendage [2, 5, 69, 120]. Ninein also associates with microtubule minus ends elsewhere in the cell besides the centriole [96, 117-119, 121, 122] suggesting that the protein has non-centrosomal functions. Based on the overexpression and localization results, the literature refers to ninein as the

'microtubule-anchoring' protein [119]. However, no rescue experiments of ninein's microtubule anchoring phenotypes have been reported. Ninein has diverse functions in the nervous system where it is believed to function in migration of neurons, radial glial cell maintenance and axon formation [93, 119, 122-124]. Humans that are homozygous for point mutations in ninein exhibit either microcephalic dwarfism [125] or skeletal dysplasia [126] depending on which splice variants are affected. It is not known whether the diverse phenotypes associated with ninein depend on its function at the subdistal appendages rather than a function at non-centrosomal sites.

ODF2/cenexin was first identified as a component of the outer dense fiber (ODF), a structure specific to sperm tails that is important for fertility [127, 128]. However, the testes specific splice variant is not the only form of ODF2. In other tissues, a broadly expressed splice variant of ODF2 (called cenexin) localizes to the subdistal appendages and is critical for the formation of the subdistal appendages [6, 7, 129-131]. While some of the published literature uses the terms cenexin and ODF2 to refer to the splice variants specifically, in this work I use the term ODF2 for all forms of the gene and protein. Although ODF2 has been reported essential for cilia formation, conflicting results have also been published [6-8, 10, 95, 132, 133]. Some publications show ODF2 to function in bipolar spindle formation or in spindle orientation [90, 95, 134] but these results seem difficult to reconcile with the relatively mild phenotypes of ODF2 mutant mice [7, 135]. ODF2 has been reported important for microtubule organization in some cell types but irrelevant in others [6, 90]. Additionally, conflicting results

exists regarding whether ODF2 plays any role in the formation of the distal appendages [6, 10, 80]. ODF2 is required for formation the basal foot, which is attached to the centrioles in multiciliated tissues [85, 136]. Loss of basal feet causes centriole position defects in the multiciliated tissues of mouse [136].

Centriolin has been reported to localize to the subdistal appendages and centriole proximal ends. This localization somewhat resembles the localization pattern of ninein. However, in comparison to ninein, centriolin staining consistently appears brighter at the subdistal appendages than at the proximal ends [6, 10, 112, 137, 138]. During late telophase of mitosis, centriolin localizes to the midbody and facilitates the final membrane abscission step of cytokinesis [137, 139, 140]. Other recent literature suggests that centriolin plays a role in transport of vesicles to the cilia [138].

Kif2a is a microtubule depolymerizing kinesin that helps facilitate bipolar spindle formation during mitosis [141-143]. Kif2a is part of the kinesin-13 family of kinesins that function to depolymerize microtubules. Kif2a itself can depolymerize microtubules from the minus ends [141, 144, 145]. Recently, Kif2a was reported to localize to subdistal appendages and function in cilia retraction [146], although the mechanism remain unclear.

Cep170 is a centriolar protein with a localization pattern similar to ninein. Cep170 binds to and stabilizes microtubules [147]. Interestingly, Cep170 interacts with Kif2a as well as two other kinesins of the kinesin-13 family, Kif2b and Kif2c [148, 149]. Furthermore, Cep170 helps target Kif2b localization to the mitotic spindle [148] and might control the localization of Kif2a as well.

The dynactin complex consists of p150glued, p62, p27, p25, dynamitin and Arp1 [150]. The complex is most well known for linking dynein motor proteins to cytoplasmic cargo and microtubules [151, 152]. However dynactin appears to have a separate function in microtubule organization in both mitosis and interphase [75, 153-155]. Overexpression of dynactin complex components or truncated components results in microtubule anchorage defects without disrupting nucleation [74, 155]. Dynactin components have also been linked to centrosome cohesion [91].

Epsilon tubulin is a specialized tubulin uniquely found at centrioles. Epsilon tubulin colocalizes with ninein at the subdistal appendages. Because of epsilon tubulin's critical role in centriole formation, it is impossible to study the sDAP specific functions of e-tubulin by normal depletion experiments. However, in an artificial system using frog egg extracts, e-tubulin was found necessary for formation of microtubule asters that also contained ninein [88].

### **1.4.3 The Centrosome cohesion, intercentrosomal linker, ciliary rootlet and other structures**

The ciliary rootlet/flagellar rootlet is a structure attached to the proximal end of the basal body (Figure 1.8). The rootlet is present in diverse organisms from single celled choanoflagellates to insects to

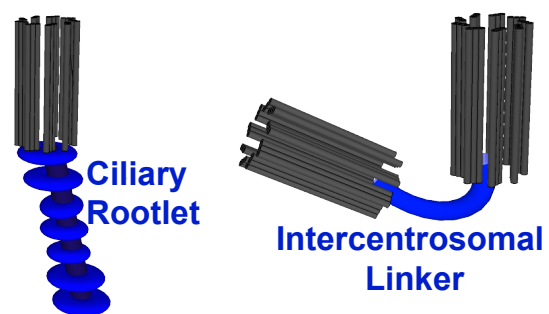


Figure 1.8 The Ciliary Rootlet and Intercentrosomal Linker



mammals [110, 156]. The ciliary rootlet is composed of rootletin, a protein that forms very stable fibers [157, 158]. The rootlet is not needed for cilia formation but supports the long-term stability and sensory functions of the cilia [156, 158]. Rootletin also forms a fibrous linker between centriole pairs to facilitate centrosome cohesion [156, 159, 160] ([Figure 1.8](#)).

During the interphase of vertebrate cells, the two centrosomes remain closely associated to each other, functioning as a single microtubule organized center. At the end of the G2 phase (prior to mitosis) the centrosomes separate and move to opposite ends of the cell. The close link between the two centrosomes is referred to as centrosome cohesion. When cohesion is lost before G2, the phenotype is referred to as centrosome splitting [161]. Two distinct mechanisms contribute to centrosome cohesion. In the most well understood mechanism, a physical linker structure connects the proximal ends of both centrioles. The linker is composed of rootletin and Cep68 [9, 159, 160]. Linker formation and centrosome cohesion require C-Nap1, a protein localized to the centriole proximal ends [160, 162, 163]. Without C-Nap1, several other proteins implicated in centrosome cohesion including rootletin, Centlein, Cep68 and LRRC45 cannot be targeted to the centrosome [160, 164-166]. Prior to mitosis, the kinase Nek2 phosphorylates C-Nap1, Cep68, Centlein, rootletin and LRRC45, triggering the disassembly of the linker [160-162, 164, 165, 167]. Protein phosphatase 1 (PP1) is able to oppose the effects of Nek2 and stabilize the linker [168-170]. Phosphorylation of Cep68 by PLK1 also contributes to cohesion loss [171]. Although the centrosomes are able to separate more than 2

microns apart after depletion of linker components, the centrosomes still remain within 3-5 of each other, suggesting that other mechanisms contribute to cohesion.

The second mechanism of centrosome cohesion involves cytoskeletal dynamics and interactions between the centrosomes and the microtubule cytoskeleton [172-174]. Microtubule depolymerizing agents like nocodazole can trigger centrosome splitting [169, 174]. Split centrosomes can later rejoin, using a microtubule dependent mechanism [60, 174]. Furthermore, if the intercentrosomal linker becomes compromised by C-Nap1 depletion, centrosome cohesion becomes more sensitive to nocodazole and Taxol [175] indicating that there is some redundancy. Centrosome cohesion also requires pericentrin and Cep215, two components of the pericentriolar material that are also important in microtubule nucleation [9, 33, 176]. Cep68, a component of the intercentrosomal linker is known to interact with pericentrin and Cep215 suggesting that the PCM and linker cooperate to maintain centrosome cohesion [171].

Even though centrosome separation is only necessary before mitosis, multiple pathways regulate centrosome cohesion independently of mitosis. The Hippo pathway proteins MPS1 and 2 promote centrosome splitting by phosphorylation of Nek2 [177]. Several Wnt pathway components localize to the centrosome and regulate centrosome splitting [178, 179]. Centrosome splitting can also be induced by DNA damage [180]. Clearly, centrosome cohesion must also be important for some processes during interphase or such complex

regulation would not have evolved. However, functional consequences of interphase separation of centrosomes are not understood.

#### **1.4.4 The Centriolar Satellites**

The **centriolar satellites** are granules of protein that are found in the vicinity of the centrosomes during interphase. Originally identified by electron microscopy, the satellites are kept near centrosome by the minus end directed motor activity of the dynein-dynactin complex. PCM1, a satellite specific protein is believed to organize the structures by binding a wide variety of proteins [45]. The satellites contain mostly proteins that are also known to localize to the cilia, PCM or appendages. The predominant model of satellite function holds that centriolar satellites transport centrosome components to regulate centrosome composition. Satellites function in the delivery of many centrosomal proteins including Cep164, C-Nap1, ninein, pericentrin, and centrin [45, 70, 181]. Consequently the satellites are important for multiple centrosome functions including cilia formation and microtubule organization.

#### **14.4.5 Centrosome Cycle**

During each cell cycle, all organelles must be duplicated once and divided between daughter cells during mitosis. Naturally, the number of centrioles also doubles once per cell cycle. During G1, vertebrate cells have two centrioles, each surrounded by a distinct matrix of PCM, making two centrosomes total (Figure 1.9). However, only one of the two centrioles has distal and subdistal

appendages during G1 (Figure 1.9). An intercentrosomal linker connects the two centrioles (Figure 1.9). During S-phase, a daughter centriole grows on the side of each preexisting centriole [182]. After formation, the new daughter centrioles are firmly attached (engaged) to the side of their mothers [183] (Figure 1.9). The

## Centrosome cycle

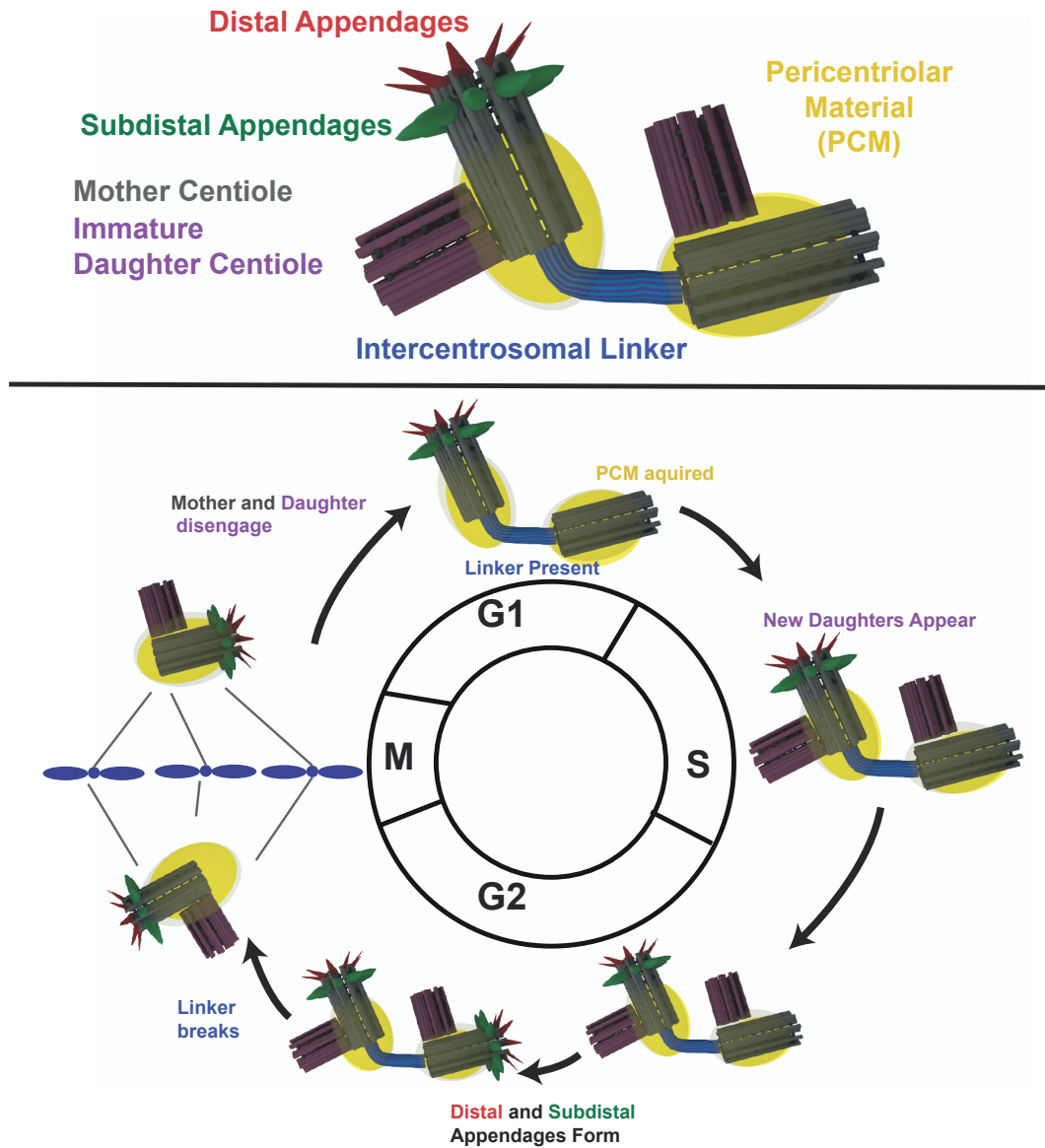


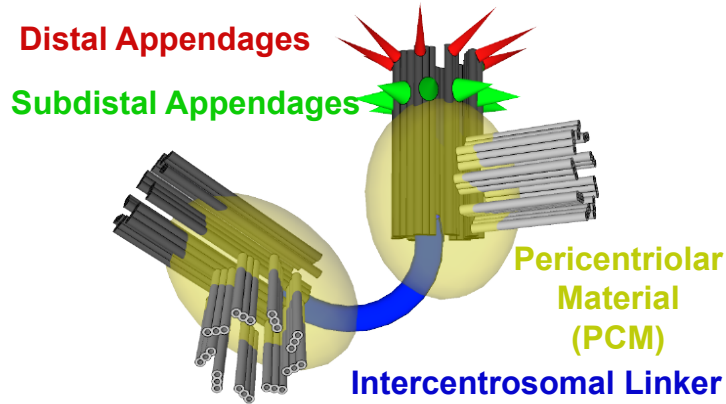
Figure 1.9 Centrosome during the Cell Cycle

second of the two mother centrioles gains appendages during G2 [80], possibly at the G2/M transition (Figure 1.9) [182]. Prior to mitosis the linker breaks, and the spindle poles form. During mitosis, each centrosome contains one mother centriole that has its own daughter engaged to it. That engagement allows each daughter centriole to segregate to a new cell with its mother despite the daughter centrioles' lack of PCM. During mitosis, the engagement between mother and daughter centrioles is broken. Activity of the kinase Plk1 modifies the daughter centriole, allowing it to mature [37]. The daughter centriole then matures, gains PCM and becomes a centrosome with the start of G1 (Figure 1.9). At G1, the intercentrosomal linker reforms to connect the mother to the newly mature daughter centriole [182]. Importantly, an ordered sequence of centrosome maturation events helps maintain centrosome hemostasis. Each step in centriole maturation 1) only occurs during a particular cell cycle stage and 2) requires the previous step in centriole maturation to have already occurred (in an earlier cell cycle stage). Centrioles only mature and acquire PCM at G1. Only those matured centrioles can become mothers during S-phase. Any new centrioles produced in a given S-phase lack PCM and are not yet mature enough to act as mothers. Only centrioles that have become mothers in S phase acquire appendages during the subsequent G2 (if they do not already have appendages from the previous G2) [182]. Using this sequence of maturation events, a cell ensures that only one centriole at a time has appendages and can grow primary cilia.

#### **14.4.6 Summary of structural modifications on Centrosomes**

The major structural modifications of the vertebrate centrosome and their respective functions are summarized in [Figure 1.10](#). Each structure must have evolved to benefit the cell in some way. In the case of some structures, like the distal appendages, that benefit is clearly understood (DAPs are required for cilia formation). At present, the ultimate purposes of the intercentrosomal linker and of the subdistal appendages have yet to be explained ([Figure 1.10](#)).

# Summary of Structural modifications of ciliated vertebrate centrosomes








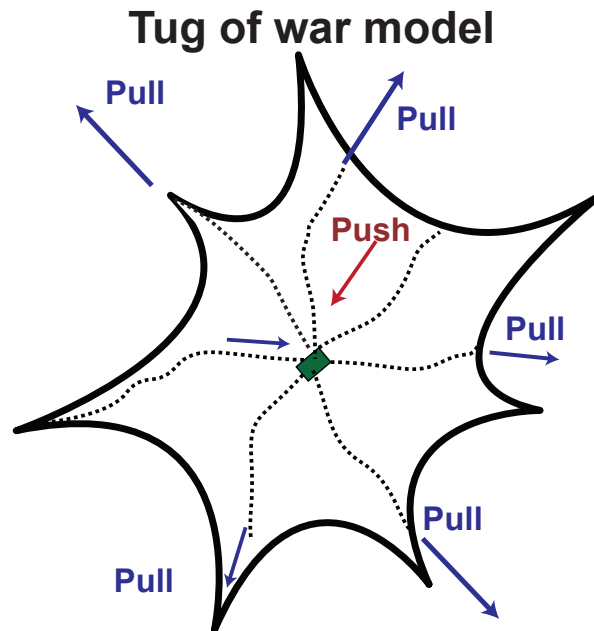
Component		Direct Role	Why?
Distal Appendage		Attach Membrane	Form Cilia
Subdistal Appendage		Attach Microtubule	????
Centriole		Template 9 fold Symetry of cilia	Form Cilia
Linker		Attach Centrosomes	???
Pericentriolar Material		Nucleate Microtubule Attach Microtubule	Organize Spindle Organize interphase array

Figure 1.10 Structural Modifications of Vertebrate Centrosome

## 1.5 Centrosome, Cilia and Golgi position

### 1.5.1 Control of Centrosome and Cilia position.

As the 'central body', the centrosome is often located at the center of interphase cells [59]. However, centrosome position must be off-centered in many cell types. For example, centrosomes in polarized epithelia are located at the apical surface [60]. Migrating cells will position their centrosome to face the



**Figure 1.11** The tug-of-war model

direction of migration [184]. And cytotoxic T cells orient their centrosomes at the immunological synapse where they contact infected cells [185]. Since the cilium grows from the distal end of one of the centrioles, the cilia's position depends on the location of the centriole. Consequently, decentering of the centrosome is necessary to form a cilium at the cell surface. The array of cytoskeletal microtubules attached to the centrosome appears critical for centrosome centering [59]. Mechanical forces exerted on the microtubules at the cell periphery push and/or pull on the MTOC from all directions (Figure 1.11). Tensile forces created by dynein motors (which are fixed in place) can pull on



microtubules from the cell edge. Microtubule flux, a pulling force driven by microtubule depolymerization can also pull on microtubule. Since the minus end directed depolymerizing activity of Kif2a is able to drive microtubule flux, a pulling force could originate from the centrosome (where Kif2a localizes). Retrograde flow, an actin mediated process pushes backward on the microtubule array from the leading edge of the cell [186]. Due to the viscosity of the cytoplasm, friction exerts a force to resist movement of the microtubule array [187]. Compression forces of microtubule plus ends against the edges of cells can “push” the array [58]. However, these pushing forces are small compared to the pulling of dynein motors [187]. Remarkably, the forces from all directions in this tug-of-war balance out to keep the centrosome in the cell center ([Figure 1.11](#)). Without highly stable anchoring of microtubule minus ends to centrioles, the pulling/pushing forces exerted would simply rip microtubules from the MTOC. It follows that microtubule anchorage should be essential for control of centrosome position. An imbalanced pulling/pushing force from one end of the cell can decenter the centrosome. Larger numbers of stabilized microtubules can push an MTOC away from the cell center toward one edge [188]. Cell polarity proteins like Cdc42 and Par3 regulate dynein motors to ensure the centrosome faces the right direction while keeping the centrosome centered during cell migration [189, 190]. Prior to my work, no research had considered the mechanisms of how centrosome-positioning forces regulate the position of cilia.

### 1.5.2 Golgi Position, Centrosome position and cell polarity

The centrosomes and Golgi are associated throughout interphase. The centrosome, in fact, defines the location of Golgi formation [78]. Golgi fragments travel along centrosomal microtubules to form stacks of cisternae beside the centrosome. Loss of centrosome cohesion has also been shown to

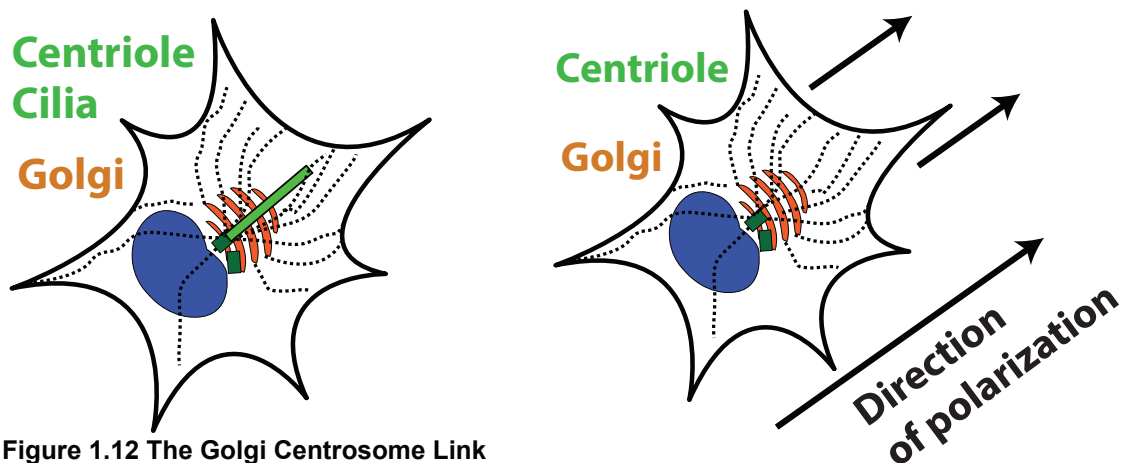


Figure 1.12 The Golgi Centrosome Link

affect Golgi morphology [175]. Also, Golgi derived vesicles are known to provide membrane and associated proteins to the cilia [191, 192]. Centrosome-nucleated microtubules are believed to provide tracks that Golgi vesicles travel upon during directional secretion. This directional secretion, in turn, is important for cell migration [55]. However, it is unclear how physical proximity of the Golgi to the cilia/centrosome contributes to physiology. Previous attempts to address the question of why the Golgi and centrosome/cilia are closely associated have been limited by lack of tools to separate the two without compromising the integrity of one or the other organelle [193, 194]. Although Hurtado et al were able to separate the organelles with AKAP450 fragment overexpression, the Golgi under these conditions was malformed and reporter effects could be explained as

overexpression artifacts [195]. Both centrosome and Golgi act as microtubule organizing centers (MTOCs). Several centrosomal proteins also localize to the Golgi apparatus including CDK5rap2, IFT20, AKAP450, and CAP350 [25, 196]. These same proteins are involved in microtubule nucleation and anchorage [25, 196], indicating shared mechanisms of MTOC activity. Because of the close proximity of Golgi and centrosomes, the structures resemble a single MTOC.

Most migrating cells polarize with a specific cellular geometry. The centrosome/cilia face the direction of cell migration. The Golgi apparatus is in front of the centrosome positioned perfectly for vesicle transport to occur in the direction of cell migration (Figure 1.12). Meanwhile the nucleus is in the back [55, 186, 197]. In this arrangement, both Golgi associated microtubules and centrosome-associated microtubules are oriented with plus ends toward the direction of migration. Using laser ablation, Wakida et al showed that the centrosomes help maintain polarized cell morphology during migration. After ablation, microtubule arrays became symmetric and nonpolarized [198]. The centrosome is important for direction cell migration in some models of wound healing but dispensable in many others [199]. Furthermore, during polarization of rat hippocampal neurons and Drosophila ganglion cells, the centrosome location defines the site of axon formation [200] suggesting that proper regulation of centrosome position could be important for neural development and function.

### **1.5.3 The position of the cilia on the edge of the plasma membrane:**

#### **Surfaced, submerged and non-emergent cilia**

The membrane structure at the base of the cilia in vertebrates is organized in a manner similar to the flagellar pocket of protozoa [201]. The cilia rests in a membrane invagination called the ciliary pit, pouch or pocket by various authors [201]. Although, the term 'ciliary pocket' is sometimes used to refer to the enlarged space at the bottom of the

## Morphology of Cilia Pit

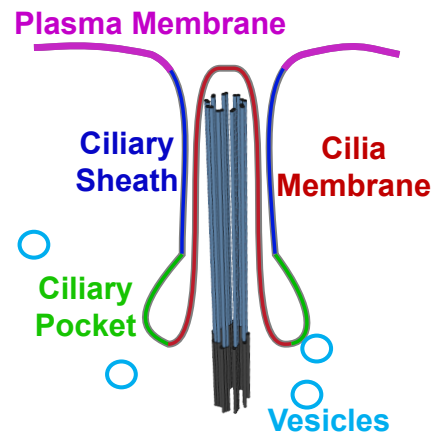


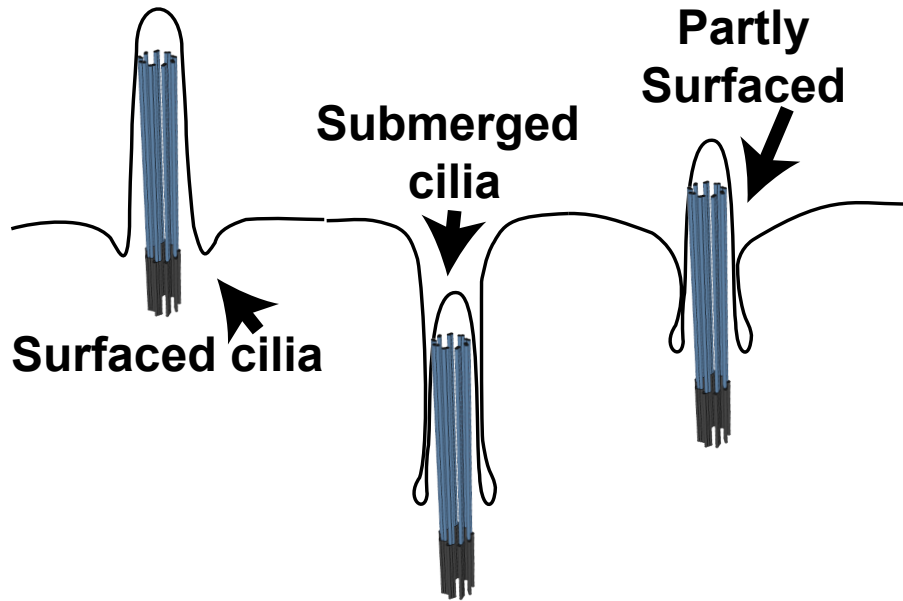
Figure 1.13 The ciliary membranes

ciliary pit [202] rather than the pit as a whole, many authors use the term ciliary pocket to refer to the entire membrane cavity [201]. Toward the distal end of the ciliary pit, the ciliary membrane and the adjacent plasma membrane are closely apposed. The plasma membrane in this region is called the ciliary sheath [201] (Figure 1.13). At the proximal end of the ciliary pit, there is a larger space separating the ciliary membrane and the plasma membrane. That space is sometimes specifically referred to as the pocket (Figure 1.13). Like the trypanosome's flagellar pocket, the vertebrate ciliary pocket is a site of endocytosis [203, 204]. The depth of the ciliary pit varies depending on the cell type studied. Cilia are commonly depicted projecting directly from the cell surface or inside a very shallow pit. Such a depiction accurately describes motile cilia that lack any apparent pit or pocket structure [85, 205]. However, depending on the depth of the ciliary pit, it may contain anything from the most proximal portions of the cilia [206, 207] to the entire length of the cilia [203, 208]. We have coined the

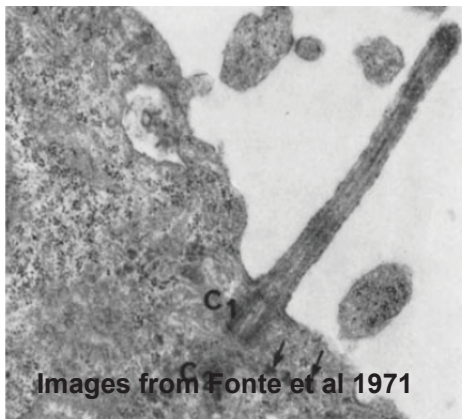
terms ‘surfaced’ to describe cilia that either rest in a shallow pit or no pit (Figure 1.14). In contrast we coin the term ‘submerged’ to describe cilia in deep pits that confine most of the axoneme (Figure 1.14). Vertebrate cells of several tissue types are able to maintain submerged cilia that are confined to a deep pit [201, 203, 209-211]. The same tissue can contain both submerged cilia that rest in deep pits and surfaced cilia that lack any pit [212]. Interestingly, spermatozoa have deep ciliary pits during intermediate stages of development that are lost when fully differentiated [201]. Surfaced cilia sometimes extend into a cavity between adjacent cells rather than a lumen [213-215]. Although in a suitable location for juxtacrine signaling, these types of surfaced cilia may behave similarly to submerged cilia with respect to fluid flow and ligand accessibility.

Most known functions of the cilia require a cell surface organelle. What function the ‘submerged cilia’ perform despite their limited exposure to the extracellular environment is unknown. They are certainly protected from mechanical stimuli and might even be shielded from some chemical signals. How cilia are maintained in a submerged position has not previously been investigated. Furthermore, no genetic means of manipulating cilia position has previously been available, making it impossible to answer questions about the function of submerged cilia. The pocket and plasma membrane at the bottom of the pit is the site of endocytosis and exocytosis for import/export of ciliary membrane proteins. Would the dynamics of import/export of proteins into surfaced cilia be different?

# Cilia Positions



## Surfaced Cilia



## Submerged Cilia



Images adapted with permission of Journal of Cell Biology. Fonte, V.G., R.L. Searls, and S.R. Hilfer, *The relationship of cilia with cell division and differentiation*. J Cell Biol, 1971. **49**(1): p. 226-9. doi: 10.1083/jcb.49.1.226

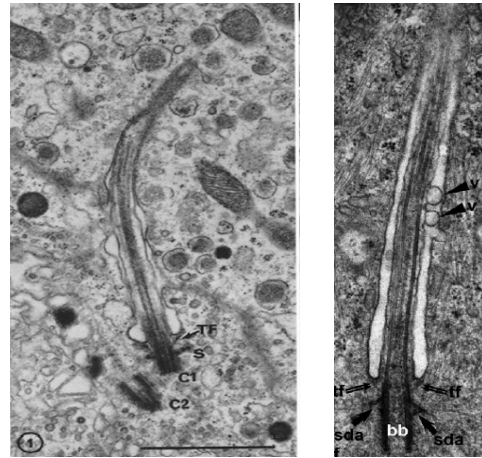
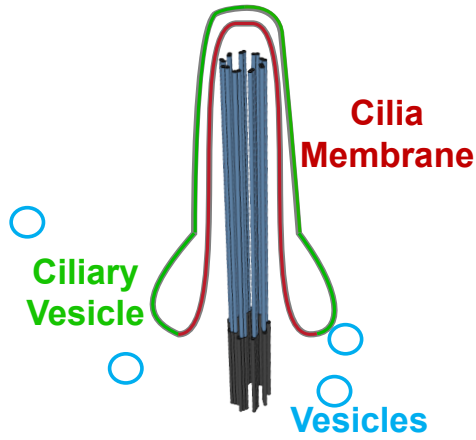
### Figure 1.14 Surfaced and Submerged Cilia

Fully formed cilia are sometimes found completely enclosed in a cytoplasmic vesicle [3, 210] (Figure 1.15). These 'non-emergent' cilia are completely isolated from the extracellular environment and are likely deaf to

some types of signaling. Emergence of the cilia might work like an on/off switch, keeping the cilia in a nonfunctional mode until the cell needs to move it to its functional location. Although non-emergent cilia are frequently reported, it is difficult to distinguish a fully non-emergent cilia from one that merely has a very deep ciliary pit [212]. To prove that a given cilia is non-emergent, one needs a complete set of serial electron microscopy (EM) sections containing the distal tip of the cilia. However, serial sectioning and EM preparation of the cilia are difficult and time consuming in practice. As a consequence, it is unknown how common non-emergent cilia are. Many published images of non-emergent cilia may in fact simply be submerged cilia inside of deep pits with unseen openings. Alternatively, non-emergent cilia may be an intermediate stage in the formation of submerged cilia.

# Non-Emergent Cilia

## Plasma Membrane



Right EM panel is reproduced and adapted with permission from Journal of Cell Science [2].  
doi: 10.1242/jcs.085852

Figure 1.15 Non-Emergent cilia

Left EM panel is reproduced and adapted with permission from Journal of Cell Biology [3].  
Dingemans, K.P., *The Relation Between Cilia And Mitoses In The Mouse Adenohypophysis*. The Journal of Cell Biology, 1969. **43**(2): p. 361-367.  
doi: 10.1083/jcb.43.2.361



#### **1.5.4 The ciliary membrane and periciliary membranes**

Despite being topologically continuous with the plasma membrane, the ciliary membrane has distinct protein composition. Proteins are delivered to the ciliary membrane primarily by fusion of vesicles at the base of the cilia [13]. Members of the Rab family of GTPases regulate vesicle trafficking to the cilia [216]. A variety of ciliary targeting domains and mechanisms target specific proteins to the cilia [217]. A barrier to membrane protein diffusion at the base of the cilia prevents free diffusion of proteins into the cilia [218]. The cilia membrane also has a lipid composition distinct from the rest of the plasma membrane [13].

The plasma membranes lining the ciliary sheath and ciliary pocket are called the periciliary membrane [219, 220]. The membrane shaping proteins EHD1 and EHD3 localize to the ciliary sheath and pocket [221]. Some membrane proteins are excluded or enriched in a circular region of the plasma membrane around the cilia [222]. This ring-shaped domain of non-invaginated plasma membrane surrounding the cilia is also referred to as part of the periciliary region [223]. There may be a second diffusion barrier that separates periciliary membrane. However, neither the unique membrane protein composition of the periciliary membrane nor the barriers have been fully characterized. Since some ciliary membrane proteins like Smoothed travel laterally from the plasma membrane to the cilia, there must be a mechanism for proteins to cross all diffusion barriers [224].

The connecting cilium of photoreceptor cells has a domain resembling a ciliary pocket located between the cilia and the periciliary collar like extension

(PCLE) [225, 226]. Like the ciliary pocket, the pocket-like region of the photoreceptor is the site of endocytosis and exocytosis [227]. In the PCLE, the connecting cilium membrane is attached to the nearby plasma membrane cilia via extracellular linkers formed by a complex of usher syndrome associated proteins (including Usherin, Whirlin and VLGR1b) [225, 226]. It is not known whether such extracellular linkers are present in the ciliary pits of normal cell (none have been reported).

## **1.6 Cilia signaling**

### **1.6.1 Several signaling pathways are linked to the primary cilia**

Primary cilia are non-motile cilia that function in signaling. With few exceptions [228, 229], there is only one non-motile signaling cilium in any given cell. This contrasts to the hundreds of motile cilia present with the cells of some tissues [84]. The cilium has roles in several signaling pathways, including hedgehog, TGF-beta, PDGF, serotonin, dopamine, somatostatin, MCH and olfactory receptor [15, 228-237]. The localization of receptors to the ciliary membrane is important for function [228, 236]. In some of these pathways, removal of the receptor from the cilia occurs upon activation. For example, Patched, SSTR3, Neuropeptide Y receptor 2 (NPRY2) and Dopamine Receptor 1 (D1) are present at the cilia membrane in absence of their respective ligands but exit the cilia after ligand binding [15, 233, 234, 236, 238, 239]. Endocytosis of certain receptors is necessary for signaling to occur normally [219, 230, 240]. That endocytosis occurs at the ciliary pocket [203, 219, 230, 240]. Receptor

endocytosis can either be a pathway activation step or a feedback that desensitizes the pathway to ligand. In the case of the Hedgehog pathway, for example, Patched must be at the cilium to mediate signaling [236] that requires the removal of GPR161 from the ciliary membrane via clathrin mediated endocytosis [240]. The entry or exit of receptors into/out of the cilia is controlled via the BBSome, a complex that structurally resembles a caveolin coat [217, 241].

Animals have evolved both cilia-membrane specific and plasma membrane localized versions of the receptors for PDGF, Dopamine, Serotonin, and Somatostatin [232, 235, 242] indicating that cilia are not strictly required for signaling. The existence of non-ciliary alternatives leads one to ask why cilium mediated signaling is used at all? Some authors propose that the proximity of the cilia to the Golgi apparatus could help relay signals from cilia to Golgi [215]. Other models hold that concentration of receptor molecules in an organelle as small as the cilia facilitates activation or results in greater ligand sensitivity [243]. Alternatively, cilia specific second messengers could produce distinct signaling outputs. Conceivably, different cell types may express different versions of the same receptor depending on the need for cilia-mediated signaling.

Cilia also mediate non-ligand signals. The light detecting photoreceptor cells within the retinas rely on a specialized cilium called the connecting cilium to function. The connecting cilia contains discs of membrane where Rhodopsin, the light sensing molecule actually resides [229]. Within kidney tubules, cilia function to sense fluid flow and ion concentrations [14]. Without these cilia, polycystic

kidney disease develops. During symmetry breaking at the embryonic node, cilia produce a leftward flow of fluid that causes expression of genes critical proper left-right patterning to occur on the left side of the embryo [205]. Cells on the periphery of the node, contain non-motile sensory cilia that help sense that flow [244]. Primary cilia are transiently necessary for the formation of an actin based structure called the stereocilia, which is required for hearing [229]. In summary, the cilia's role in signaling is important for many biological processes. Vertebrates need cilia to form a body, to see, to hear, to smell, to sense our hunger, to feel and much else.

### **1.6.2 Hedgehog signaling**

The most biologically important and well-studied signaling pathway mediated by the primary cilium is the Hedgehog pathway (Figure 1.16). Ligand responsiveness of the Hedgehog signaling pathway requires the primary cilia [245, 246]. The mechanisms of how this works are complex and not yet perfectly understood. A summary of the pathway (as it is currently understood) follows. In the absence of ligand, the membrane receptor Patched (PTCH1) normally represses entry of the GPCR like protein, Smoothened (Smo) into the cilia. Without Smoothened in the cilia, another component, GPR161 promotes the production of cyclic AMP. High cAMP levels activate protein kinase A (PKA) at the cilia. PKA phosphorylates the HH pathway transcription factors Gli2 and Gli3 [240, 247, 248]. Phosphorylation promotes efficient processing of Gli2 and Gli3 into their repressor forms (Gli2/3R) within the cilia [219, 249] while inhibiting

conversion to Gli2/3 activator forms (Gli2/3A) [250]. Meanwhile, in the cytoplasm, Sufu binds any unprocessed molecules of Gli in order to keep them from entering the nucleus and functioning as activators [251]. Binding of hedgehog ligands to Patched causes Patched to leave the cilia and stops inhibition of Smoothened entry. Smoothened can then enter the cilia and be converted to its activated form [15, 252] [236, 239]. Smoothened inhibits cyclic AMP production and causes the removal of GPR161 (a promoter of cAMP production) from the cilia [240, 248] (Figure 1.16). The reduced cyclic AMP levels lead to less Gli

## The Cilia's role in the Hedgehog Pathway

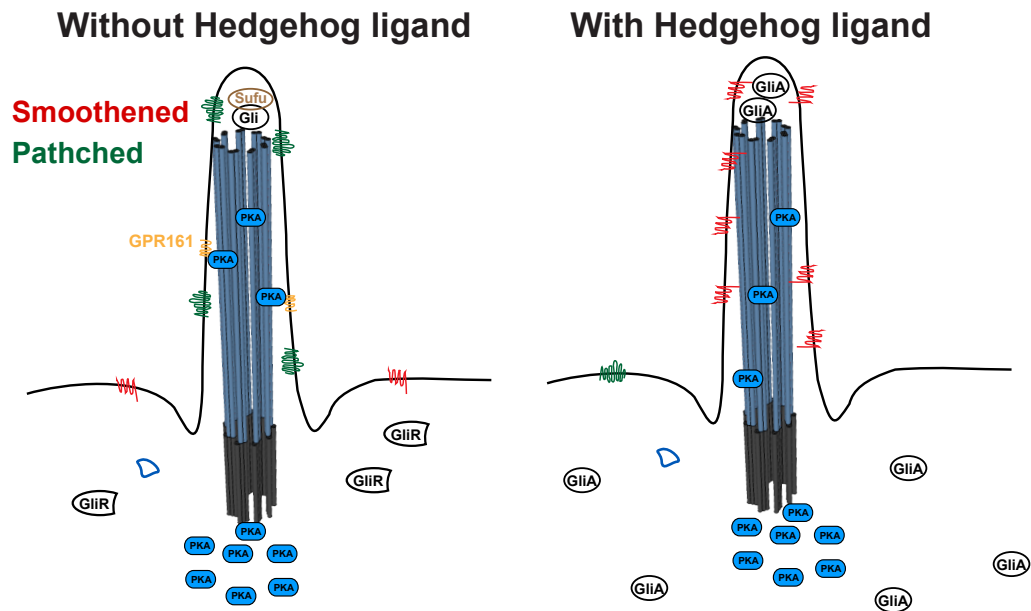


Figure 1.16 The Hedgehog Pathway

phosphorylation, resulting in less GliR production [247, 253]. At the highest levels of Hedgehog ligand concentration, Gli2 and Gli3 accumulate at cilia tips, are converted to their activator forms by phosphorylation [250], lose the ability to interact with SuFu and enter the nucleus [251]. The balance between the amount

of GliA to GliR, activator and repressor forms controls the level of signaling output. The complex control of signaling levels allows different cellular responses to occur depending on the level of ligand in each part of a developing neural tube or limb. In mutants that lack cilia, Gli2/3s can neither be efficiently processed to their repressor form nor to their activator form and Smoothed activation can no longer affect Gli2 nor Gli3 function [245, 246].

## **1.7 Centrosomes, Cilia and human disease**

### **1.7.1 Centrosome Amplification and Clustering**

Excessive numbers of centrosomes are a common feature of cancer cells in both tumors and precancerous lesions [254]. Cells with extra centrosomes are said to have undergone centrosome amplification (CA). Common oncogenic phenotypes like deregulation of the cell cycle or p53 loss-of-function can cause CA [255, 256]. The number of centrosomes can be used as a prognostic biomarker in many tumors. More centrosomes typically correlate with worse prognosis and more advanced tumors [257, 258] or response to some treatments [259]. The presence of extra centrosomes also correlates with chromosomal instability (CIN). Since each centrosome promotes the formation of a spindle pole, multipolar division was once thought to be behind the CIN. However, this appears not to be the case because centrosomes can form clusters during interphase and mitosis. After clustering, bipolar spindles can form with a cluster of several centrosomes in each pole. Chromosomal instability results from merotelic attachments that occur when bipolar spindles form with clustered

centrosomes [260]. Since multipolar cell divisions do not produce viable daughter cells, centrosome clustering is essential for the growth of cells with CA [260]. Centrosome declustering drugs show some therapeutic potential [57]. Interestingly, loss of clustering during interphase can inhibit cell migration and lead to apoptosis of cells with CA [57]. A better understanding of centrosome clustering in interphase and mitosis could inform the development of new treatments.

### **1.7.2 Ciliopathies**

Loss of cilia formation causes midgestation lethality in which embryos have neural tube closure defects due to a failure in the hedgehog-signaling pathway. Milder mutations that can impair the function of cilia without a complete block of cilia formation occur in a family of disorders known as ciliopathies. Different forms of ciliopathy have a diverse but overlapping myriad of symptoms including retinal degeneration, deafness, anosmia, obesity, hyperphagy, polycystic kidneys, nephronophthisis, polydactyly, Hepatic fibrosis, skeletal abnormalities, cognitive defects, cerebellar vermis aplasia, and sinus inversus [261]. Although these many symptoms appear arbitrary, most have been linked to the function of the cilia in specific tissues. The connecting cilium of the photoreceptor must be maintained for a lifetime to preserve visual function [229]. Neuronal cilia function to control of appetite and their loss leads to hyperphagy and obesity [238, 262]. Cilia at the embryonic node must create and sense fluid flow in order to produce proper left-right symmetry [205]. Lack of olfactory cilia

causes anosmia [229]. Defects in the cilia renal tubule epithelia (which sense fluid flow) can contribute to Kidney cysts [261]. Hedgehog signaling contributes to multiple developmental steps: stimulating growth of the cerebellum's granule cell neural progenitor cells, controlling formation of digits and neural tube organization [15]. In summary, patients with ciliopathies display an interesting mix of phenotypes because different kinds of cilia serve several distinct signaling functions.

### **1.7.3 Cilia, hedgehog and Cancer**

Hedgehog signaling drives Medulloblastoma, Basal cell carcinoma and some Rhabdomyosarcomas [263-266]. Activating mutations can occur at multiple points in the pathway either upstream of the cilia (Patched loss) or downstream (Sufu mutations). Hedgehog signaling also contributes to the growth of some breast, pancreatic and colon cancers [266]. Upregulation of this pathway can increase expression of G1 cyclins, suppress apoptosis via BCL2 and maintain stemness [265]. The importance of cilia for tumor growth seems to vary from tumor to tumor [263, 267, 268]. Cilia are essential for initiation and growth of tumors driven by Patched mutations or Smo activating mutations [263, 268]. In contrast, cilia suppress the growth of tumors that are driven by Gli2 activation [263]. The position of the cilium (surfaced versus submerged) in most tumor models is unknown.



## **Chapter 2: Spatial Control of Primary Ciliogenesis by Subdistal Appendages Alters Sensation-Associated Properties of Cilia**

### **2.1 Introduction**

Cilia are membrane bound structures that extend from the cell surface. At the surface, cilia can beat to create a mechanical force, or perform chemical-sensory functions. In vertebrates, the centrioles also function as the core of the centrosome, which functions as the microtubule-organizing center (or MTOC). Just as its name suggests (literally, 'central body'), The centrosome is located at the cell center, far away from the plasma membrane. Those cilia that grow from centrally located centrioles have an interesting morphology. These cilia are confined in a deep ciliary pit, exposed to the environment through a narrow opening at the top of the pit. We refer to these as 'submerged cilia' in contrast to the "normal" or 'surfaced cilia'. Each aforementioned function of the cilia naturally requires a cell surface organelle, making the existence of submerged cilia a paradox. In contrast, vertebrate centrioles and their cilia are often located far from the cell surface. Published literature describes a cavity around the cilia base as the "ciliary pocket". However, the term 'pocket' is not unique to animal cells. In many cell types, a shallow pocket that resembles that flagellar pocket of trypanosomes is present. However, the cilia formed from these shallow pockets are fully surfaced. To clarify, both surfaced and submerged cilia contain a ciliary pocket at their base. To avoid confusion, we use the term "deep ciliary pit" to

specifically refer to the pronounced structure that traps submerged cilia in vertebrate cells.

Submerged cilia can be easily found in non-polarized stromal cells including fibroblasts and smooth muscle cells that carry centrally located centrosomes. Interestingly, some fully polarized tissues such as retinal pigment epithelia form and maintain submerged cilia despite having apically located centrosomes [210, 211]. Cultured cell lines that generally form submerged cilia can be coaxed into forming surfaced cilia under some conditions [269]. This suggests that cells have a mechanism to regulate spatial configuration of their cilia. However, neither the purpose nor the mechanism for maintaining cilia in a submerged configuration is understood.

To facilitate the formation of submerged cilia, vertebrate centrioles may have acquired additional structural complexity. Indeed, vertebrate centrioles are heavily decorated or modified with many accessory structures, including the distal and sub-distal appendages that project radially from the distal part of centrioles, and less distinct structures such as the pericentriolar material (PCM) or the centrosome cohesion linkers that attach to the proximal end of centrioles. In contrast, neither the appendage structures nor the cohesion linkers are seen in the centriole of some lower animals like *Drosophila* or *C. elegans* [102, 270, 271], where no submerged cilia have been reported. Although the distal appendages (DAPs) mediate the docking of centrioles to membranes, they are necessary for cilia formation regardless of cilia position and therefore DAPs not likely to mediate cilia position control. In contrast, the potential link between subdistal

appendages and cilia position has not yet been explored. The sDAP is dispensable for cilia formation but are required for proper alignment of basal bodies at the cell cortex in postmitotic, multiciliated epithelia [136] [7], which exclusively grow surfaced cilia. Furthermore, proteins that localize to the sDAP have been reported to help maintain stable microtubule anchorage [70, 72, 77]. However, it is not yet clear what biological advantage cells may obtain from a centrosome-attached microtubule array. How the sDAP may contribute to primary ciliogenesis has not been fully elucidated, and seems to vary among cell types.

DAP and sDAP are distinct structures composed of different core components, including *CEP83*, *CEP89*, *SCLT1*, *CEP164* and *FBF1* for DAPs, and *ODF2*, *CNTRL* and *NIN* for sDAPs. DAP components are well preserved in all vertebrates and other deuterostomes, but are highly conserved only in some protostome lineages such as mollusks and annelids [80, 272]. A similar evolutionary profile is also seen for sDAP components *CNTRL* and *NIN* [272], suggesting that DAP and sDAP may somehow be co-selected for specific functions. Perhaps one such function could be to maintain submerged cilia. To explore the idea, here we systematically characterized the assembly and function of sDAP in the retinal pigment epithelial cell line (RPE1), which, comparable to their in vivo counterpart [210, 211], nearly exclusively grow submerged cilia.

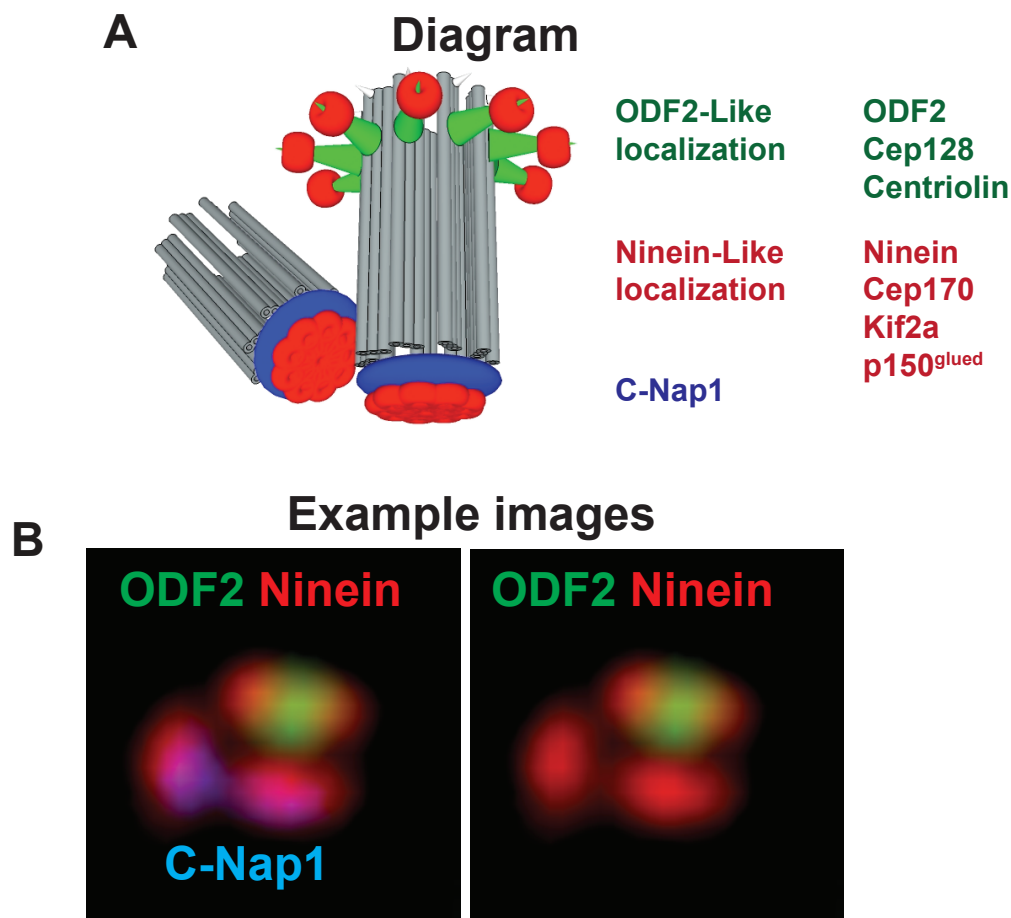
## **2.2 Results**

### **2.2.1 Initial Approach**

To screen for components of the sDAP, we focused on mother centriole specific proteins using the quantitative proteomic approach described previously [80, 273]. We checked the subcellular localization of candidate proteins for ones with localization patterns similar to the known sDAP components: ODF2 or ninein (Figure 2.1). Including the novel and those previously known [6, 91, 112, 138, 147], we identified seven proteins or protein complexes associated with sDAP, including ODF2, Cep128, centriolin (*CNTRL*), ninein (*NIN*), p150glued/dynactin complex, Cep170, and Kif2a. These components were divided into two groups, based on their detailed localization patterns. ODF2 appears as a bar or focus near the distal end of the mature mother centriole where the sDAP are located [6]. ODF2, Cep128 and centriolin exhibit a similar localization pattern, and were thus referred to as members of the ODF2 Group (Figure 2.1A, 2.2A). Ninein, however, localizes both to the sDAP of mother centrioles and to the proximal ends of both mother and daughter centrioles. When the orientation of both centrioles is parallel to the focal plane, ninein appears as a total of four foci, two for the sDAP and two for the centriole proximal ends [6, 112]. We refer to proteins with a ninein-like localization as members of the Ninein Group. The Ninein Group includes ninein, Cep170, Kif2a and p150glued/dynactin complex (Figure 2.1A, 2.2A).

### **2.2.2 The assembly hierarchy of sDAP components**

We next examined the assembly hierarchy of sDAP components. Experiments were done in clonal RPE1 cell lines permanently depleted of specific sDAP components by the CRISPR-Cas 9 method (Figure 2.2B; Table 1) [274]. RNAi experiments were also performed in HeLa cells to confirm the results. We first checked the ODF2 Group members. ODF2 mutation impairs the recruitment of both Cep128 and centriolin to centrioles (Figure 2.2C; centriolin lost in 98%, n>100). Cep128 loss abolishes centriolin recruitment while having a partial effect on the level of ODF2 recruitment (ODF2 lost entirely from 47% while



**Figure 2.1. Different types of sDAP protein localization are distinguishable through immune fluorescent staining.**

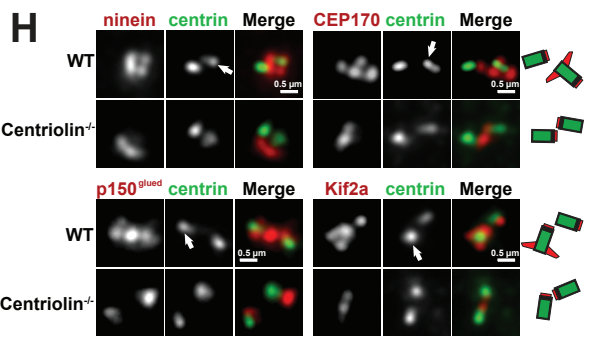
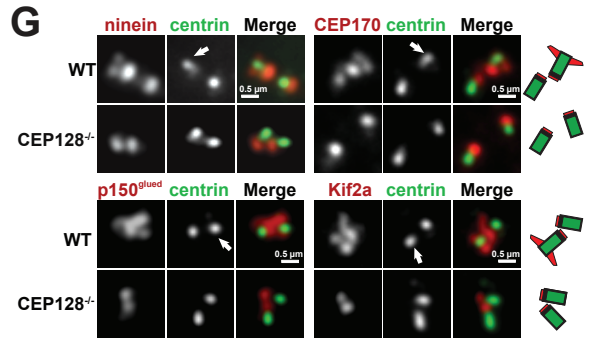
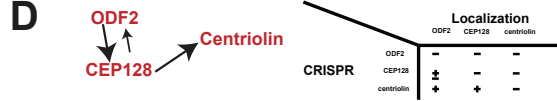
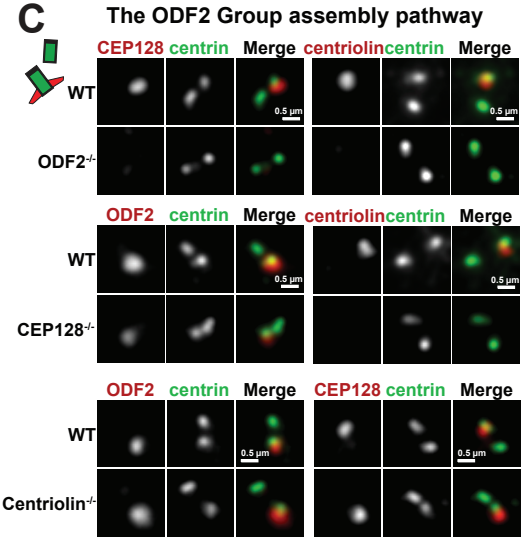
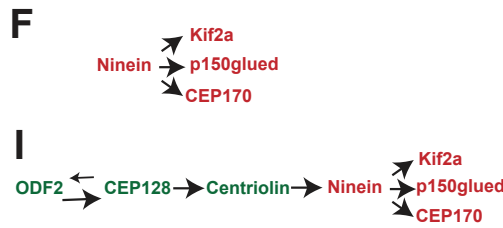
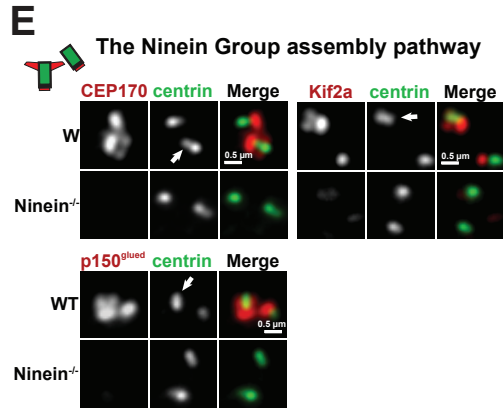
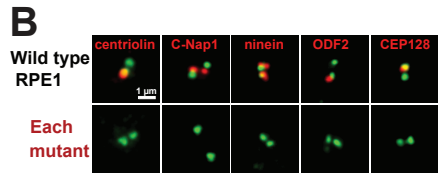
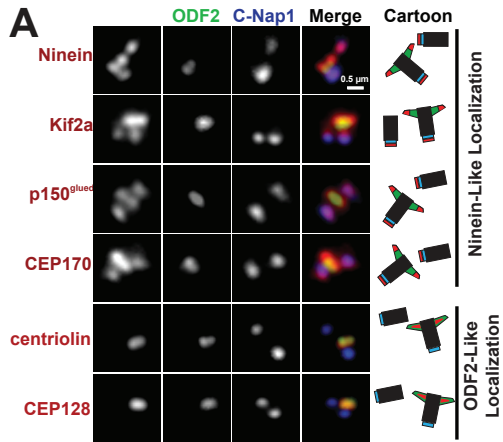
(A) Detailed illustration explaining the localization patterns of sDAP proteins.

(B) Immunofluorescence images of ODF2, Ninein and C-Nap1.

intensity diminished in rest, n>100). In contrast, centriolin loss does not affect the recruitment of ODF2 nor Cep128 (Figure 2.2C; normal intensity in 98% and 96%, n>100). Thus, ODF2 Group assembly follows a hierarchy in the order of ODF2, Cep128 and centriolin (Figure 2.2D). The dependence of Cep128 and centriolin on ODF2 further confirms that Cep128 and centriolin are bonafide sDAP components. We next examined the Ninein Group. Ninein loss prevents the proper recruitment of all other Ninein Group members including Cep170, Kif2a and p150glued (Figures 2.2E and F; lost in 94%, 91% and 98% respectively, diminished in rest, n>100). This suggests that ninein acts as a scaffold for the rest of the Ninein Group. Similar results were seen in HeLa cells using RNAi (Figure 2.3).

Previous work has shown that ODF2 loss eliminates ninein from the subdistal appendages while having no effect on ninein localization at centriole proximal ends, leading to a reduction in the number of ninein foci associated with centrioles [6, 136]. We found that ODF2 depletion by RNAi in HeLa cells has precisely the same effect on Cep170, Kif2a and p150glued localization (Figure 2.3). We next determined whether deletion of the other ODF2 Group members could produce a similar effect on ninein localization. In WT RPE1 cells each member of the Ninein Group appears as 4 foci (Figures 2.2G and H), three associated with the mature mother (indicated by arrow) and one with the other centriole. In *CEP128*<sup>-/-</sup> or *centriolin*<sup>-/-</sup> cells, all Ninein Group members appear as two foci total, one at the proximal end of each centriole (Figures 2.2G and H; >90%, n>100), indicating that while Ninein Group members required

ODF2/Cep128/centriolin to localize to sDAP, their recruitment to centriole proximal ends is independent of the ODF2 Group. The same results were obtained using CEP128 siRNA in HeLa cells (Figure 2.3). Our results are consistent with an assembly hierarchy with ODF2 being the most upstream, followed by Cep128, centriolin, ninein and the rest of the Ninein Group members (Figure 2.2I). While we were unable to deplete Cep170 using CRISPR, Cep170 knockdown had no effect on ninein and p150glued (data not shown). Cep170 knockdown produced inconsistent results with regard to its effect on Kif2a localization (data not shown) possibly because of incomplete depletion. Knockdown of Kif2a did not affect the localization of any Ninein Group nor ODF2 Group protein (data not shown).





**Figure 2.2. The assembly hierarchy of subdistal appendage components**

(A) The localization patterns of sDAP-associated proteins. Localization of respective proteins (red) was shown in relation to centrosome markers for proximal ends (C-Nap1 in blue) and subdistal appendages (ODF2 in green). Results are summarized in diagram and shown in respective colors.

(B) CRISPR-mediated knockout cell lines for each sDAP component (red). Mutant RPE1 cell lines were stained with indicated antibodies (red). Proteins targeted by CRISPR are shown in red along with centrosome markers in green.

(C), Wild-type (WT) or clonal RPE1 cells lines knocked out (KO) of indicated proteins by CRISPR are stained with indicated antibodies. Loss of ODF2 disrupts localization of CEP128 and centriolin at centrioles. Loss of CEP128 disrupts localization of centriolin from centrioles and reduces ODF2 levels at centrioles. Loss of centriolin has no effect on the localization of CEP128 nor ODF2.

(D) A schematic of the assembly hierarchy of the ODF2 group members.

(E) Loss of ninein impairs the localization of CEP170, Kif2a and p150glued to the centrosome.

(F) A schematic of the assembly hierarchy of the Ninein Group.

(G and H) The centrioles of wild-type RPE1 cells have 4 foci positive for each of the Ninein Group members. In CEP128 depleted or centriolin-depleted cells, the foci at the sDAP disappear, leaving only two foci. Arrows indicate the mature mother centrosome.

(I) A schematic of the assembly pathway at the sDAP including both ODF2 Group and Ninein Group members.

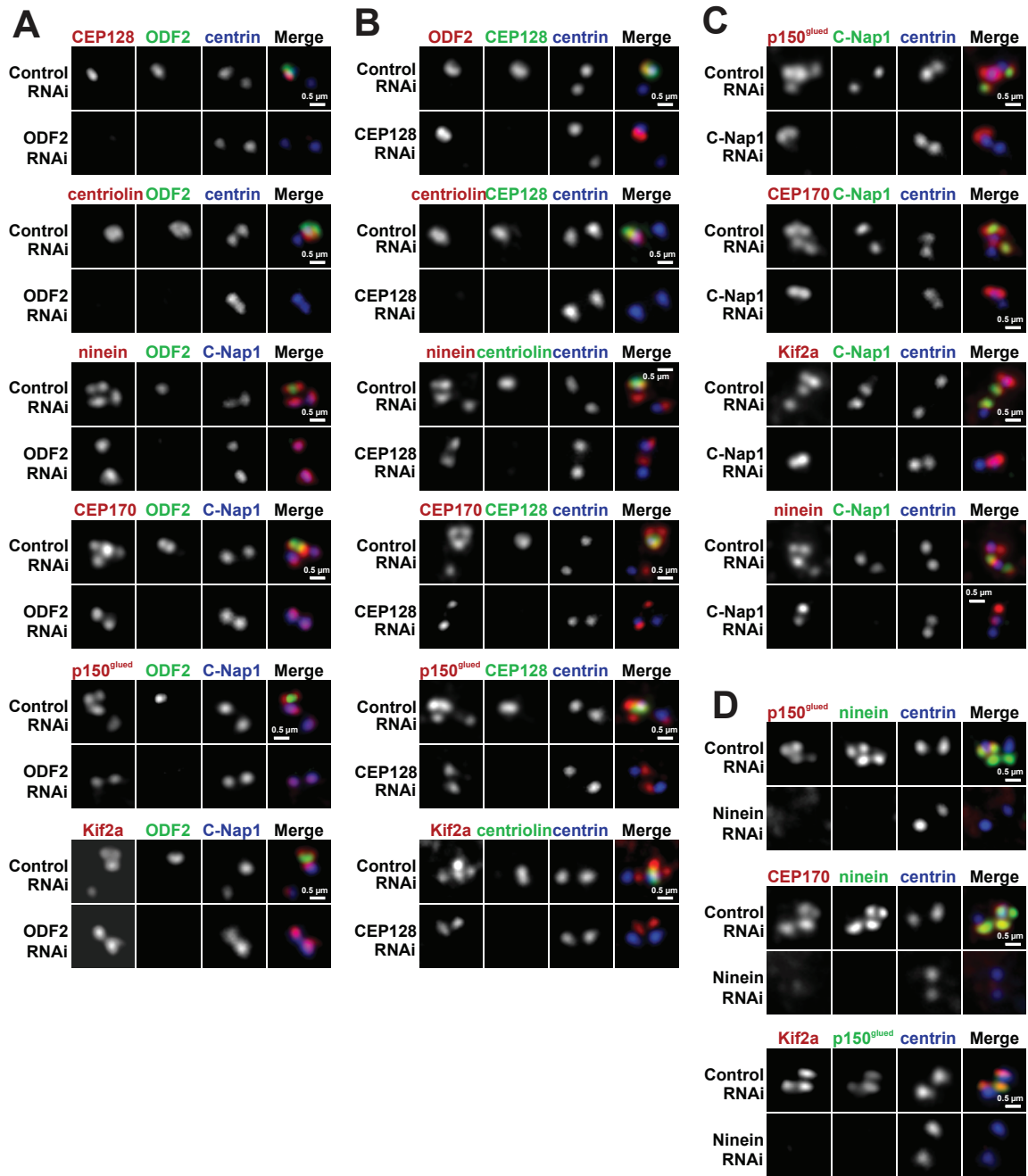


Figure 2.3. Depletion of sDAP-associated proteins by RNAi phenocopies depletion by CRISPR.

(A through D) HeLa cells transfected with siRNAs against the indicated centrosomal proteins or with control siRNA for 60-80 hours. Cells were stained with indicated antibodies to mark the centrosomes (blue) and show the RNAi effects (green and red).

Cell line #	Genotype	Genetic Lesion(s) introduced to one allele	Genetic Lesion(s) introduced to the second allele	Lesion Description and other comments
1	<i>ODF2</i> <sup>-/-</sup>	GAGTGTCGGGGTGA AAAACCAAGG	GAGTGTCGGGGTGA AAAACCAAGG	Small insertions. Result frameshift
2	<i>ODF2</i> <sup>-/-</sup>	GAGGAACAGCACTG6AAAAGAGG	GAGGAACAGCACTG6GGTAAAGAGG	Small deletion and insertion. Result frameshift
3	<i>Cep128</i> <sup>-/-</sup> (3 gRNAs)	lesion 1 (exon 3): GCTGCCAGATCAACGCAGAGGG lesion 2 (exon 14): <b>6CTTGAG6A</b> TCTCAGAGCTGACTC	lesion 1 (exon 3): GCTGCCAGATCAACGCAGAGGG lesion 2 (exon 13 and 14): AACTTCAGCG <large deletion 38.2 KB> ATCTCAGAGCTG	At the first gRNA target site, there are small indels that result in a frameshift of both alleles. At the other two gRNA target sites, there is one small and one large deletion. The large deletion eliminates everything between two gRNA target sites.
4	<i>CNTRL</i> <sup>-/-</sup> (CNTRL was targeted by 2 gRNAs)	lesion 1 (exon 14): ACATTATGTTTGAAAAA <196 bp deletion extending into intron> ACATTATGTTTGAAAAA lesion 2 (exon 15): CTCAGTGCCTATGAAGCTGAGGTAAGAGGCTCGGCTAAACCT	lesion 1 (exon 14 and 15): ATAGCAGCAATGAAGC <25KB large deletion> CTATATTTGTAGGTA	In one allele one there is a large deletion (196bp) that results in a frameshift and small in frame deletion at downstream site. On the second allele a very large deletion includes and goes beyond the cut sites of both gRNAs.
5	<i>Nlrp</i> <sup>-/-</sup>	GCTCAGGGCCAAAATA <b>TGTTAGAGGGTGGGAAGGG</b> TTACGGAGC AA	GCTCAGCCCCAAAATATGTTGCAGAGG	Small deletion and insertion. Result frameshift.
6	<i>C-Map1</i> <sup>-/-</sup>	GGAGCCACTGGGAT <b>ACTFAGAGAGGCGAGG</b> TCCAGGAGGCT	GGAGCCACTGGGAT <b>ACTFAGAGAGGCGAGG</b> TCCAGGAGGCT	Small deletion in both alleles. Result frameshift
7	<i>C-Map1</i> <sup>-/-</sup> ; <i>ODF2</i> <sup>-/-</sup>	GAGGAACAGCACTGC AAAAGAGG	<b>GAGGGAAAGAGCACTG6AAAAGAGG</b>	Small deletion and insertion. Result frameshift. ODF2 mutation was created in cell line #6
8	<i>C-Map1</i> <sup>-/-</sup> ; <i>Cep128</i> <sup>-/-</sup> (Cep128 was targeted by 3 gRNAs)	lesion 1 (exon 3): GCTGCCAGATCAACGCAGGG lesion 2 (exon 13 and 14): AACTTCAGCG <large deletion 38.2 KB> ATCTCAGAGCTG	lesion 1 (exon 3): GCTGCCAGATCAACGCAGAGGG lesion 2 (exon 13 and 14): AACTTCAGCG <large deletion 38.2 KB> ATCTCAGAGCTG	At one gRNA target site, there are small 1 bp indels that result in a frameshift of both alleles. Downstream of the first site, there is a very large deletion of the sequences between the other two gRNAs target sites. Cep128 mutation was created in cell line #6
9	<i>C-Map1</i> <sup>-/-</sup> ; <i>CNTRL</i> <sup>-/-</sup> (CNTRL was targeted by 2 gRNAs)	lesion 1 (exon 14): GTGTTATCAGTGGGTTGCCAGAGAT <b>ACCTGGGGACCA</b> lesion 2 (exon 15): GTGCCTATGAAGCTGAGC <266bp insertion> TAGAGGCTCGGCTAAAC	lesion 1 (exon 14 and 15): GATTTAGAAGGTTTATC <b>TGT</b> <large 10KB deletion> AGGCTGGCTAAACCTAA	In one allele there is a small deletion that produces a frameshift at one site and a large insertion at the second site. On the second allele, there is a very large deletion of sequences in between the two gRNA target sites. Centriolin mutation was created in cell line #6
10	<i>Cep128</i> <sup>-/-</sup> ; <i>C-Map1</i> <sup>+/+</sup> 'Restoration'	GGAGCCACTGG <b>ATACTFAGAGAGGCGAGG</b> TCCAGGAGGCT	GTGGGATATGATTTTATATAT <large deletion 379 bp> TCCAGGAGGCTCAACGGGAG	A small 1bp deletion in one allele that had previously been altered (14bp deletion) in creation of the <i>C-Map1</i> <sup>-/-</sup> . Results in an open reading frame. Other allele has large deletion that does not. <i>C-Map1</i> 'Restoration' was done in cell line #8.

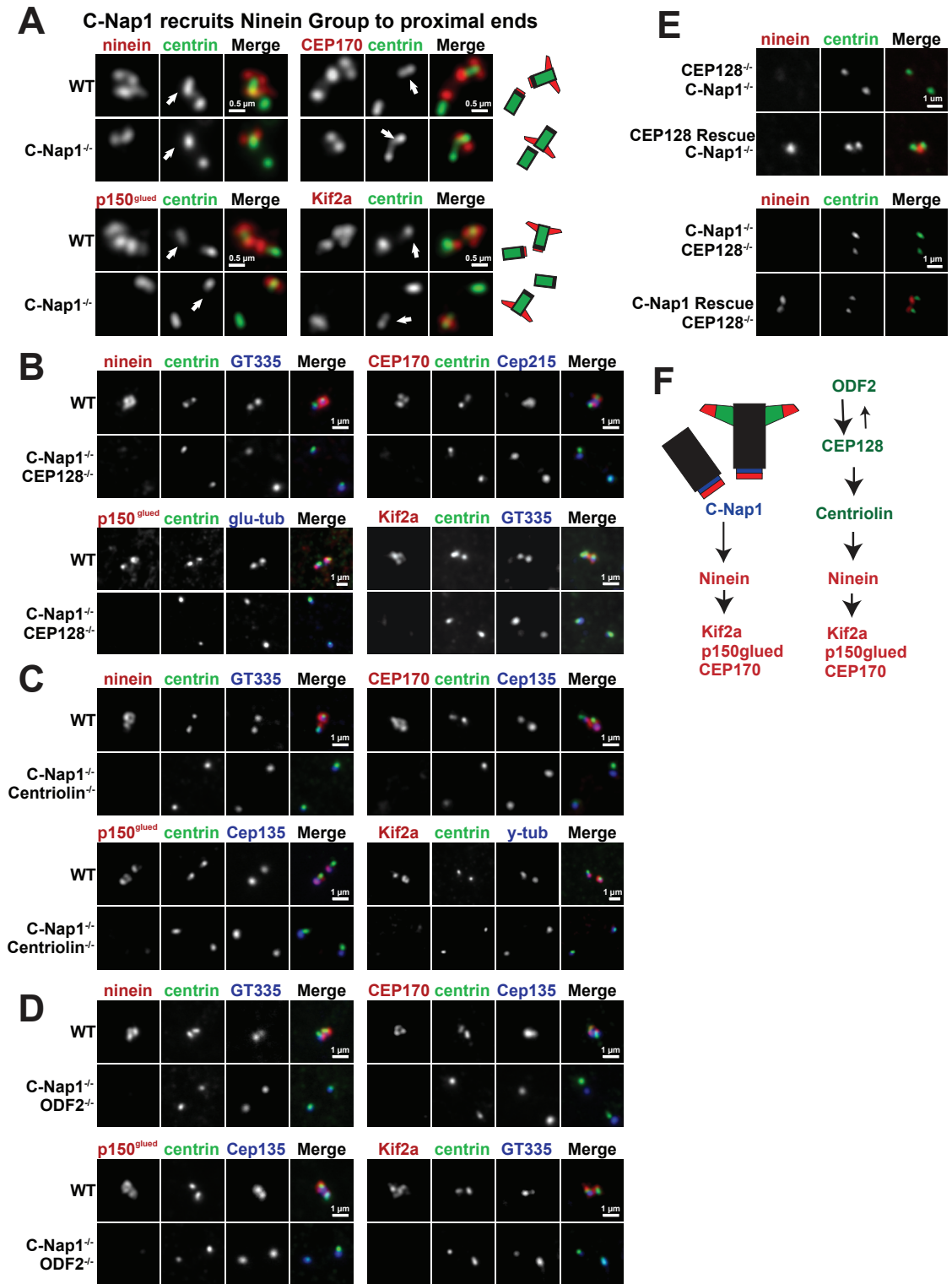
**Table 1**  
Sequence analyses of the mutation in each CRISPR knockout cell line generated in this study. Deleted nucleotide residues are depicted in red. Inserted nucleotides are depicted in green.

### **2.2.3 sDAP associated proteins are independently targeted to centriole proximal ends through C-Nap1**

Next, we examined the mechanism responsible for recruitment of ninein to centriole proximal ends. We reasoned that a protein located exclusively at the proximal ends of centrioles should mediate ninein localization. Among the candidates, C-Nap1, which localizes to proximal ends of both centrioles [162, 163], is essential for ninein recruitment. C-Nap1 depletion in CRISPR knockout cells resulted in displacement of all Ninein Group members from the proximal ends of centrioles without affecting their localization at sDAP (Figure 2.4A; >90%, n>100). C-Nap1 RNAi produced a similar effect in HeLa cells (Figure 2.3). To remove the Ninein Group from both ends of mother centrioles, we subsequently performed CRISPR targeting of each ODF2 Group protein in C-Nap1 knockout background. Loss of both C-Nap1 and any one ODF2 Group member resulted in displacement of the entire Ninein Group from both centrioles (Figure 2.4B-D). Note that ninein localization could be rescued (Figure 2.4F), confirming the specificity of our results. Taken together, our results suggest that sDAP-associated proteins, such as the Ninein Group and perhaps other molecules not yet identified, are independently targeted to both the distal and proximal ends of the mature mother centriole (Figure 2.4E). The underlying function, however, is unclear.

### **2.2.4 sDAP at mother centrioles are not essential for cilia assembly nor microtubule aster formation**

Previous work has suggested some involvements of sDAP in cilia assembly and cilia length control, although inconsistent results were also reported [6, 8, 95, 132, 136]. To verify, we examined the functions of subdistal appendages and sDAP-associated proteins using our CRISPR knockout cell lines. Surprisingly, in mutant cells where the ODF2 Group, Ninein Group, or both groups are removed from mother centrioles, cilia grew efficiently and had a similar average length to controls (Figures 2.5A-B). These results indicate that unlike the DAP which is required for ciliogenesis, the sDAP-associated proteins are dispensable for cilia assembly and cilia length. sDAP components have also been previously implicated in mediating microtubule anchorage/organization at the centrosome [70, 72, 77, 147, 154, 155]. Therefore, we expected to see a dramatic defect in microtubule organization in our sDAP mutant cells. However, to our surprise, grossly normal looking microtubule asters were seen to associate with nearly all centrosomes in our mutant cells, both at steady state and after a microtubule regrowth procedure (Figures 2.5C-D). Microtubule arrays looked entirely normal even when we mutated proteins previously implicated in microtubule organization (ODF2 and ninein) (Figures 2.5C-D). Additional attempts using siRNA or alternate CRISPR targeting sequences also failed to produce any detectable microtubule organization defect (data not shown). While we cannot rule out the presence of very subtle defects, these results suggest that at least in RPE1 cells, sDAP do not play an essential role in the formation of microtubule asters at the centrosome.



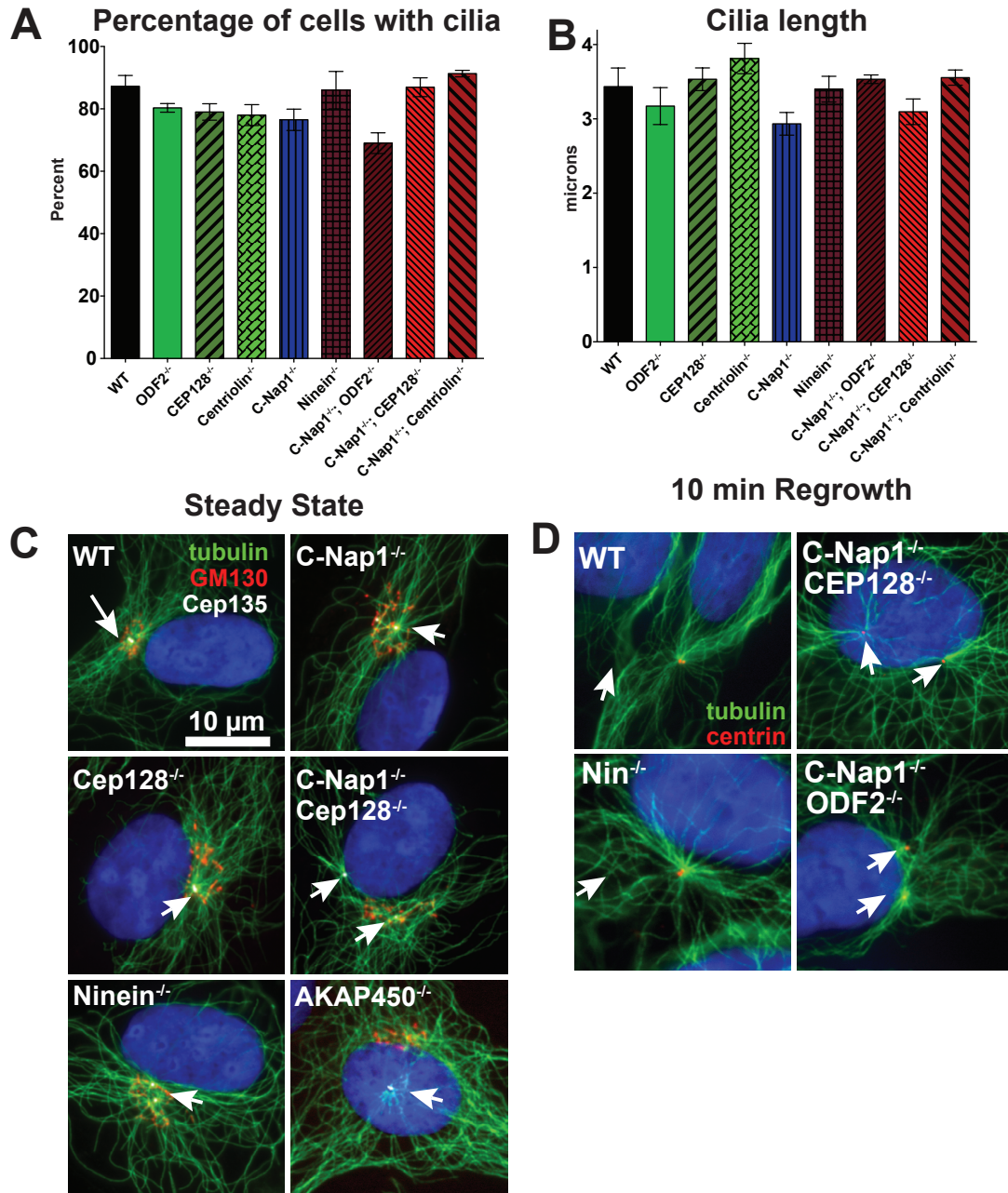
**Figure 2.4. Removal of sDPA-associated components from both ends of centrioles**

(A) C-Nap1 is necessary to target each member of the Ninein Group to the proximal ends of centrioles. WT or C-Nap1 knockout (KO) cells were stained with indicated antibodies. Arrows indicate the mature mother centrosome.

(B, C and D) The localization of each Ninein Group protein in RPE1 cell lines depleted of indicated proteins by CRISPR is shown.

(E) Rescue of ninein localization. CEP128 was exogenously expressed in RPE1 cells that lacked both endogenous CEP128 and C-Nap1. Also shown included the restoration of C-Nap1 expression in CEP128 and C-Nap1 double KO cells by a second round of CRISPR-mediated gene editing (see Experimental Procedures).

(F) A full schematic of the assembly hierarchy of sDAP components.



**Figure 2.5. C-Nap1 and sDAP depletion do not affect cilia formation or MTOC activity**

(A) The percentage of cells with cilia for each genotype is depicted. RPE1 cells were serum starved for 48 hours prior to fixation and staining with anti-acetylated tubulin antibodies. Bars represent average of three experiments (n>100 cells each) and error bars represent the standard deviation of the three experiments.

(B) Cilia length for each genotype. Bars represent average cilia length between three experiments (n>50 cilia each) and error bars represent the standard deviation.

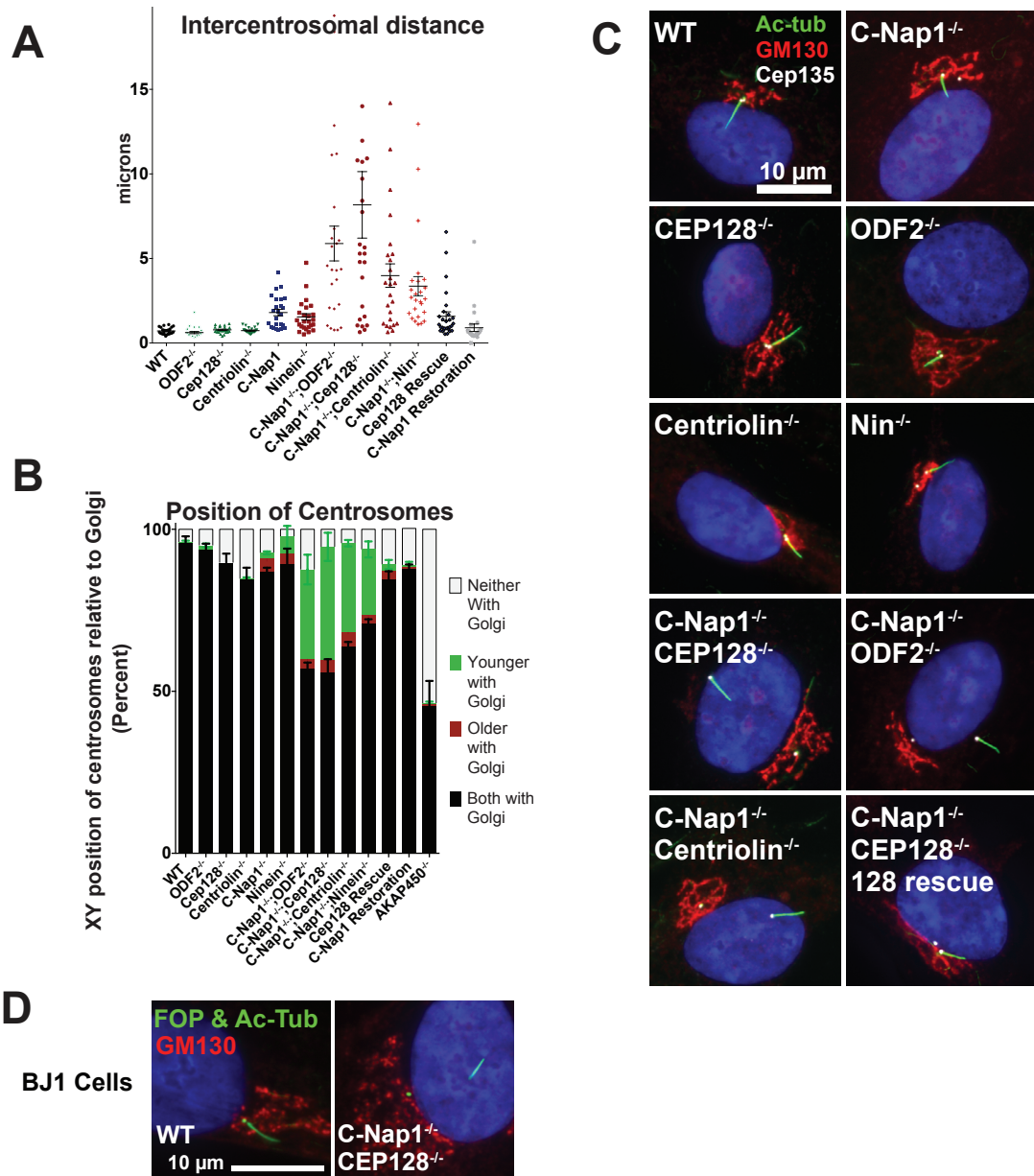
(C) Microtubule arrays in cells with indicated genotypes. White arrows point at the location of the centrosomes.

(D) After microtubule regrowth, microtubule arrays (green) are focused on the two centrosomes in both wild type and C-Nap1<sup>-/-</sup>; CEP128<sup>-/-</sup> double KO cells. White arrows point to the location of the centrosomes.



### **2.2.5 sDAP and C-Nap1 work together to establish intact centrosome cohesion**

In interphase cells, the two centrosomes are closely associated (about 1  $\mu\text{m}$  apart) through centrosome cohesion, mediated in part by C-Nap1 and ninein [163]. Consistently, loss of C-Nap1 or ninein in our knockout cells caused weakened centrosome cohesion allowing centrosomes to separate mildly ( $\sim 2 \mu\text{m}$  apart; [Figure 2.6A](#)). Centrosomes are described as “split” when the distance between them exceeds 2 microns [163]. The mild separation phenotype seen in C-Nap1 or ninein knockout cells suggests that other redundant mechanisms exist to keep centrosomes together. Intriguingly, while loss of any member ODF2 Group alone had no effect on centrosome cohesion ([Figure 2.6A](#)), when both C-Nap1 and a member of the ODF2 Group were mutated, centrosome cohesion was severely disrupted, leading to extreme centrosome separation ([Figure 2.6A](#)). In some cases, centrosomes were over 10 microns apart, placing them in opposite side of the cell or nucleus ([Figures 2.6A, C](#)). We were able to rescue centrosome cohesion by either exogenously expressing full length CEP128 in cells lacking both C-Nap1 and Cep128 ([Figure 2.6A](#)), or by restoring endogenous C-Nap1 expression through a second run of CRISPR gene editing that corrects the translational frameshift created by the 1<sup>st</sup> run ([Figure 2.6A](#); see [Experimental Procedures](#)). These results show that sDAP and C-Nap1 function together to ensure centrosome cohesion.



**Figure 2.6. C-Nap1 and sDAP depletion disrupts centrosome cohesion and Golgi-cilia association.**

(A) The intercentrosomal distances for 25 cells of each genotype are shown. Error bars represent the standard error of the mean. Cells were serum starved and stained with anti-gamma-tubulin antibodies to mark centrosomes for quantification.

(B) Cilia position in RPE1 cells of each genotype indicated is shown with acetylated-tubulin (green), GM130 (red), Cep135 (white) and DAPI (blue).

(C) Quantification of centrosome positions in the X-Y axis relative to the Golgi in each RPE1 lines. The relative position in the Z-axis is ignored. RPE1 cells were serum starved for 24 hours, and stained with markers against the centrosomes, the Golgi and distal appendage (as a marker of the older centrosome). >100 cells in each of three experiments were classified. Bars represent average of the three experiments and error bars represent the standard deviation of the three.

(D) Wild-type or mutant BJ1 cells knocked out of CEP128 and C-Nap1 by CRISPR were stained with indicated antibodies. Note that wild-type BJ1 cells proliferate poorly from a single cell, and thus could not survive the clonal selection process. C-Nap1<sup>-/-</sup>; CEP128<sup>-/-</sup> BJ1 cells were examined in the mixed population 6 days after CRISPR treatment. FOP (green) marks the centrosomes, acetylated tubulin (also green) marks the cilia, GM130 (red) marks the Golgi.

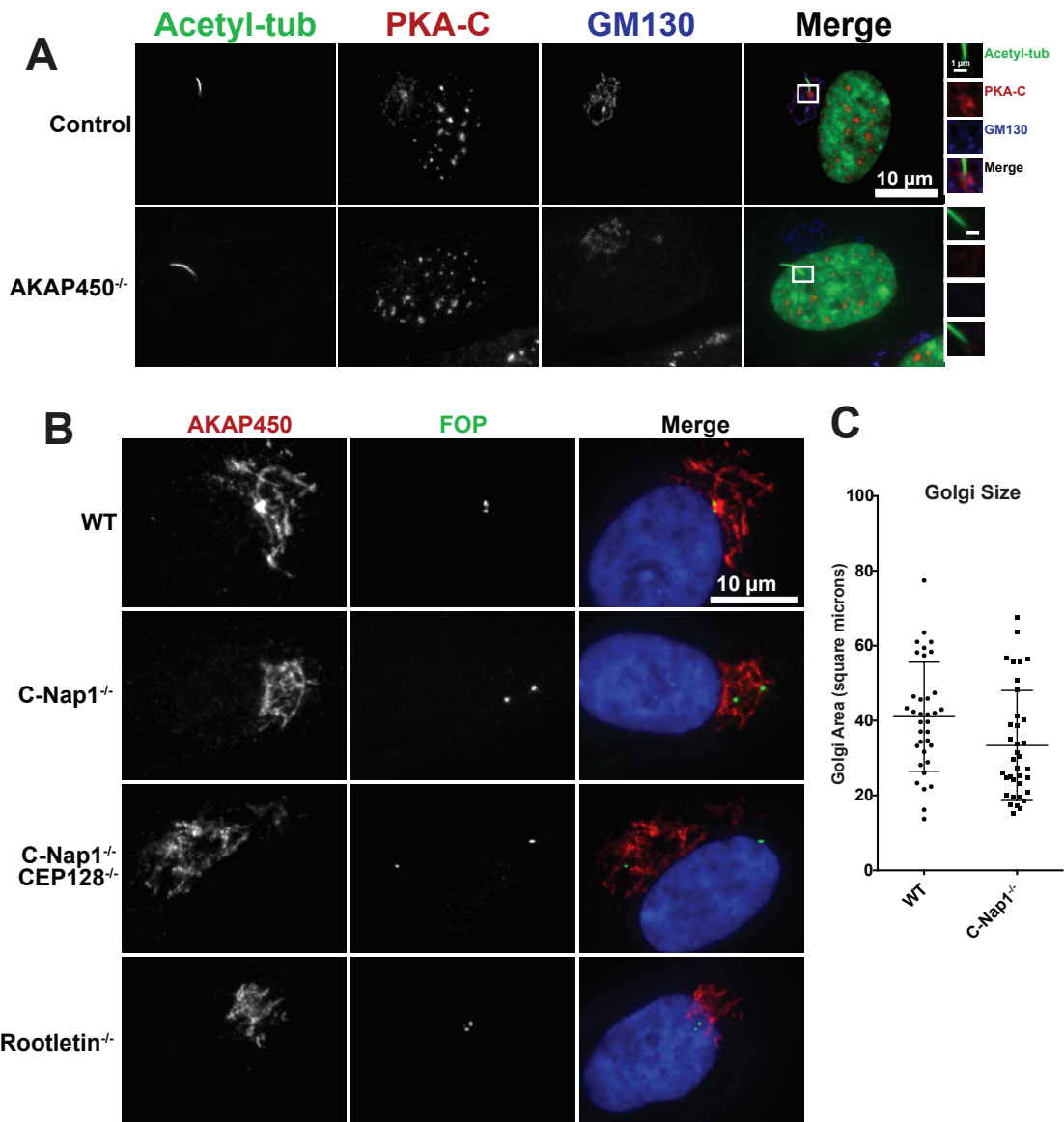
### **2.2.6 C-Nap1 and sDAP are required for stable association of ciliated centrosomes with the Golgi.**

Vertebrate centrosomes are normally associated with the Golgi apparatus [275], in turn bringing the two centrosomes in close vicinity. The purpose of this association is unknown but it might enhance the trafficking between cilia/centrosome and Golgi to facilitate cilia growth and maintenance. We reasoned that if two centrosomes are great distances apart, an intact Golgi could not simultaneously associate with both centrosomes. To test this hypothesis, we examined if centrosomes remain associated with the Golgi in each mutant cell line. Centrosome-Golgi association remained normal when the ODF2 Group, C-Nap1 or ninein was lost individually (Figures 2.6B, C). By contrast, when C-Nap1 and ODF2 were both absent, one centrosome frequently remained with the otherwise intact Golgi while the other centrosome was separate (Figures 2.6B, C). More interestingly, in 90% of the cases where the Golgi is associated with only one centrosome, it was the older, ciliated centrosome that was distantly positioned away from the Golgi (Figures 2.6B, C), while the other (younger/nonciliated) centrosome associated with the Golgi. The same pattern occurred when Cep128, centriolin or ninein was eliminated in the C-Nap1 knockout background (Figures 2.6B, C). Restoring either C-Nap1 or Cep128 expression in *C-Nap1<sup>-/-</sup>; CEP128<sup>-/-</sup>* double knockout cell lines rescued normal centrosome-Golgi association (Figures 2.6B, C). Depletion of the same proteins in non-transformed BJ1 cells using CRISPR resulted in a similar Golgi-cilia

separation phenotype, indicating that the function is not an idiosyncrasy of RPE1 cells (Figure 2.5H). Our results show that loss of both C-Nap1 and any member of the ODF2 Group (or ninein) can break the stable cilia-Golgi association. It is known that ciliary vesicles derived from the Golgi play a key role in ciliogenesis [138, 209, 221, 276], providing a potential reason why the Golgi is often closely associated with cilia. To our surprise, at least in RPE1 cells, the close cilia-Golgi association is neither essential for cilia formation nor for cilia length control.

Previous studies showed that expression of dominant-negative fragments of AKAP450, a protein localizing to both the Golgi and centrosome, impairs Golgi organization and centrosome-to-Golgi attachment [195]. Because of these results we decided to look for a connection between AKAP450, the sDAP and C-Nap1. Since many published conclusions regarding AKAP450 are based on fragment overexpression and not depletion, we first verified that previous AKAP450 results were reproducible. Consistent with the kinase anchor protein function of AKAP450, PKA no longer localized to the Golgi nor the centrosome in AKAP450 KO cell (Figure 2.7A). Also, consistent with published work, depletions of AKAP450 CRISPR prevented the Golgi from organizing microtubules and caused the Golgi to separate from centrosomes (Figure 2.5C, 6B) [195, 277]. We found that AKAP450 localized normally to the Golgi apparatus in all of our C-Nap1<sup>-/-</sup>;Cep128<sup>-/-</sup> cells, regardless of whether or not the Golgi was stably associated with cilia (Figure 2.7B). However, C-Nap1 and rootletin were required for centrosomal localization of AKAP450. Despite the loss of AKAP450 from centrosomes, C-Nap1 or rootletin mutation alone had no effect on Golgi-cilia

association (Figure 2.7B; Figures 2.6B, C). Therefore, AKAP450's function in Golgi-centrosome association must be mediated through Golgi targeted AKAP450, consistent with previous work [195]. Despite the link between AKAP450 and C-Nap1, AKAP450 mutation alone only cause separation of centrosome from Golgi and did not cause centrosome splitting (Figure 2.8D). Contrary to published work [175], Golgi size was no larger in C-Nap1 mutant cells than controls (Figure 2.7C). Thus, the Golgi-cilia detachment phenotype seen in our double mutant cells is not a result of non-specific disruption of the Golgi organization through AKAP450 or through C-Nap1.



**Figure 2.7. AKAP450 localizes normally to the Golgi in C-Nap1<sup>-/-</sup>; CEP128<sup>-/-</sup> double mutant cells**

(A) Wild type and AKAP450<sup>-/-</sup> cells are staining with antibody against PKA-C catalytic subunit as well as the indicated markers of cilia, Golgi and nuclei.

(B) AKAP450 depicted in red. RPE1 cells with indicated genotypes were stained with indicated antibodies. Note that the centrosomal localization of AKAP450 is lost in C-Nap1 knockout and Rootletin knockout cells.

(C) Scatterplot of Golgi Area based on GM130 staining in C-Nap1 mutant and Wild Type RPE1 cells, showing that Golgi area is similar.

### **2.2.7 The Golgi does not contribute to centrosome cohesion.**

As mentioned earlier, centrosomes in the absence of C-Nap1 remain about 2 microns apart despite having no physical linker between them. Given that several mutants simultaneously break that 2-micron limit and centrosome-Golgi attachment, we speculated that associated with the Golgi apparatus indirectly linked the two centrosomes, keeping them close. To test this hypothesis, we treated C-Nap1<sup>-/-</sup> cells with Brafeldin A, a drug that causes collapse of the Golgi. Despite lack of an observable Golgi, the two centrosomes remained about 3-5 microns apart (Figure 2.8A), suggesting that Golgi attachment is not required to keep the two centrosomes close. In contrast, treatment of C-Nap1<sup>-/-</sup> cells with nocodazole (ultimately depolymerizing the microtubule array) caused extreme centrosome splitting (Figure 2.8A). Therefore, in the absence of a centrosomal linker, the microtubule array but not the Golgi keeps the centrosomes in the same location.

### **2.2.8 The sDAP does not function to maintain the linker.**

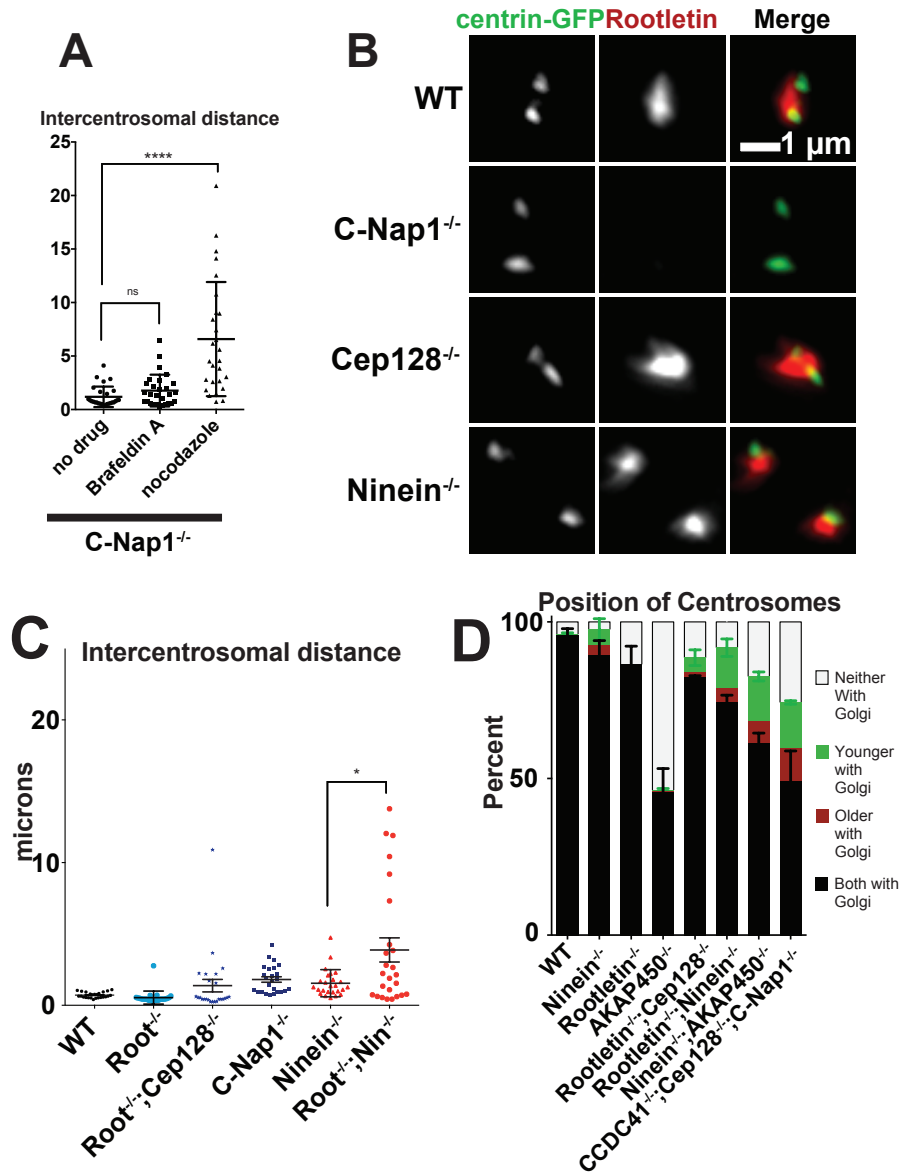
C-Nap1 is believed to mediate centrosome cohesion by recruiting rootletin, a component of the intercentrosomal linker. Since depletion of ninein caused a similar centrosome splitting to C-Nap1, we checked if ninein functioned in rootletin linker assembly. Unlike, C-Nap1<sup>-/-</sup> cells, centrosomes in ninein<sup>-/-</sup> cells still had rootletin as did WT and CEP128<sup>-/-</sup> cells (Figure 2.8B). Interestingly, rootletin localized into two masses in ninein mutant cells formed, rather than forming a link between centrosomes. sDAP proteins do not function as C-Nap1

does in linker assembly.

### **2.2.9 Simultaneous mutation of Rootletin linker and sDAP does not produce the phenotypes characteristic of C-Nap1-sDAP mutants.**

Among our most surprising observations is the extreme centrosome splitting phenotype produced by depletion of both C-Nap1 and any one of several sDAP proteins. We sought to better understand why this synthetic effect existed. As C-Nap1 functions in the formation of the intercentrosomal linker, we speculated that simultaneous loss of the linker and the sDAP might contribute to this phenotype. This was not the case as *Rootletin<sup>-/-</sup>;CEP128<sup>-/-</sup>* mutants did not show extreme centrosome splitting (Figure 2.8C) nor separation of centrosomes from Golgi (Figure 2.8D). Although *Rootletin<sup>-/-</sup>;ninein<sup>-/-</sup>* cells did show an increase in centrosome-Golgi separation and extreme centrosome splitting (Figure 2.8C-D), the strength of the phenotype was mild compared to that of *C-Nap1<sup>-/-</sup>;CEP128<sup>-/-</sup>* cells. The phenotypes of *C-Nap1<sup>-/-</sup>; CEP128<sup>-/-</sup>* mutants cannot be explained by a loss of linker. Interestingly, *Rootletin<sup>-/-</sup>* mutation alone did not produce as severe a centrosome splitting as depletion of C-Nap1 (Figure 2.8C), suggesting that C-Nap1 might promote centrosome cohesion by rootletin-independent mechanisms.





**Figure 2.8. Neither intercentrosomal linker loss alone nor Golgi detachment alone can help recapitulate the centrosome cohesion defects in C-Nap1 and sDAP mutants**

(A) Intercentrosomal distance in C-Nap1 mutant cells treated with indicated drugs (5ug/ml nocodazole; 10ug/ml Brafeldin A) are plotted

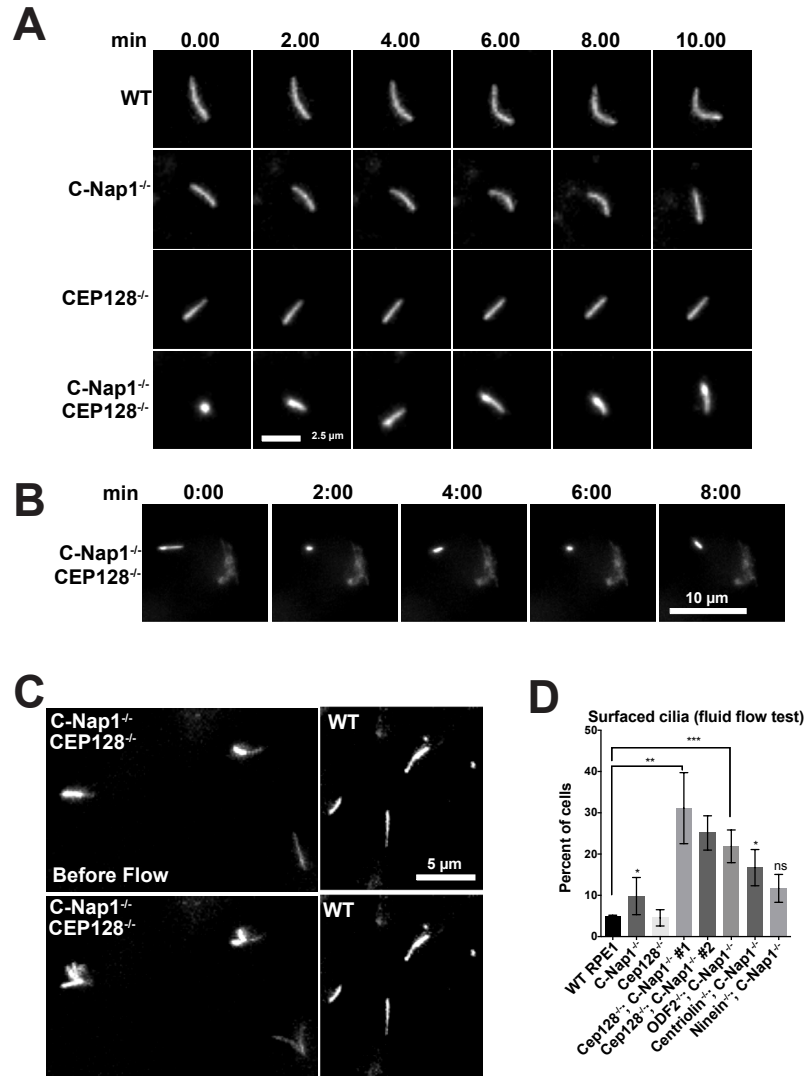
(B) Rootletin staining (red) is shown from cells of indicated genotypes is shown.

(C) The intercentrosomal distances for 25 cells of each genotype are shown. Error bars represent the standard error of the mean. RPE1 cells were serum starved and stained with anti gamma-tubulin antibodies to mark centrosomes for quantification.

(D) Quantification of centrosome positions in the X-Y axis relative to the Golgi in each RPE1 lines. The relative position in the Z-axis is ignored. RPE1 cells were serum starved for 24 hours, and stained with markers against the centrosomes, the Golgi and distal appendage (as a marker of the older centrosome). >100 cells in each of three experiments were classified. Bars represent average of the three experiments and error bars represent the standard deviation of the three.

**2.2.10 *C-Nap1*<sup>-/-</sup>; *CEP128*<sup>-/-</sup> double mutant cells grow surfaced cilia capable of responding to fluid flow with motion.**

Cilia form with normal frequency and length in *C-Nap1*<sup>-/-</sup>; *CEP128*<sup>-/-</sup> double mutant cells, despite not associating with the Golgi. To examine if these cilia behave differently in ways that cannot be easily detected in fixed cells, live cell imaging was performed. Wild-type or mutant cells were induced to express Arl13b-GFP to mark the cilia, and filmed by time lapse microscopy for hours. Cilia in wild-type, *C-Nap1*<sup>-/-</sup> knockout, or *CEP128*<sup>-/-</sup> knockout cells behaved similarly, exhibiting a confined, leisurely motion, rarely changing direction and remained parallel to the XY plane (Figure 2.9A; Movie 1), consistent with them being submerged. On the contrary, cilia in *C-Nap1*<sup>-/-</sup>; *CEP128*<sup>-/-</sup> double mutant cells had frequent episodes of erratic motion in which the cilia changed direction randomly, often pointing along the Z-axis (Figure 2.9A; Movie 2), a pattern nearly unseen in wild-type RPE1 cells. Moreover, live-cell imaging also confirmed that the wide-range motion of cilia occurred while cilia were detached from the Golgi (Figure 2.9B; Movie 3). These observations suggest that the cilia formed in double mutant cells are not trapped in a deep membrane invagination. A trapped cilium could never move so freely. To further test the idea, we examined the bending of the cilium in response to fluid flow; a mechanical force that can only reach surfaced cilia. As expected, cilia in wild-type RPE1 cells were stationary, showing no bending when fluid was pumped over cells, consistent with being submerged (Figures 2.9C- D; Movie 4 and 5).



**Figure 2.9. Cilia mobility and position are altered upon depletion of sDAP and C-Nap1**

(A) Still images extracted from long time-lapse movies of indicated RPE1 cell lines expressing Arl13b-GFP. Row labels indicate genotypes of the imaged cells. Column labels indicate the time intervals (in minutes). Each row represents time lapse. The movie for WT or C-Nap1<sup>-/-</sup>; CEP128<sup>-/-</sup> mutant cells was provided (see Movie 1 and 2).

(B) Still frames from long time-lapse movies of C-Nap1<sup>-/-</sup>; CEP128<sup>-/-</sup> double knockout cell lines expressing both Arl13b-GFP and GalT-GFP, a Golgi marker (see Movie 3). Note that cilia showed wide-range motion while detach from the Golgi.

(C) Fluid was pumped over the cultured cells during the time lapse imaging of Arl13b-GFP expressing RPE1 cells. Frames from a short time-lapse movie (10 seconds) are shown. Genotypes of the imaged cells are indicated. Images taken before and during fluid flow are shown. Note that cilia fluttered upon flow activation (see Movie 4 and 5).

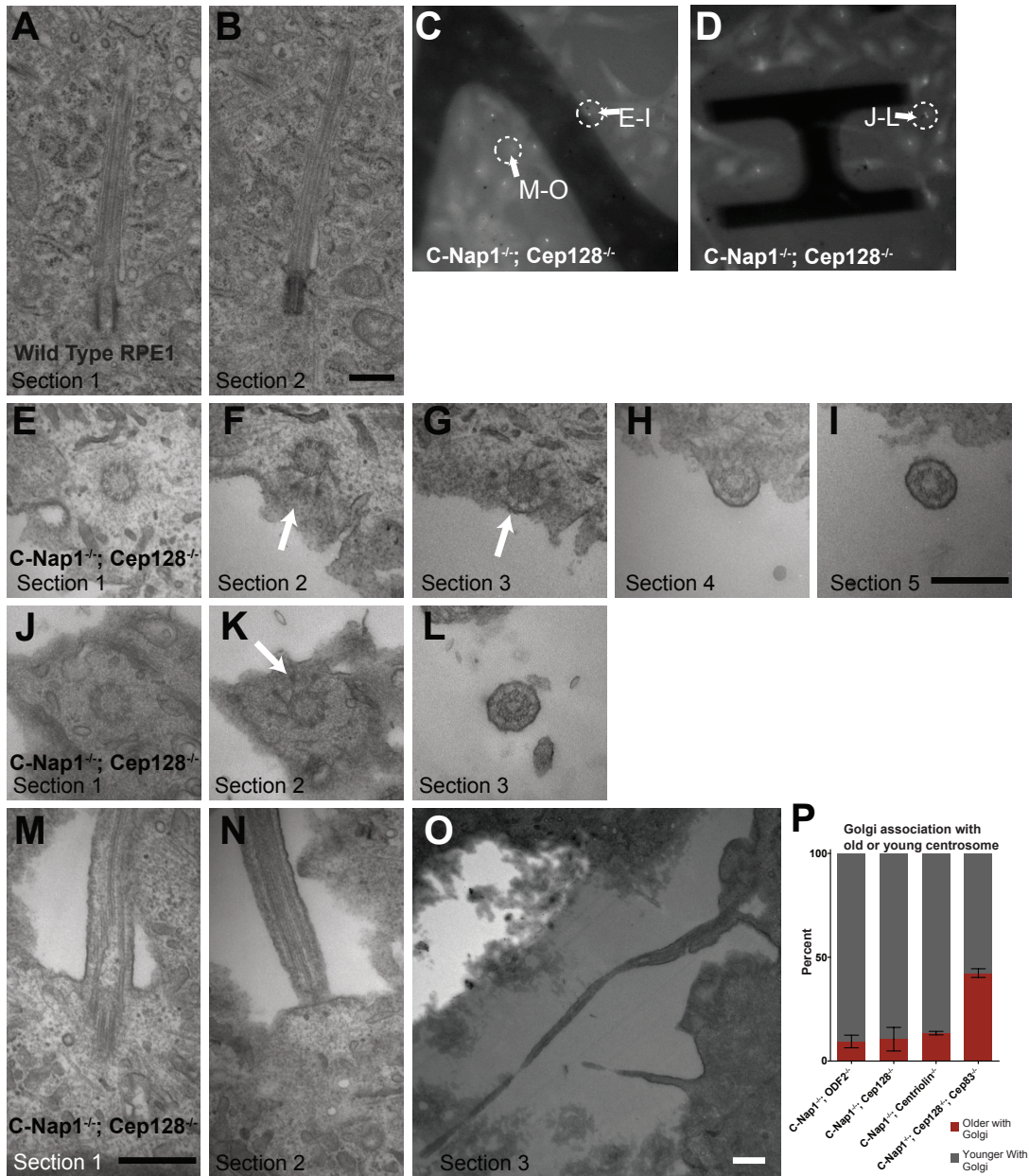
(D) The percentage of cilia that respond to fluid flow in WT or indicated mutant cell lines. The average of 3-4 independent experiments is shown. Two independently derived clones of C-Nap1<sup>-/-</sup>; CEP128<sup>-/-</sup> mutant cells (#1 & #2) were analyzed. 100-150 cells were scored to determine percentage in each of 3-4 separate experiments. Error bars represent the standard deviations.

In contrast, about 25-32% of cilia in *C-Nap1*<sup>-/-</sup>; *CEP128*<sup>-/-</sup> cells, 23% in *C-Nap1*<sup>-/-</sup>; *ODF2*<sup>-/-</sup> and 17% of *C-Nap1*<sup>-/-</sup>;centriolin<sup>-/-</sup> cells fluttered violently in response to fluid flow (Figures 2.9C-D; Movie 5), strongly suggesting that these cilia project from the apical cell surface. Similar behaviors were seen in independently derived clones of cells (Figure 2.9D). However, unlike the other three double mutants mentioned, the percentage of *C-Nap1*<sup>-/-</sup>; *Nin*<sup>-/-</sup> cilia that responded to fluid flow, did not significantly differ from *C-Nap1*<sup>-/-</sup> single mutant cells (Figure 2.9D).

#### **2.2.11 *C-Nap1*<sup>-/-</sup>; *CEP128*<sup>-/-</sup> double mutant cells grow cilia not trapped in a deep membrane invagination**

To further characterize cilia position in detail, serial sectioning transmission electron microscopy (TEM) was performed. TEM analyses confirmed that wild-type RPE1 cilia are submerged in a deep membrane invagination (the ciliary pit) surrounded by cytoplasm (100%, n=16) (Figures 2.10A-B). In *C-Nap1*<sup>-/-</sup>; *CEP128*<sup>-/-</sup> double mutant cells, however, some cilia respond to flow and others do not. We thus used correlated light and electron microscopy (LM/EM) to explore why these cilia behave differently (Figures 2.10C-D; Movie 6 and 7). LM/EM analyses showed that flow-sensitive cilia indeed projected from the apical cell surface (n=5/5), lacking a detectable ciliary pit, with the centriole docked to the plasma membrane via distal appendages (Figures 2.10E-I and 2.10J-L) and the axoneme growing from the edge of the cell into the environment (Figures 2.10E-I and 2.10J-L). Surprisingly, in addition to

flow-sensitive cilia, we found that cilia that are non-responsive to flow also lacked intact ciliary pits (n=2/2) (Figures 2.10M-O); these cilia, instead of protruding from the apical surface, were found to grow out of the basal surface, where they were trapped in a cavity devoid of cytoplasm underneath the cell (Figures 2.10M-O), consistent with their static behavior in response to fluid flow. We hypothesized that the physical anchoring of the ciliated centrosome to the plasma membrane at the cell surface can perhaps explain why only the non-ciliated (or daughter) centrosome can “freely” stay at the cell center with the Golgi (Figure 2.6F, G). Indeed, consistent with this prediction, when ciliogenesis (membrane docking) was disrupted by abolishing the DAP component CEP83 in *C-Nap1<sup>-/-</sup>; CEP128<sup>-/-</sup>; CEP83<sup>-/-</sup>* triple knockout cells, we found that the biased association between the Golgi and daughter centrosomes disappeared (Figure 2.10P). Together, these results indicate that factors from both distal and proximal ends of centrioles are required to maintain the normal morphology of the ciliary pit.



**Figure 2.10 Loss of the deep ciliary pit in *CEP128*<sup>-/-</sup>; *C-Nap1*<sup>-/-</sup> double knockout cells**

(A and B) Two serial TEM sections of a wild type RPE1 cell carrying a submerged cilium buried in a deep membrane invagination. Scale bar represents 500nm.

(C and D) Still light microscopy images of *C-Nap1*<sup>-/-</sup>; *CEP128*<sup>-/-</sup> double knockout cells carrying either flow-sensitive or insensitive cilia, extracted from time-lapse movies (see Movie 6 and 7). Arrows mark the cells that were processed for TEM and shown in panels below as indicated.

(E, F, G and I) LM/EM analyses of a flow responsive cilium from *C-Nap1*<sup>-/-</sup>; *CEP128*<sup>-/-</sup> double mutant cells. A series of successive EM sections revealed that the cilium was at the apical surface. Section 1 contained the centriole. Section 2 and 3 showed visible distal appendages (arrows) with tip of centriole clearly on edge of the cell while the immediate next two sections showed the ciliary axoneme clearly outside of the cell. Scale bar represents 500nm.

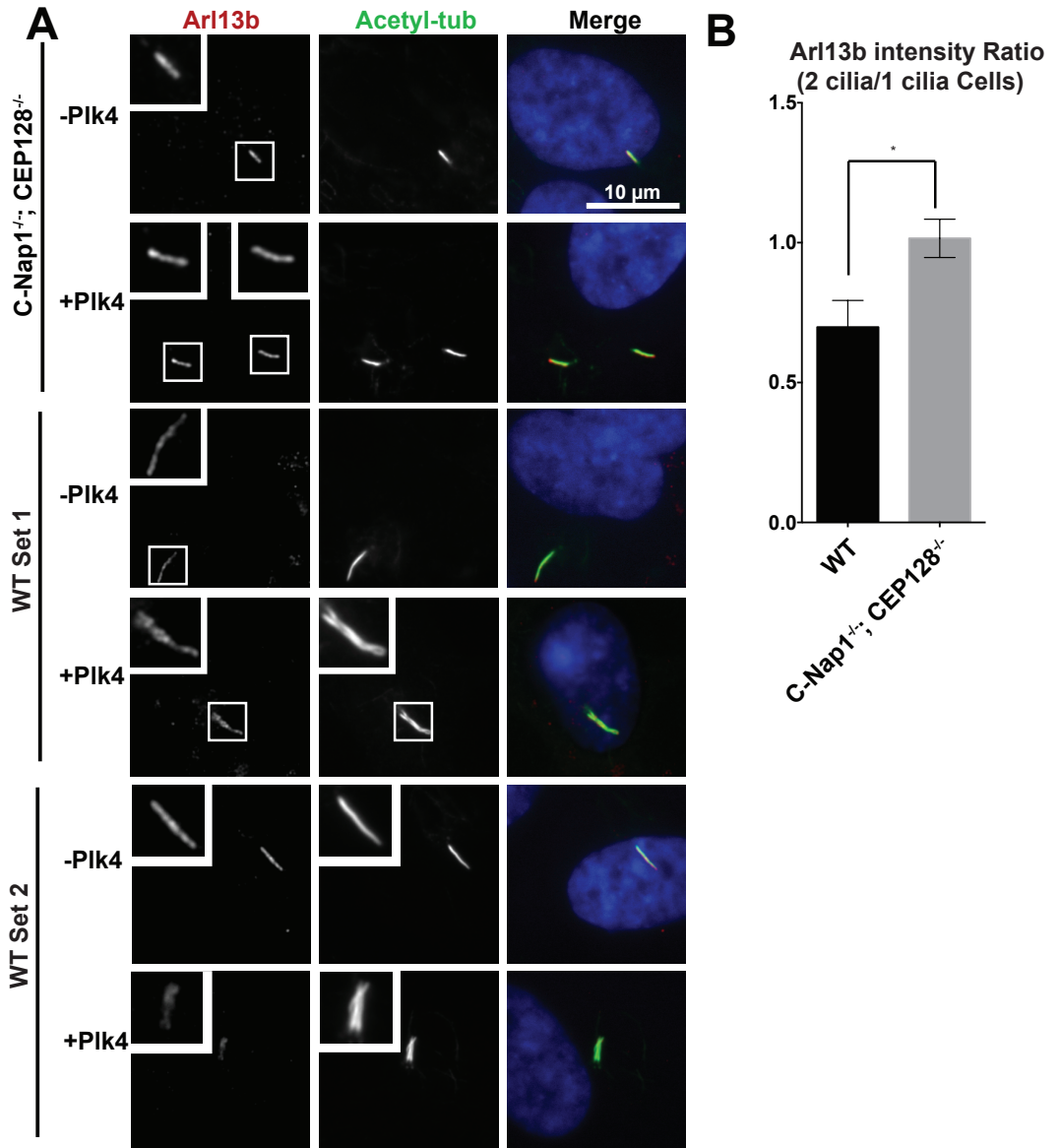
(J, K and L) A series of EM sections of another *C-Nap1*<sup>-/-</sup>; *CEP128*<sup>-/-</sup> double mutant cilium that had been shown to respond to fluid flow under time-lapse microscopy. Sections 1 and 2 showed the distal end of the centriole while section 3 showed an axoneme outside the apical cell surface. Scale bars represent 500nm.

(M and O) Serial EM sections of a *C-Nap1*<sup>-/-</sup>; *CEP128*<sup>-/-</sup> double mutant cilium that could not respond to flow. Section 1 and 2 showed that the deep ciliary pit is disrupted, while sections 3 at a lower magnification showed that the rest of the cilium was trapped below the cell, outside of the basal cell surface. All scale bars are 500nm.

(P) The biased separation of the older/ciliated centrosome from the Golgi depends on CEP83. Quantification shows the percentage of the indicated mutant cell lines in which the older or younger centrosome associates with the Golgi. Numbers were collected from cells in which the two centrosomes are distantly separated and only one is associated with the Golgi. Older centrosomes in *C-Nap1*<sup>-/-</sup>; *CEP128*<sup>-/-</sup>; *CEP83*<sup>-/-</sup> triple KO cells were identified by ODF2 staining. Error bars represent standard deviations. Data of *C-Nap1*<sup>-/-</sup>; *ODF2*<sup>-/-</sup>, *C-Nap1*<sup>-/-</sup>; *CEP128*<sup>-/-</sup> and *C-Nap1*<sup>-/-</sup>; *CNTRL*<sup>-/-</sup> double KO cells are extracted from Figure 2.6.

## **2.2.12 Loss of deep ciliary pit allows multiple intact cilia to form individually in the same cell**

Over-duplication of centrosomes in RPE1 cells can lead to the production of multiple cilia that are clustered in the same ciliary pit [278]. These clustered cilia are diluted of membrane-bound components and therefore functionally compromised as compared to a solitary cilia that is not in a cluster [278] (Figure 2.11). This reveals that the deep ciliary pit, while important in some cell types, could be a liability for multi-ciliated cells [278]. To test whether loss of the ciliary pit can liberate cilia and allow multiple cilia to form with undiluted membrane components, we induced centrosome over-duplication in *C-Nap1*<sup>-/-</sup>; *CEP128*<sup>-/-</sup> double mutant cells (which lack a proper ciliary pit) (Figures 2.12A and B).

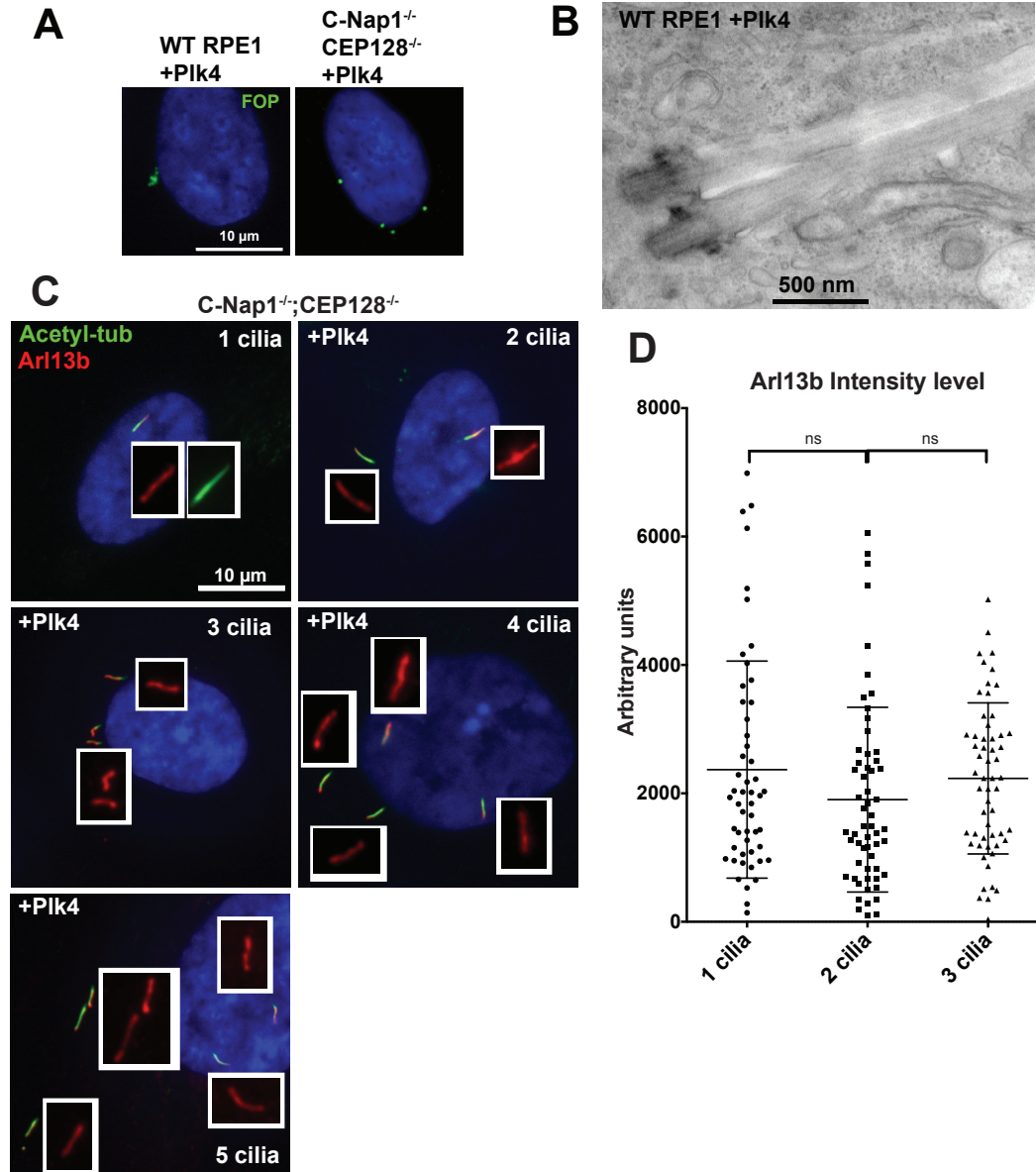


**Figure 2.11. Dilution of Arl13b in cells with two clustered cilia.**

(A) Multiple cilia formed in wild type RPE1 cells were clustered and diluted of Arl13b while multiple cilia in *CEP128*; *C-Nap1* double knockout cells were distantly separated with undiluted Arl13b. Two sets of images for wild type cells are shown. Multiple cilia formation in the same cell was induced by overexpression of the PLK4 kinase, followed by 48 hours of serum starvation. Cells were stained with indicated antibodies.

(B) Quantification of Arl13b intensity. Mean value of Arl13b intensity in regions surrounding cilia was taken. Plot displays a ratio of Arl13b intensity per cilia in bi-ciliated (clustered or separated) cells over single ciliated cells. The bar lengths are an average of three independent experiments (n=10-20 cilia). Error bars represent standard deviation among the three. Significance was determined by unpaired two-tailed t-test with Welch's correction ( $p < 0.05$ ).





**Figure 2.12. Loss of the deep ciliary pit allows multiple intact cilia to form with undiluted membrane composition in one cell**

(A) Indicated RPE1 cell lines were infected with lentiviral vectors carrying tet-inducible PLK4 expression construct and induced to overexpress PLK4. Doxycycline was applied to cells for 2 days before examination. FOP (green) marks centrosomes. Wild type RPE1 cells have centrosomes cluster in a small area. In contrast, centrosomes are well separated in the *CEP128*<sup>-/-</sup>; *C-Nap1*<sup>-/-</sup> double KO cells.

(B) EM images of two clustered cilia that grew from two centrosomes in the same ciliary pit. PLK4 was expressed in wild type RPE1 cells to induce formation of extra centrosomes before serum starvation and preparation for TEM.

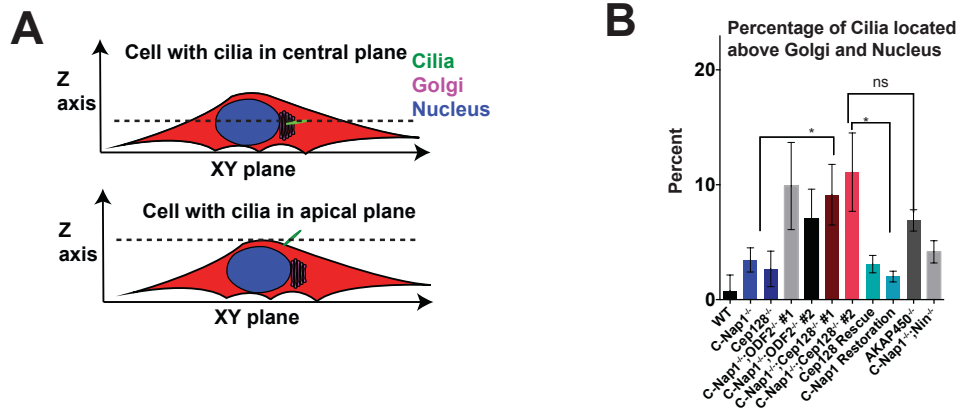
(C) Multiple cilia in *CEP128*<sup>-/-</sup>; *C-Nap1*<sup>-/-</sup> double knockout cells were distantly separated with undiluted Arl13b. Multiple cilia formation in the same cell was induced by overexpression of the PLK4 kinase, followed by 48 hours of serum starvation. Cells were stained with indicated antibodies.

(D) Quantification of Arl13b intensity. Mean value of Arl13b intensity in regions surrounding cilia was taken. Plot displays Arl13b intensity per cilia in bi-ciliated or tri-ciliated cells. Error bars represent standard deviations.

While overexpression of PLK4 in wild-type RPE-1 cells drove the formation of clustered centrosomes and cilia (Figures 2.12A left; Figures 2.12B), such was not the case in mutants. In *C-Nap1*<sup>-/-</sup>; *CEP128*<sup>-/-</sup> cells, multiple individual centrosomes or cilia at distinct locations were formed and maintained (Figures 2.12A right and Figures 2.12C). The distance between these cilia indicates that they are not physically linked. Furthermore, cilia growing in separate locations in the same cell had full levels of Arl13b (Figures 2.12C-D), similar to that seen in the single primary cilium. Together, our observations suggest that forming a ciliary pit is not essential for trafficking of ciliary membrane components (such as Arl13b), neither for cilia assembly nor for length control. Instead, C-Nap1 and sDAP function to confine primary cilia in deep pits in specific cell types. Confinement of multiple cilia in a shared, deep cavity can negatively impact the function of cells that carry more than one cilia (such as olfactory neurons).

### **2.2.13 Abnormally positioned cilia at the apical cell surface results in ectopic accumulation of Hedgehog signaling components.**

We next examined if cilia composition changes upon changes in cilia position. Submerged cilia are found in the same focal plane as the Golgi and nucleus while surfaced cilia are often at the top of cells (Figure 2.13A), making it possible to distinguish likely surfaced from likely submerged cilia. However, only a small percentage of surfaced cilia can be identified as surfaced using this method. The same mutations that caused cilia to separate from the Golgi and



**Figure 2.13. Apically surfaced cilia can be identified with light microscopy based on the focal plane of the cilia.**

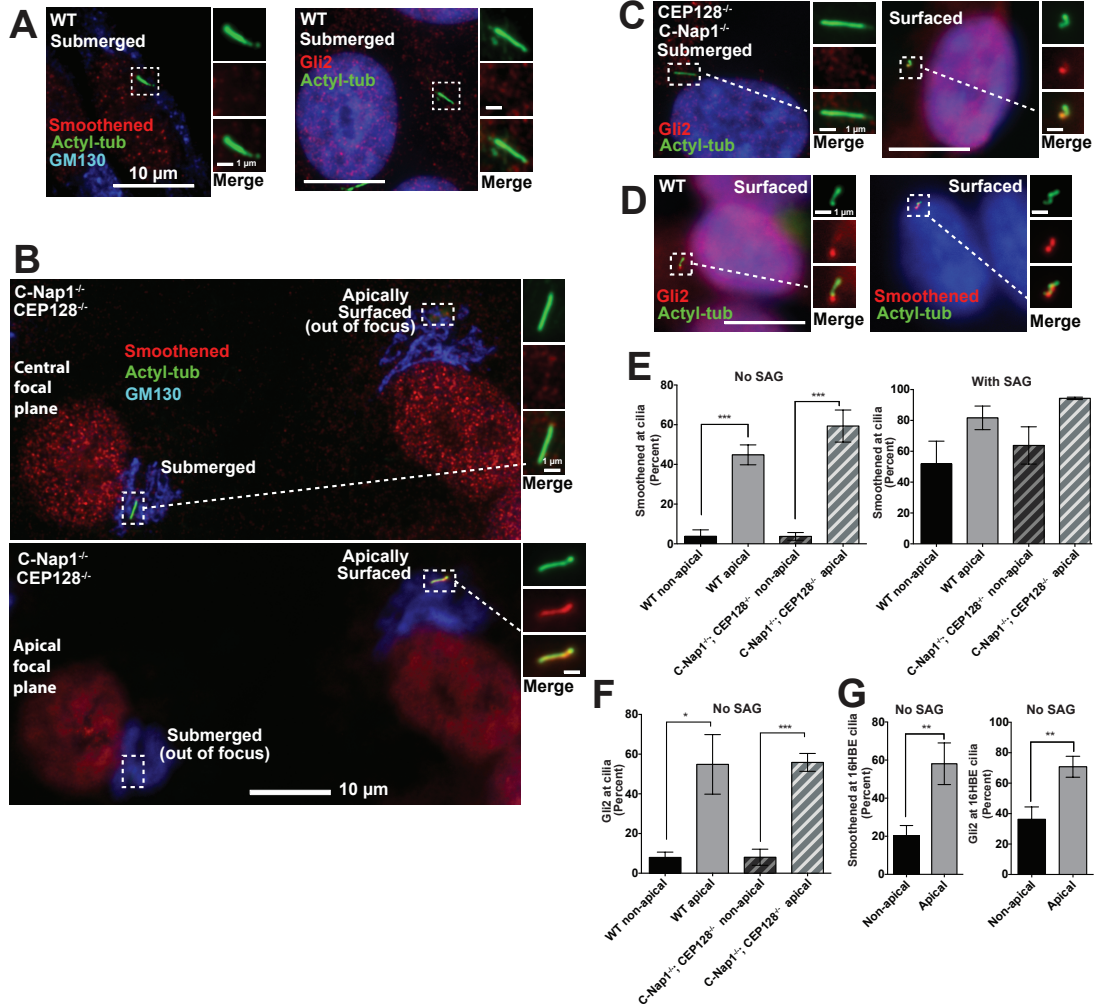
(A) Cartoon depicting submerged or apically surfaced cilia in fixed RPE1 cells guided by the relative position between the cilia, Golgi, and nucleus. Only the cilia positioned at an apical focal plane not overlapping with the Golgi or nucleus were considered “apically surfaced”. Cilia at the same focal plane with the Golgi and nucleus were considered submerged.

(B) Percentage of cells in cells of each genotype that were “apically surfaced” is plotted. N>100 cells were counted for 3 replicates of each cell line. Error bars represent the standard deviations. Wild-type RPE1 cilia are mostly submerged, with only 1-2% surfaced apically. In contrast, apical cilia can be easily found in *CEP128*<sup>-/-</sup>; *C-Nap1*<sup>-/-</sup> double knockout cells.

respond to fluid flow also put a fraction of cilia in an elevated focal plane (Figure 2.13B). The same mutations that caused cilia to separate from the Golgi and respond to fluid flow also put a fraction of cilia in an elevated focal plane (Figure 2.13B). Using the focal plane method, we found that submerged cilia in both wild-type and *C-Nap1*<sup>-/-</sup>; *CEP128*<sup>-/-</sup> mutant RPE1 cells, mostly lacked Hedgehog signaling components Smoothed and Gli2 (Figures 2.14A, 2.14B and 2.14E), unless treated with the Smoothed agonist (SAG) (Figure 2.14E). In striking contrast, apically surfaced cilia in *C-Nap1*<sup>-/-</sup>; *CEP128*<sup>-/-</sup> mutant cells, identified by their location at a focal plane above the nucleus and Golgi (Figures 2.14B-C), frequently accumulated Smoothed and Gli2 even in the absence of SAG (Figures 2.14B, C and E). Moreover, in the 1-2% of wild-type RPE1 cells in which cilia were apically surfaced (Figure 2.14D), as identified by their location above the Golgi and nucleus, similar accumulations of Smoothed or Gli2 were observed (Figures 2.14D-F). To further confirm the link between apical cilia and

Smoothened accumulation, we examined 16HBE cells, a human bronchial epithelial cell line. Prior to forming a fully polarized monolayer, 16HBE cells frequently grew submerged cilia that were mostly devoid of Smoothened and Gli2 (Figure 2.14G). After polarization, 16HBE cells were found to form surfaced cilia that accumulated high levels of Smoothened or Gli2 in the absence of SAG (Figure 2.14G).

The accumulations of Smoothened and Gli2 in surfaced cilia were also seen in *C-Nap1<sup>-/-</sup>; ODF2<sup>-/-</sup>* cells as well as in BJ5, a fibroblast cell line in which about 10% of cilia are apically surfaced (Figure 2.15A-B). Importantly, Smoothened enrichment at surfaced cilia is seen in Triton-extracted, methanol fixed cells, suggesting that the pattern is unlikely due to a difference in antigen accessibility (Figure 2.15D). To further rule out antigen accessibility issues, we expressed Smoothened-GFP (Smo-GFP) in *C-Nap1<sup>-/-</sup>; CEP128<sup>-/-</sup>* mutant cells. Under these conditions, overexpressed Smo-GFP was seen in most cilia, but more Smo-GFP was observed in surfaced cilia (Figure 2.15C), consistent with our observations using the endogenous Smoothened. Thus, the properties of primary cilia can be altered through spatial changes in the ciliogenesis, a previously unreported type of regulation. In summary, our work identified redundant functions of the sDAP and the proximal end factor C-Nap1 in centrosome cohesion, cilia-to-Golgi association, and ciliary pit maintenance, all spatial properties of ciliogenesis.



**Figure 2.14. Apically surfaced cilia can ectopically recruit Smoothened and Gli2 in the absence of agonist.**

(A) Wild-type RPE1 cilia are devoid of Smoothened (left) and Gli2 (right) in the absence of SAG.

(B) Two *CEP128*<sup>-/-</sup>; *C-Nap1*<sup>-/-</sup> mutant cells in the same field, one carrying apically surfaced cilia (right) and the other submerged cilia (left), were stained with Smoothened, cilia, and Golgi antibodies as indicated. At the central focal plane (top panel), submerged cilia, the Golgi and nucleus were in focus. At the apical focal plane, only surfaced cilia was in focus (bottom panel, right).

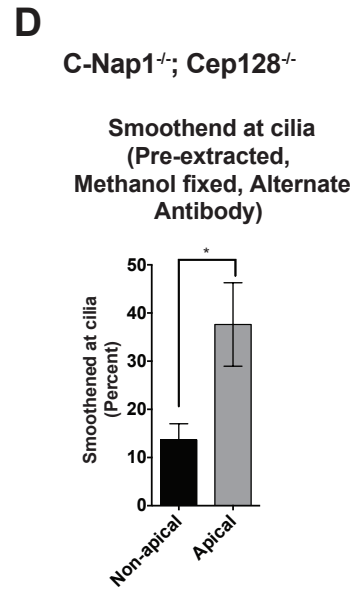
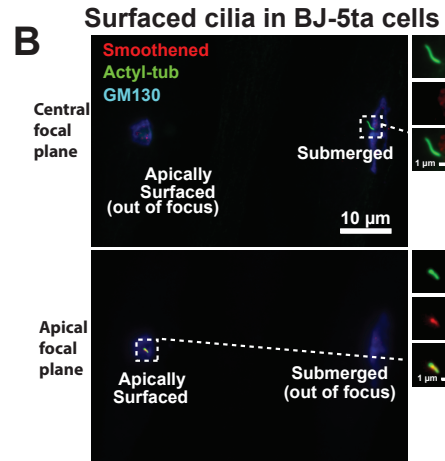
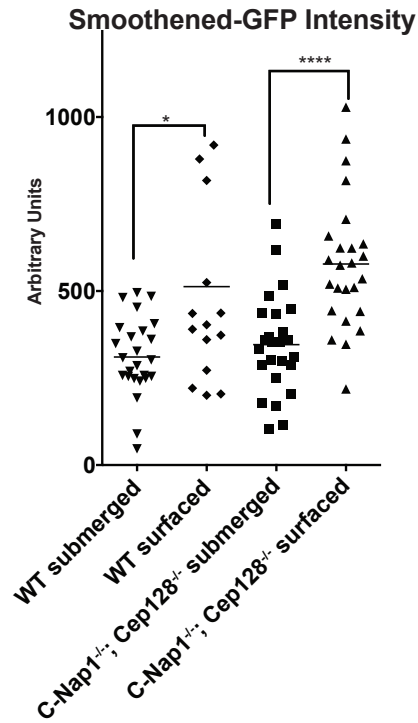
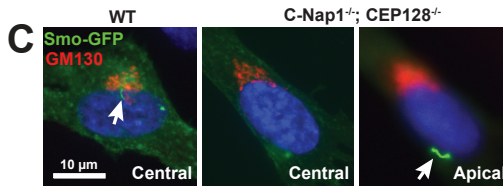
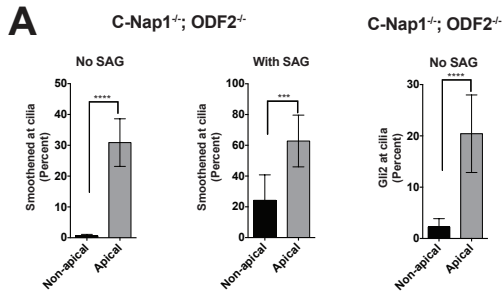
(C) *CEP128*<sup>-/-</sup>; *C-Nap1*<sup>-/-</sup> mutant cells carrying either submerged (left) or apically surfaced (right) cilia were stained with Gli2 antibodies.

(D) Rare wild-type RPE1 cells carrying apically surfaced cilia were stained with Smoothened or Gli2 antibodies as indicated.

(E) Quantification of the ciliary accumulation of Smoothened for each indicated genotype and cilia position in the presence or absence of SAG. Mean and standard deviation are depicted as bars and error bars respectively. 30-60 cilia were scored for each of the three repeats, except for the rare surfaced cilia in wild type cells, which were 10 cilia per repeat. Significance determined by unpaired two-tailed t-test with Welch's correction ( $p < 0.001$  corresponds to \*\*\*).

(F) Quantification of the ciliary accumulation of Gli2 for each indicated genotype and cilia position in the absence of SAG. Mean and standard deviation are depicted. 30-60 cilia were scored for each of the three repeats, except for the rare surfaced cilia in wild type cells, which were 10 cilia per repeat. Significance determined by unpaired two-tailed t-test with Welch's correction ( $p < 0.05$  for \*) ( $p < 0.001$  for \*\*\*).

(G) Plot depicting the percentage of 16HBE cells with Smoothened or Gli2 accumulation in cilia for each cilia position. 20-40 cilia were scored for each of three repeats. Mean percentage of the 3 experiments is shown. Error bars correspond to standard deviation. Significance determined by unpaired two-tailed t-test with Welch's correction ( $p < 0.01$ \*\*).



**Figure 2.15 Accumulation of Smoothened at surfaced cilia is robustly seen in multiple cell lines and staining conditions**

(A) Quantification of the ciliary accumulation of Smoothened for C-Nap1<sup>-/-</sup>; ODF2<sup>-/-</sup> and cilia position in the presence or absence of SAG. Mean and standard deviation are depicted. 20-60 cilia were scored for each of the three repeats. Significance was determined by unpaired two-tailed t-test with Welch's correction (p<0.001).

(B) Two *BJ-57a* cells in the same field, one carrying apically surfaced cilia and the other submerged cilia, were stained with Smoothened, cilia, and Golgi antibodies as indicated. At the central focal plane, submerged cilia, the Golgi and nucleus were in focus. At the apical focal plane, only the surfaced cilium was in focus.

(C) WT and C-Nap1<sup>-/-</sup>; Cep128<sup>-/-</sup> cells expressing Smoothened-GFP are shown. Plot depicts the Smoothened-GFP intensity for 25 cells of each location. Lines depict means. Significance was determined by unpaired two-tailed t-test with Welch's correction (p<0.0001).

(D) Quantification of the ciliary accumulation of Smoothened for C-Nap1<sup>-/-</sup>; Cep128<sup>-/-</sup>. Cells were triton pre-extracted, fixed with -20C methanol and then stained with a different smoothened antibody from that used elsewhere. Mean and standard deviation are depicted. 20-60 cilia were scored for each of the three repeats. Significance was determined by unpaired two-tailed t-test with Welch's correction (p<0.05).

### **2.3 Brief summary and discussion of results**

This work began as a detailed examination of the subdistal appendages. We identified novel sDAP components and developed a more complete understanding of how sDAP protein is required to centrioles. This knowledge allowed us to disrupt the sDAP's function and explore for new phenotypes. Most importantly, we identified several molecules required to maintain primary cilia in submerged configurations. The process involves the redundant functions of accessory structures located at both the distal ends (sDAP: Cep128, Odf2, centriolin) and proximal ends of centrioles (C-Nap1). Elimination of all these structures from centrioles has no effect on cilia assembly, but instead causes multiple defects in cilia/centrosome position. Upon mutation, normally submerged cilia fully surface, and lose the deep ciliary pit, also causing a separation of the Golgi from ciliated centrosomes. Importantly, surfaced cilia respond to fluid flow with motion, a process relevant for mechanosensation. Surfaced cilia also recruit signaling molecules that are normally not seen in submerged cilia, revealing a

potential link between the sensation functionality and cilia position. Also, our studies support the published model that the deep ciliary pit can trap a group of cilia together [279], and argue that abolishing the clustering of cilia within a shared pit could be an important process to ensure proper function of cells that have multiple surfaced cilia, such as multi-ciliated epithelia or olfactory neurons.

The cilium is historically described either as a cellular antenna that receives extracellular signals or as a hair-like structure that produces and senses motions. Yet vertebrate cilia are often maintained in a submerged configuration, where they certainly cannot generate nor detect motions, and perhaps might even be shielded from properly receiving chemical signals, raising many interesting ideas and questions for future studies. The possibilities and implications will be discussed in the next chapter. These results do not reveal the mechanical mechanisms by which sDAP maintain submerged cilia in complete detail. Possible future research that can establish such details will be discussed in the next chapter as well.

## **2.4 Experimental Procedures**

### **2.4.1 Cloning and Plasmids**

Full-length HA tagged CEP128, Smoothed-GFP (from Addgene: 25395 [280]), Arl13b-GFP, GalT-GFP (A Golgi marker from Addgene:11929 [281]), and Arl13b-mCherry were cloned into pLVX-Tight-Puro vector (Clontech). For constant Arl13b and GalT expression, CMV promoter was cloned into pLVX vector to replace the tetracycline-inducible promoter in Arl13b-GFP, GalT-GFP



and Arl13b-mCherry constructs. Both tetracycline-inducible and non-inducible Arl13b constructs were used in this work.

### **2.4.2 CRISPR**

CRISPR/Cas9 mediated gene targeting was used to inactivate C-Nap1 and various sDAP components as described previously [282]. The targeting sequences of gRNAs used for CRISPR are as follows: C-Nap1 gRNA4 (5'-GATACTACAGACCCAGCTCCAGG-3'), ODF2 gRNA1 (5'-GAGGGAACAGCACTGCAAAGAGG-3'), ODF2 gRNA2 (5'-GAGTGTCCGGGTGAAAACCAAGG-3'), Ninein gRNA0 (5'-GCTCAGCCCAAATATGTTAGAGG-3'), CEP128 gRNA2 (5'-GCTGCCAGATCAACGCACAGGG-3'), CEP128 gRNA4 (5'-GAGTCAGCTCTGAGATCTGAAGG-3'), CEP128 gRNA5 (5'-GCAGCTGAACTTCAGCGCAATGG-3'), Centriolin gRNA6 (5'-AGTGGGTTGCAAGAATACCTGG-3'), Centriolin gRNA9 (5'-GTGCCTATGAAGCTGAGCTAGAGG-3'), Cep83 gRNA1 (5'-GGTGGAGACAGTGGATTGACAGG-3'), Cep83 gRNA2 (5'-GATATTA ACTCCACAAAATTGG-3'), Rootletin gRNA 4 (5'-GGACATCACGAGCTGTCCAGG-3'), AKAP450 gRNA 2 (5'-GTCTGATAATCTTCTAATAAGTGG-3'), AKAP450 gRNA4 (5'-GAGAAATGGAGAATGCTTTAAGG-3')

Frame shift mutations in each target gene were confirmed by sequence analyses of clonal cell lines (see Table S1). To achieve complete protein

depletion, multiple gRNAs targeting different exons were used for CEP128 and centriolin as shown above. For rescuing C-Nap1 expression, a second lesion near the site of the 1<sup>st</sup> lesion was introduced by CRISPR to put the sequence back into frame, with the targeting sequence (5'-GAGCCTCCTGGAATCCCAGTGG-3').

#### **2.4.3 Cell culture.**

hTERT-RPE1 cells were cultured in DME/F-12 10% FBS, 1% penicillin/streptomycin. hTERT-BJ1 cells were cultured in DMEM medium supplemented with 199 media (1:4 ratio) 10% FBS, 1% penicillin/streptomycin. 16HBE cells were cultured in MEM supplemented with Glutamax (Gibco), 10% FBS, 1% penicillin/streptomycin. All other cells were cultured in DMEM medium, 10% FBS, 1% penicillin/streptomycin. Stable expression of various gene constructs was achieved with the Lentiviral pLVX-tight-Puro vector.

#### **2.4.4 Antibodies**

Mouse monoclonal antibodies used in this study are anti-centrin2 (clone 20H5; 04-1624, Millipore), anti-centrin3 (clone 3E6; H00001070-M01; dilution 1:200), anti-FOP (clone 2B1, H00011116-M01; dilution 1:1000) (Abnova), anti-Cep170 (72-413-1; dilution 1:200; Invitrogen Antibodies), anti-ODF2 (1a1, H00004957-M01; dilution 1:200; Novus Biologicals), anti-GM130 (610822; dilution 1:2000), anti-AKAP450 (611518; dilution 1:500), anti-p150glued (610473; dilution 1:1000)(BD Transduction Laboratories), anti-Gli2 (C-10, sc-271786;

dilution 1:200), anti-gamma tubulin (TU-30, sc-51715; 1:500 dilution), anti-Centriolin (C9, sc-365521; dilution 1:200), anti-rootletin (sc-67824; dilution 1:500) (Santa Cruz Biotechnology), anti-acetylated alpha tubulin (clone 6-11B-1, T7451; dilution 1:1000), anti-alpha tubulin (clone DM1A, T9026; dilution 1:2,000) (Sigma-Aldrich). Rabbit polyclonal antibodies used in this work include anti-ODF2 (HPA001874; dilution 1:500), anti-CEP128 (HPA001116; dilution 1:500) (Sigma-Aldrich/Atlas), anti-Ninein (A301-504; dilution 1:3000; Bethyl Labs), anti-FBF1 (11521-1-AP; dilution 1:500; Proteintech Group), anti-Kif2a (ab37005; dilution 1:3000), anti-CEP135 (ab75005; dilution 1:1000) and anti-Smoothened (ab38686; dilution 1:200) (Abcam). A rabbit polyclonal antibody against the human C-Nap1 was produced as previously described [183]. Anti-Arl13b rabbit polyclonal antibody was a gift from the Kathryn Anderson lab as was the Smoothened Antibody used in Figure 2.15. A rat monoclonal anti-tubulin (clone Y11/2, MCA77G; dilution 1:500; AbD Serotec) was also used in this work. Secondary antibodies Alexa-Fluor 405, 488, 594, 680 were from Molecular Probes.

#### **2.4.5 Immunofluorescence**

Cells were washed with phosphate-buffered saline (PBS) or extracted in PTEM (20 mM PIPES pH 6.8, 0.2% Triton X-100, 10 mM EGTA, 1 mM MgCl<sub>2</sub>) for 2 minutes, before fixation with methanol at -20°C or with 4% paraformaldehyde for 10 minutes. Fixed cells were blocked in 3% BSA 0.1% TritonX100 in PBS before incubation with antibodies. DNA was visualized using 4',6-diamidino-2-

phenylindole (DAPI). An upright microscope (Axio imager; Carl Zeiss) with a 100X objective (NA 1.4) and a camera (ORCA ER; HamamatsuPhotonics) was used to collect still images. For p150glued or Kif2a staining at centrosomes, microtubules were depolymerized by cold treatment for 20-30 minutes to remove microtubule associated staining (centrosomal Kif2a and p150glued were not affected by the cold treatment). For microtubule regrowth assay, the same cold treatment described above was followed by a 10-minute incubation at 37C to allow microtubule aster formation, before fixation and examination. To induce cilia growth, RPE1 cells were switched to media without FBS. SAG treatments were done for 20 hours with 200nM SAG. If rat anti-tubulin and any mouse igg1 antibody needed to be stained on the same coverslips, igg1 primary and secondary staining were performed prior to rat primary and secondary staining to prevent cross reactivity issues. ImageJ and Adobe Illustrator software were used to prepare images for figures. Graphs, plots and statistical analysis were done in Prism software. P-values and significance were determined by unpaired t-test with Welch's correction. Multiple 3D illustrations were done with Sketchup software.

#### **2.4.6 Arl13b level and Smoothened-GFP quantification**

Cells were induced to express modest amounts of Smoothened-GFP under tetracycline-inducible promoter. Regions of interest were drawn around the cilia in ImageJ using the wand tool and measured.

To produce the Arl13b ratios, the following formulas were applied

Arl13b Level = ((‘Mean Intensity’-‘Background Level Mean’) \* ‘Area’) /  
(‘Number Cilia in Roi’ \* ‘Major Axis Length’)

**Ratio**= ‘Average Arl13b Level in cells containing 2 cilia’ / ‘Average Arl13b  
Level in cells containing 1 cilia’

#### **2.4.7 Time-lapse microscopy and generation of fluid flow**

For live cell imaging, cells expressing fluorescent protein-labeled Arl13b or Golgi marker (GalT-GFP) were grown in glass bottom plates. A Zeiss Axiovert microscope equipped with 40X objective, a motorized temperature-controlled stage, an environmental chamber and a CO2 enrichment system was used for time-lapse microscopy. Images in time-lapse movies were acquired and processed by an electron-multiplying charge-coupled device (EMCCD) camera (from Hamamatsu Photonics) and axiovision software (Zeiss). To generate fluid flow, holes were melted into the lid of glass bottom plate using a soldering iron. Silicone tubing (1/16", Fisher Scientific) was filled with media, put through the openings, submerged in the media, and positioned near the field of view of the objective. The other end of the silicone tubing was attached to a 6V peristaltic pump with a maximum flow rate of ~40ml/min. Fluid direction was reversed at two-second intervals. Details of the control apparatus are shown in the included circuit diagram.

#### **2.4.8 Correlated light and Electron Microscopy.**

Aclar sheets with Carbon patterns were glued onto glass bottom plates (Cellvis). Cells expressing tet-inducible GFP-Arl13b were split onto the aclar sheets and grown for 4 days. Cells were then serum starved and treated with 1ug/ml doxycycline for two more days. Using the same microscope and flow apparatus as described above, we imaged cilia movements on the patterned aclar sheets at 20x. We then fixed rapidly by adding 8% Paraformaldehyde, 4% Glutaraldehyde, 4mM CaCl<sub>2</sub>, 40mM Sodium Cacodylate PH7.4 buffer to an equal volume of media. We incubated for 45 minutes. We then changed to 4% Paraformaldehyde, 2% Glutaraldehyde, 2mM CaCl<sub>2</sub> in 0.1M Sodium Cacodylate buffer with 0.2% tanic acid for a 2h treatment. Plate was left in 4% Paraformaldehyde, 2% Glutaraldehyde, 2mM CaCl<sub>2</sub> in 0.1M Sodium Cacodylate buffer at 4C for storage. Cells were post-fixed in 1% reduced OsO<sub>4</sub> with 1.1% potassium ferrocynide in 0.1M sodium cacodylate buffer for 60 min on ice, stained with 1% uranyl acetate for 30min, dehydrated in a graded series of ethanol, infiltrated with Eponate12 resin (Electron Microscopy Sciences) and then embedded in the resin. Based on live cell imaging, serial sections (~ 70-nm thickness) in regions containing cells of interest were cut on a microtome (Ultracut E; Leica). Samples were examined on JOEL 100CX transmission electron microscope (TEM) with the digital imaging system (XR41-C, Advantage Microscopy Technology Corp, Denver, MA) at 80kV or 100kV in the electron microscopy resource center in The Rockefeller University.

#### **2.4.9 siRNA for knockdown**

RNAi was performed using RNAiMax transfection reagent and siRNAs obtained from Life Technologies. Trypsinized cells were counted and plated with reagent-siRNA mixtures. Cells were fixed and stained 3 days after transfection. The control siRNA used was the Silencer® Select Negative Control No. 1 (Life Technologies). The antisense sequences of siRNA used to target Cep128 are 5'-UCACGUAUGAAAUCUUGGAC-3' and 5'-UAACCUUCGAGAUAGCUCCAA-3'.

Those for ODF2 are 5'-UUUACAAGAUCUGUUACCCGG-3' and 5'-UUGGUUUUCACCCGGACACUC-3'. Those for ninein are 5'-AUACUCCUCACUGCGUUGCGU-3' and 5'-UUUGACCUCAUCGUAACUCUU-3'. That for Cep250 was 5'-UGACAU AUGGGCUUGCUC CAG-3'.

## **Chapter 3: Findings, Conclusions, Discussion and Future**

### **work**

#### **3.1 Subdistal appendages**

##### **3.1.1 The role of sDAP in microtubule organization**

The apparent lack of apparent microtubule organization phenotypes in any sDAP mutant strongly conflicts with literature on ODF2 and ninein [72, 90]. We attempted to deplete the proteins with 3 distinct ninein CRISPR gRNAs, two ninein siRNA oligos, 2 ODF2 CRISPR gRNAs and 2 ODF2 siRNA oligos (data not shown). Depletion was attempted in HeLa and RPE1 cells. Although all splice variants were targeted and the proteins disappeared from the centriole, no trace of a microtubule anchoring phenotype was visible at steady state. Nor did we observe any defects with the widely used 10-minute microtubule re-polymerization assay. The sDAP appears to be dispensable for microtubule organization in RPE1 cells. By contrast, depletion of a non-appendage centriolar protein known to be involved in anchorage (FOP) caused clear microtubule organization phenotypes in about half of cells (data not shown). Furthermore, while others observed that only the older mother anchors interphase microtubules, we observe that both the mother and daughter centriole organize microtubules. Why do our observations not match the literature? For one, other groups use various other cell lines and not RPE1 for their experiments [70, 72, 90], not RPE1 nor HeLa. Likely, distinct mechanisms might contribute to microtubule organization in different cell lines. In the future, we can deplete sDAP components in U2OS, a cell line that has sDAP dependent microtubule



organization [70, 90]. If we can reproduce the microtubule phenotypes in U2OS, then we may hypothesize that RPE1 cells maintain radial microtubule arrays by distinct mechanisms from U2OS. There are a few possibilities for the distinct mechanism, 1) The PCM is believed to have microtubule anchoring capacity [17] that might be unregulated in some cell types but unused in others. 2) Constant nucleation of microtubules from PCM combined with high turnover could produce a radial array without anchorage at the sDAP. Each of these hypotheses are testable. For the first possibility, the main challenge is imaging at high enough resolution to distinguish a PCM attached microtubule from an sDAP associated one. That resolution can be attained with EM or STORM. To address the second possibility, we can determine the rates of microtubule nucleation using a live imaging. We can express EB1-GFP to label growing ends and tubulin-mCherry to label existing microtubules. We can compare microtubule growth and disappearance rates between RPE1 and U2OS.

Regardless of how some cells form sDAP independent radial microtubule arrays, it is interesting that multiple mechanisms exist for radial microtubule organization. Since self-assembly of radial microtubule arrays has been demonstrated without centrosomes [56], it is not clear why centrosomes are necessary to organize interphase microtubule arrays. Multiple mechanisms to assemble similar looking radial arrays around centrosomes seem like needless redundancy. I propose that only certain kinds of microtubule-to-centrosome attachments might be secure enough to be used for centrosome positioning. A pulling force strong enough to move the MTOC might break weak forms of

microtubule anchorage. Relocation of the MTOC is important for changes in cell polarization and cilia position.

### 3.1.2 The assembly of the sDAP

We divided the sDAP proteins into ODF2 Group and Ninein Group based on their localization. This two-group classification turned out to be more than just a heuristic for thinking about sDAP-associated proteins. The requirement of ninein for the localization of the entire Ninein Group shows that the Ninein

## The Assembly Hierarchy of centriolar proteins

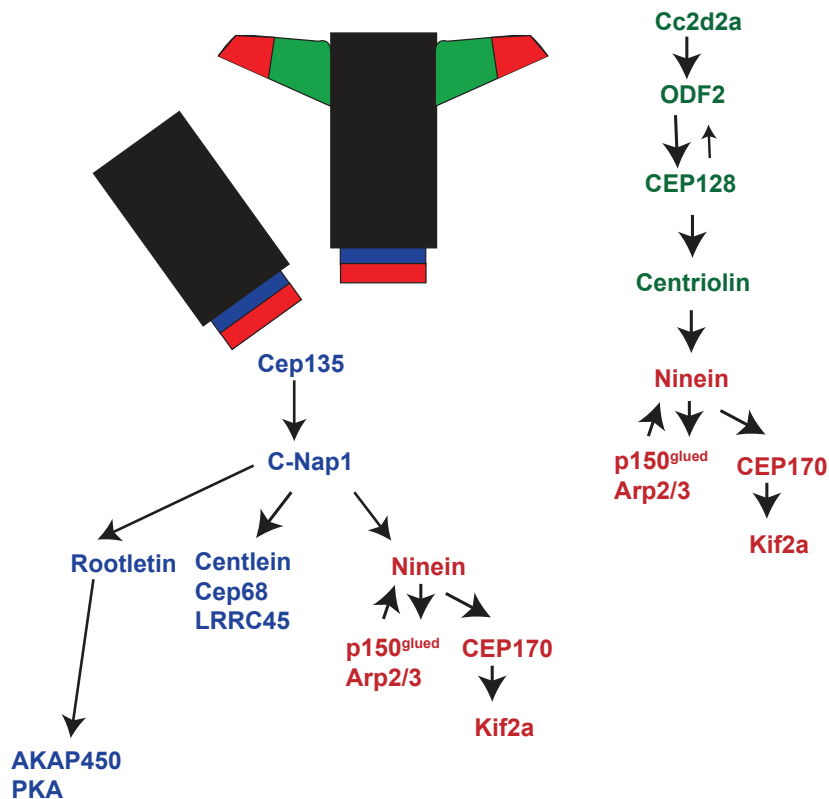


Figure 3.1 Assembly hierarchy of centriolar proteins

Group's proteins have a functional link beyond their similar localization. Similarly,

the ODF2 Group followed an assembly hierarchy of ODF2, Cep128 then Centriolin. Therefore, the two groups represent modules of the sDAP. Presumably, the proteins at the top of the assembly hierarchy (ODF2 and ninein) simply function as a structural scaffold for other proteins (Cep170, Kif2a, dynactin...) whose activities directly mediate the function of the sDAP. Previous research on the sDAP has focused on few or individual sDAP associated proteins without the benefit of a complete assembly hierarchy [6, 7, 10, 72, 75, 77, 91, 111, 112, 114, 117, 118, 147, 155, 180, 283, 284]. As a consequence, ideas regarding how the sDAP worked have been incomplete. Our assembly hierarchy of subdistal appendage proteins provides the most complete understanding of sDAP assembly created to date. We initially looked for an assembly hierarchy analogous to that of the distal appendages [80]. Based on published research on ODF2 and ninein [6], we correctly expected ODF2 to mediate Ninein Group localization to the sDAP. We made an educated and ultimately correct guess; C-Nap1 functions to recruit the Ninein Group specifically to the centriole proximal ends. Since our initial observation on C-Nap1, Conroy et al reported C-Nap1 to be generally required for ninein localization to centrioles regardless of location [180]. Although our work appears to contradict Conroy et al, there is in fact no inconsistency. Conroy quantified a specific population of centrioles in which only 12% had ODF2, preventing them from analyzing subdistal appendage associated ninein. Figure 3.1 above shows a complete assembly diagram of the sDAP and proximal end of centrioles that combines our

work with other published results (Figure 3.1). Most likely, not every molecular component of the sDAP has yet been identified.

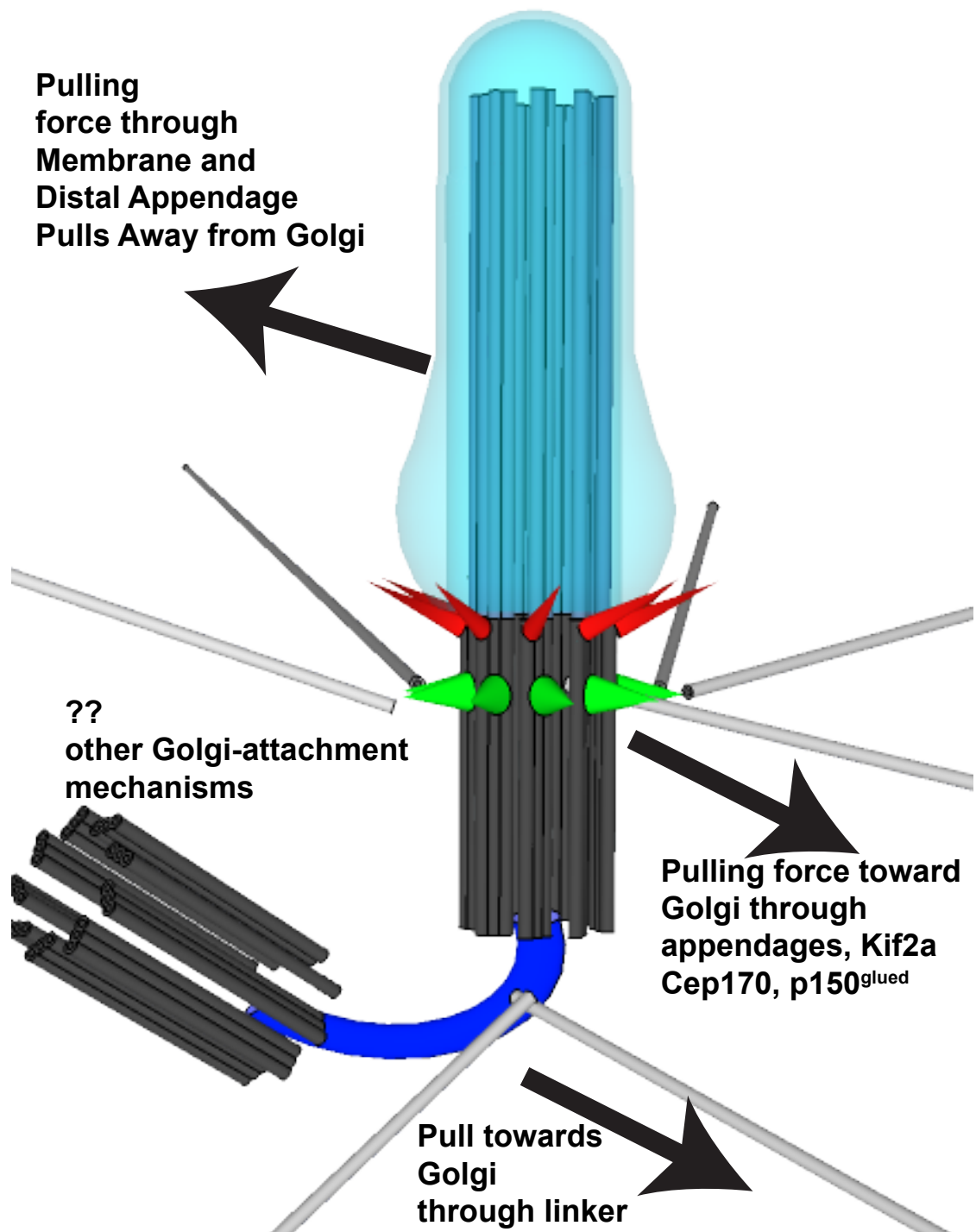
### **3.1.3 The limitations of the assembly hierarchy and future directions**

We have shown that several proteins at the subdistal appendages are required to recruit other proteins to the sDAP. Proteins like ninein, Cep128, C-Nap1 and ODF2 are apparently structural scaffolds onto which microtubule binding proteins like Kif2a, dyactin and Cep170. Another group showed that p150glued was important for centrosomal localization of ninein and Cep170 [91]. As we did not attempt to prove a protein-protein interaction between any two proteins, we cannot claim that recruitment of any one protein by another depends on direct physical interactions. Nor did we attempt to explore interactions from previously published papers, like the interaction of the microtubule binding protein EB1 with ninein, Cep170 and C-Nap1 [2]. To better understand the mechanisms of sDAP assembly, future work could use yeast 2-hybrid approaches to identify interacting partners. Simply the knowledge of additional sDAP associated proteins might lead to new insights regarding sDAP assembly and function. A more complete sDAP proteome could be helpful in understanding the structure. Currently, there are multiple proteomics techniques that could help identify novel sDAP proteins. Biotin ligase fusion proteins are used for proximity labeling, followed by pull-down and proteomics. In the future, we could express a ninein-BirA or ODF2 fusion protein to identify currently unknown sDAP proteins.

## **3.2 Centrosome Positioning**

### **3.2.1 Models of centrosome position control**

We successfully identified a group of proteins required for mediating Golgi-centrosome attachment. However, we have not yet provided a mechanistic model for how the two structures come together. The presence of microtubule interacting proteins at the sDAP strongly suggests a microtubule-based mechanism. But how is this motion achieved? Does the process really require interactions between sDAP and microtubules? Previous work on centrosome centering supports models in which forces from other parts of the cell pull on the microtubule array. The sDAP might contribute to this tug-of-war by pulling on the microtubules from the centrosome side. Although our work shows that multiple redundant mechanisms must contribute, we are only able to make detailed hypothesis about the few motor proteins known to be located to the sDAP. So far, the only motor protein that certainly localizes to the sDAP is Kif2a. Unlike a prototypical kinesin motor, Kif2a does not function by moving laterally along microtubules. Instead, Kif2a generates a pulling force by depolymerizing microtubules. The production of pulling forces by microtubule de-polymerization from secure ends has been extensively studied [285, 286]. Since the mechanisms of force generation from depolymerizing microtubules require secure microtubule binding, Cep170 or dynactin could contribute by binding the minus end. As microtubules are depolymerized, the centrosomes would be pulled toward the structure onto which the opposite ends of the microtubules are attached. Besides the centrosome, there is another structure that organizes



**Figure 3.2** The forces pulling on the centrosome microtubules: the Golgi apparatus. Hence, the centrosome is pulled toward the Golgi. Consistent with this model, mutation of AKAP450, a protein that is required for the Golgi to organize microtubules also causes the Golgi and centrosome to separate. However, this model alone does not explain two observations: 1) the

functional redundancy between sDAP and intercentrosomal linker and 2) the tendency for only the older centrosome to separating from Golgi. Based on our results, there must be multiple redundant mechanisms to bring Golgi and centrosome together. One mechanism (mediated by the C-Nap1/rootletin linker) functions redundantly to the sDAP. Rootletin is known to interact with kinesins that could pull the centrosome toward the Golgi [157, 287], working in parallel to the sDAP. When both the sDAP and centrosome cohesion are broken, the younger centrosome remains with the Golgi while the older does not. Under these conditions, the older centrosome has only one unique structure: the distal appendages (DAP). The DAP, mediate attachment of the centrosome to lipid membranes. Through the plasma membrane, the older mother centriole is subjected to any pulling forces that the plasma membrane or vesicle is exposed to. Therefore, the attachment of centrioles to membranes provides a means for the older centriole to be ripped away from the Golgi. Consistent with this explanation, younger and older centrioles detach from Golgi with equal frequency in triple mutants that lack C-Nap1, distal and subdistal appendages (see [Figure 2.10](#)). The younger centriole is not subject to the same mechanical forces so can remain tethered to the Golgi through a weaker mechanism. The different types of mechanical forces that may contribute to centriole position are summarized in [Figure 3.2](#). As a cell changes shape, polarizes and migrates, the organelles are subjected to a variety of mechanical forces through to cytoskeleton. In order to maintain appropriate position of centrioles in the face of these stresses, animals have evolved several mechanisms.

### **3.2.2 Testing models of Centrosome positioning**

Most aspects of the above model regarding centrosome position are testable. One could deplete Kif2a or Cep170 in a C-Nap1 deficient cell line and check for microtubule phenotypes to show that they have a role. The need for AKAP450 in linking centrosome and Golgi, suggests that Golgi organized microtubules are needed for Golgi-centrosome link. To test this, I could deplete other Golgi proteins involved in microtubule organization like GM130, IFT20 and CLASP1/2. I predict that these mutants should also have centrosomes separate from Golgi.

### **3.3 Golgi and cilia positioning**

We were able to separate cilia from Golgi in two distinct ways: Mutation of AKAP450 and simultaneous mutation of C-Nap1 and sDAP. Intriguingly, both these approaches also resulted in surfaced cilia, suggesting that it is the link between cilia and Golgi that keeps a cilium submerged. However, some of our mutants like ninein; C-Nap1 double produced cilia-Golgi separation without producing surfaced cilia at significantly higher rates. At present, we do not have an explanation for this discrepancy.

#### **3.3.1 Scoring of surfaced cilia phenotypes**

In this work, we employed a few distinct means of scoring cilia as 'surfaced' versus 'submerged'. Transmission electron microscopy with serial sections is the most accurate means of determining if a cilium is surfaced. TEM



can also reveal the morphology of the ciliary pocket in detail. Despite that advantage, the expense, the high labor/time/skills required and low throughput limit the use of TEM. The fluid-flow technique we developed provides a cheap, fast, and easy alternate means of determining if one has a cilia-surfacing phenotype. Any lab with access to a fluorescent time-lapse microscope can perform our assay. To label the cilia we have created lentiviral constructs for expression of Arl13b-GFP, Smo-GFP, and SSTR3-GFP. The apparatus to produce the fluid flow takes less than a day to build with parts costing under \$150. A researcher can learn how to operate it in minutes and score a couple hundred cilia in about 1 hour. (The circuit diagram is shown in Appendix). However, the fluid flow test has important limitations. Most importantly, the fluid flow test underestimates the percentage of cilia that protrude from the cell surface because cilia protruding from the bottom of cells and cilia in between cells are shielded from flow. This was evident from the electron micrographs of cilia that did not respond to flow. In all cases, the nonresponsive cilia were 'surfaced' in a cavity below the cell. These bottom-of-cell surfaced cilia are only identifiable by electron microscopy. Less importantly, our assay provides no means to distinguish non-emergent cilia from normal submerged cilia. When implementing our fluid flow assay we scored cilia as stationary or mobile. However, several distinct movement patterns were seen. In some cells, cilia pivoted about their base with no restrictions. In others, the bending motion occurred within a limited range. The top half of some cilia moved while the bottom remained stationary (likely because the bottom half was inside a ciliary

pit). Occasionally, a swollen cilia tip would respond to flow while most of the cilia remained stationary. In one curious case, both distal and proximal cilia tips were stationary while the middle of the cilia moved. Each of these motion types provides clues regarding the cilia position and cilia pit ultrastructure. Previously, defects in ciliary pit structure could only be identified using difficult electron microscopy techniques. We would like to study ciliary morphology in more detail. With our fluid flow assay, future researchers could easily identify mutants with specific bending patterns before investing resources into electron microscopic studies.

In order to test whether surfaced cilia correlate with the localization of any specific protein using IF, we used a third method; score cilia that are in a higher focal plane than the nucleus or the Golgi as surfaced. Although feasible, the focal plane technique greatly underestimates the percentage of surfaced cilia because surfaced cilia in relatively flat cells are not guaranteed to be in a distinct focal plane.

Pitaval et al reported that cells grown on small micropatterns grow cilia from the top surface at greater frequency than those allowed to spread out [269]. Although we did not attempt our fluid flow assay on constrained micropatterns, we would like to determine if micro pattern size affects our mutants similarly to wild type cells in the future.

Efficient means of scoring cilia position are essential for more detailed studies regarding cilia position control. Many details regarding the molecular mechanisms of cilia position control are unknown. How does each protein

contribute to the process? Does the intercentrosomal linker contribute? What other proteins play a role? Does Golgi attachment simply force cilia to be submerged or does the proximity to the Golgi contribute to cilia function? What other mechanisms could be keeping non-ciliated centrosomes with Golgi?

### **3.3.2 Cilia position and Hedgehog Signaling**

We observed that Smoothened and Gli2 were enriched in surfaced cilia. Interestingly, some surfaced cilia seemed to have elevated levels of Arl13b as well. It would be interesting to determine what other ciliary membrane proteins accumulate at surfaced cilia. Could trafficking of proteins to and from cilia occur differently based on cilia position? It is entirely possible. Endocytosis-mediated removal of ciliary membrane proteins might be impaired when cilia are surfaced, leading to Smoothened accumulation.

The accumulation Smoothened at surfaced cilia suggests that cilia position may modulate the levels of Hedgehog (HH) Pathway activation. At the moment, we do not know if the small increase in smoothened levels in surfaced cilia leads to activation. Despite several attempts, we have not been able to establish an assay for Hedgehog signaling in a cell line amenable to CRISPR. Although the Gli-luciferase reporter construct can be introduced into a variety of cell lines, the HH pathway itself poses an obstacle. In many tractable cell lines (including RPE1), the HH pathway is blocked downstream of Smoothened entry, making the reporter non-responsive to both agonists and antagonists. Although 3T3 Gli-light, an established luciferase based reporter line, responds to HH

agonist and antagonists, these cells lose the responsiveness after prolonged culturing. A developmental system would be an ideal tool for studying the HH pathway in signaling.

### **3.3.2.1 Mystery of PKA at the centrosome**

Protein Kinase A (PKA) is a critical negative regulator of the sonic hedgehog pathway that also localizes to the base of the cilia and the Golgi. Based on the requirement of C-Nap1 & Rootletin for AKAP450 recruitment (which in turn recruits PKA), one may expect to see strong hedgehog signaling defects in Rootletin or C-Nap1 mutant animals. However, none of the defects observed in animals are consistent with aberrant hedgehog signaling [158, 288]. We propose that the PKA at centrioles does not function in hedgehog signaling. Although surprising, this conclusion is not irreconcilable with existing literature. A separate pool of PKA located within the cilia has been proposed to play a role in the HH pathway [289, 290]. However, what function the centrosome-associated PKA plays remains to be explained. Others have proposed that centrosomal PKA regulates the cytoskeleton by phosphorylation of microtubule-associated proteins [291]. Interestingly, ninein seems to be a PKA substrate [292] suggesting that PKA might regulate sDAP function. Since the amino acid sequence of the PKA target site is known, bioinformatics approaches can be employed to search other known centrosomal proteins for candidate PKA sites. It would be interesting to determine if PKA inhibition alone could produce centrosome-Golgi separation.

### **3.3.2.2 Important questions regarding HH signaling**

A few important questions about cilia position and hedgehog signaling remain unsolved. Do Hedgehog (HH) Pathway responsive cells *in vivo* normally have surfaced or submerged cilia? Does the position of the cilia affect basal activation levels or ligand sensitivity? Do the cilia dynamically change position to activate or suppress the HH pathway? Does HH pathway activation cause the cilia to change position? Interestingly, Lan et al observed a cilium with a deep pit in a SHH responsive cell line derived from a patient's glioblastoma [267]. However, this observation may not be representative of most HH responsive cells. Electron microscopic analysis of a few hedgehog responsive tissues and tumors could determine whether hedgehog signaling is mediated by surfaced or submerged cilia. In order to study the relationships between dynamic changes in cilia position and pathway activation, it would be necessary to establish both the fluid flow assay and a HH reporter in HH responsive cell line. For the reasons discussed above, this would be challenging and require a determined researcher.

## **3.4 Submerged cilia**

### **3.4.1 What are the roles of submerged cilia?**

Although my work has yielded important insights into the mechanisms needed to maintain submerged cilia, the ultimate purpose of submerged cilia remains unknown. Countless possibilities exist. Placing cilia in a deep pit could allow them to specialize in receiving chemical signals rather than mechanical.

Submerged cilia might even be protected from some types of ligand signals like those signals carried by small vesicles. Moving cilia to a submerged position might temporarily silence ciliary signal transduction function without a time-consuming cilia disassembly process. Alternatively, cilia might be submerged to protect them from mechanical stresses that might otherwise trigger cilia disassembly or breakage of the cilia tip. Perhaps a short exposed cilium tip could act as a less sensitive mechanical sensor than would a fully surfaced cilium. A deeper ciliary pit could provide a larger surface area for specialized endocytosis and exocytosis. More complex hypotheses are also plausible. For example, a ciliary pit could help trap protein ligands that would otherwise quickly diffuse away from the cilium. Alternatively, if a tight junction like seal existed within the cilia pit (unlikely), it could prevent some types of ligands from reaching the bottom of the pit. By identifying the mechanisms to maintain cilia position, my work has provided the means to manipulate cilia position and study its purpose. Since the possibilities regarding the function of submerged cilia are so numerous, a logical next step would be an open-ended approach. First, produce an sDAP and C-Nap1 mutant animal model. By examining the animals for phenotypes in each ciliated tissue, one could identify what biological processes require submerged cilia. Based on the phenotypes, further hypothesis regarding surfaced cilia can be made and tested.

#### **3.4.2 Characterize the ciliary pit that traps submerged cilia**

The ciliary pit that confines submerged cilia is mysterious. Its narrow space may perform a distinct function from that of the submerged cilium itself. However, neither the ciliary sheath membrane nor cortical environment of the ciliary pit is well understood. To resolve the gap in understanding we have developed a BioID based approach to systematically characterize the pit contents. We created plasmid construct to express APEX2-tagged Smoothened with APEX2 on the extracellular side of the membrane. In the presence of H<sub>2</sub>O<sub>2</sub>,

APEX2 catalyzes the oxidation of Biotin Tyramide. The oxidation produces biotin-phenoxy radicals that can react with tyrosines on nearby proteins, covalently attaching the biotin. The labeling reaction works efficiently with PEG-4-

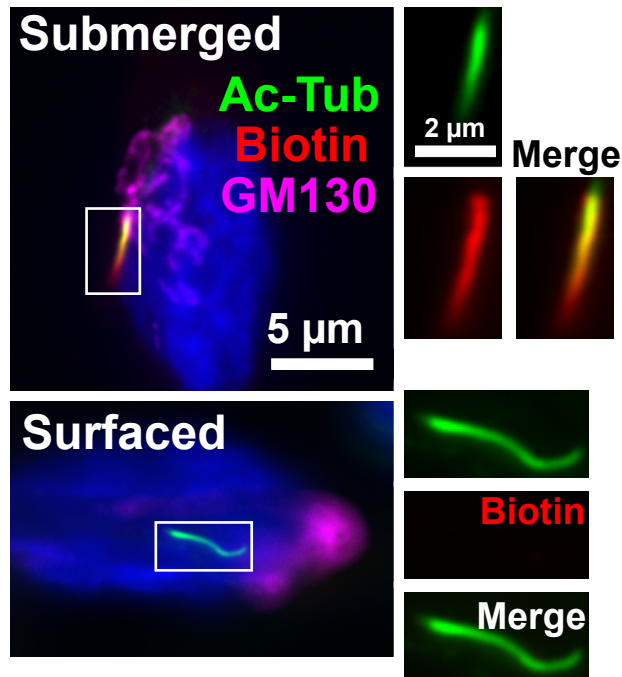


Figure 3.3 Apex2-Smo construct selectively biotinylates submerged cilia

membrane impermeable biotin derivative. Strikingly, while the biotin radicals generated from submerged cilia can robustly label the surrounding membrane proteins in the pit, nearly no biotin signal could be detected around surfaced cilia (Figure 3.3), even though a similar level of APEX2-Smo was targeted to both types of cilia. These results have important implications. The system can be used

to specifically label membrane proteins located in the ciliary pit with biotin. Biotinylated proteins can be purified for mass-spec analyses.

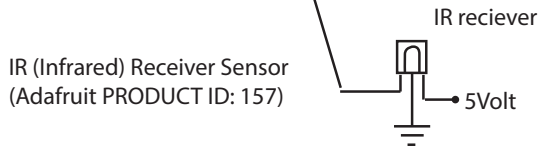
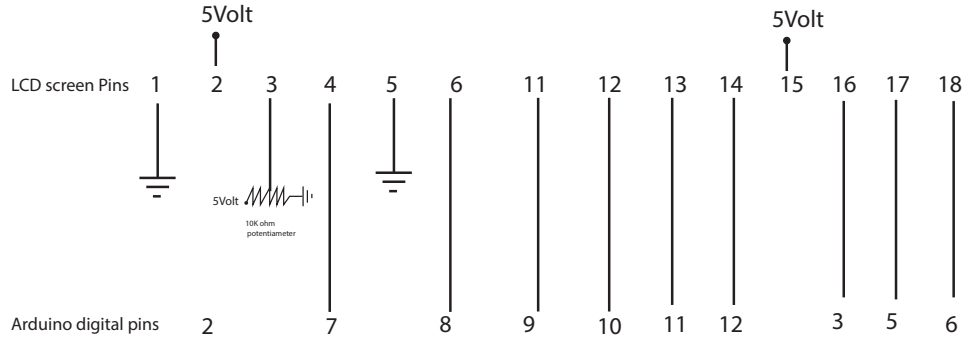
To filter out non-specific labeling, we can combine BioID with SILAC proteomics to identify proteins specifically associated with the ciliary pit, which will be relatively more abundant in WT cells that grow submerged cilia. Once identified, these membrane proteins can be further used as baits (by tagging the APEX2 at the intracellular domain) to probe the cortical environment of the ciliary pit through another run of BioID-SILAC.



# Appendix

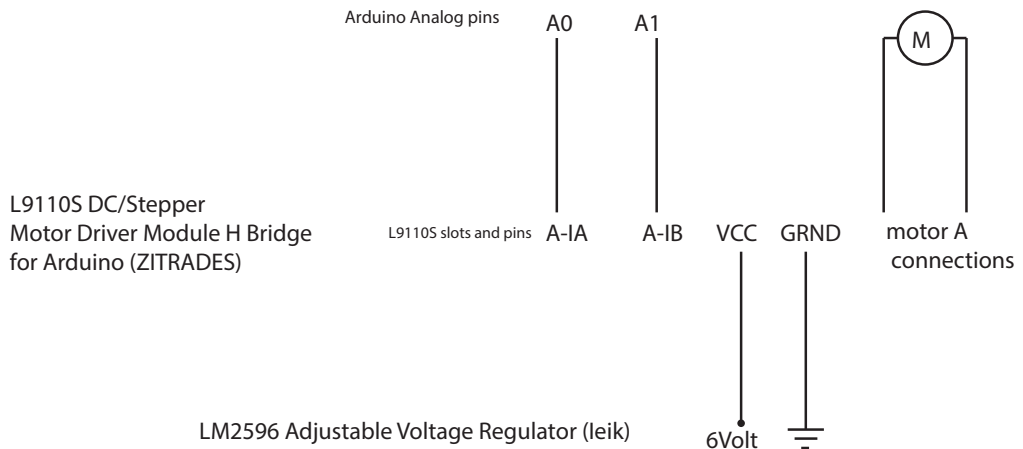
## Circuit diagram for peristaltic pump control

RGB backlight positive LCD  
(Adafruit PRODUCT ID: 398)



IR (Infrared) Receiver Sensor  
(Adafruit PRODUCT ID: 157)

6V DC  
Dosing Pump  
Peristaltic. 30mA  
40ml/min.  
20-60ml/min range  
(ZFE® GROUP LIMITED)



L9110S DC/Stepper  
Motor Driver Module H Bridge  
for Arduino (ZITRADES)

LM2596 Adjustable Voltage Regulator (leik)

Warning. DO NOT tie  
grounds of adjustable  
voltage regulator to  
arduino ground

## References/Bibliography

1. Bornens, M., *The centrosome in cells and organisms*. Science, 2012. **335**.
2. Schrøder, J.M., et al., *EB1 and EB3 promote cilia biogenesis by several centrosome-related mechanisms*. Journal of Cell Science, 2011. **124**(15): p. 2539-2551.
3. Dingemans, K.P., *The Relation Between Cilia And Mitoses In The Mouse Adenohypophysis*. The Journal of Cell Biology, 1969. **43**(2): p. 361-367.
4. Dawe, H.R., H. Farr, and K. Gull, *Centriole/basal body morphogenesis and migration during ciliogenesis in animal cells*. Journal of Cell Science, 2007. **120**(1): p. 7-15.
5. Paintrand, M., et al., *Centrosome organization and centriole architecture: Their sensitivity to divalent cations*. Journal of Structural Biology, 1992. **108**(2): p. 107-128.
6. Ishikawa, H., et al., *Odf2-deficient mother centrioles lack distal/subdistal appendages and the ability to generate primary cilia*. Nat Cell Biol, 2005. **7**(5): p. 517-524.
7. Kunimoto, K., et al., *Coordinated Ciliary Beating Requires Odf2-Mediated Polarization of Basal Bodies via Basal Feet*. Cell, 2012. **148**(1-2): p. 189-200.
8. Kuhns, S., et al., *The microtubule affinity regulating kinase MARK4 promotes axoneme extension during early ciliogenesis*. The Journal of Cell Biology, 2013. **200**(4): p. 505-522.
9. Graser, S., Y.-D. Stierhof, and E.A. Nigg, *Cep68 and Cep215 (Cdk5rap2) are required for centrosome cohesion*. Journal of Cell Science, 2007. **120**(24): p. 4321-4331.
10. Tateishi, K., et al., *Two appendages homologous between basal bodies and centrioles are formed using distinct Odf2 domains*. The Journal of Cell Biology, 2013. **203**(3): p. 417-425.
11. Carvalho-Santos, Z., et al., *Tracing the origins of centrioles, cilia, and flagella*. The Journal of Cell Biology, 2011. **194**(2): p. 165-175.
12. Rosenbaum, J.L. and G.B. Witman, *Intraflagellar transport*. Nat Rev Mol Cell Biol, 2002. **3**(11): p. 813-825.
13. Emmer, B.T., D. Maric, and D.M. Engman, *Molecular mechanisms of protein and lipid targeting to ciliary membranes*. Journal of Cell Science, 2010. **123**(4): p. 529-536.
14. Nauli, S.M., et al., *Polycystins 1 and 2 mediate mechanosensation in the primary cilium of kidney cells*. Nat Genet, 2003. **33**(2): p. 129-137.

15. Goetz, S.C. and K.V. Anderson, *The primary cilium: a signalling centre during vertebrate development*. Nat Rev Genet, 2010. **11**(5): p. 331-344.
16. Scheer, U., *Historical roots of centrosome research: discovery of Boveri's microscope slides in Würzburg*. Philosophical Transactions of the Royal Society B: Biological Sciences, 2014. **369**(1650).
17. Mennella, V., et al., *Amorphous no more: subdiffraction view of the pericentriolar material architecture*. Trends in Cell Biology. **24**(3): p. 188-197.
18. Haren, L., T. Stearns, and J. Lüders, *Plk1-Dependent Recruitment of  $\gamma$ -Tubulin Complexes to Mitotic Centrosomes Involves Multiple PCM Components*. PLOS ONE, 2009. **4**(6): p. e5976.
19. Zimmerman, W.C., et al., *Mitosis-specific Anchoring of  $\gamma$  Tubulin Complexes by Pericentrin Controls Spindle Organization and Mitotic Entry*. Molecular Biology of the Cell, 2004. **15**(8): p. 3642-3657.
20. Gomez-Ferrera, M.A., et al., *Human Cep192 Is Required for Mitotic Centrosome and Spindle Assembly*. Current Biology, 2007. **17**(22): p. 1960-1966.
21. Fong, K.-W., et al., *CDK5RAP2 Is a Pericentriolar Protein That Functions in Centrosomal Attachment of the  $\gamma$ -Tubulin Ring Complex*. Molecular Biology of the Cell, 2008. **19**(1): p. 115-125.
22. Sonnen, K.F., et al., *Human Cep192 and Cep152 cooperate in Plk4 recruitment and centriole duplication*. Journal of Cell Science, 2013. **126**(14): p. 3223-3233.
23. Murphy, S.M., et al., *GCP5 and GCP6: Two New Members of the Human  $\gamma$ -Tubulin Complex*. Molecular Biology of the Cell, 2001. **12**(11): p. 3340-3352.
24. Lüders, J., U.K. Patel, and T. Stearns, *GCP-WD is a [ $\gamma$ ]-tubulin targeting factor required for centrosomal and chromatin-mediated microtubule nucleation*. Nat Cell Biol, 2006. **8**(2): p. 137-147.
25. Rios, R.M., *The centrosome-Golgi apparatus nexus*. Philosophical Transactions of the Royal Society B: Biological Sciences, 2014. **369**(1650).
26. Dammermann, A., A. Desai, and K. Oegema, *The minus end in sight*. Current Biology, 2003. **13**(15): p. R614-R624.
27. Haren, L., et al., *NEDD1-dependent recruitment of the  $\gamma$ -tubulin ring complex to the centrosome is necessary for centriole duplication and spindle assembly*. The Journal of Cell Biology, 2006. **172**(4): p. 505-515.
28. Dictenberg, J.B., et al., *Pericentrin and  $\gamma$ -Tubulin Form a Protein Complex and Are Organized into a Novel Lattice at the Centrosome*. The Journal of Cell Biology, 1998. **141**(1): p. 163-174.
29. Muroyama, A., L. Seldin, and T. Lechler, *Divergent regulation of functionally distinct  $\gamma$ -tubulin complexes during differentiation*. The Journal of Cell Biology, 2016. **213**(6): p. 679-692.

30. Blagden, S.P. and D.M. Glover, *Polar expeditions [mdash] provisioning the centrosome for mitosis*. *Nat Cell Biol*, 2003. **5**(6): p. 505-511.
31. Sdelci, S., et al., *Nek9 Phosphorylation of NEDD1/GCP-WD Contributes to Plk1 Control of  $\gamma$ -Tubulin Recruitment to the Mitotic Centrosome*. *Current Biology*, 2012. **22**(16): p. 1516-1523.
32. Zhang, X., et al., *Sequential phosphorylation of Nedd1 by Cdk1 and Plk1 is required for targeting of the  $\gamma$ TuRC to the centrosome*. *Journal of Cell Science*, 2009. **122**(13): p. 2240-2251.
33. Barr, A.R., J.V. Kilmartin, and F. Gergely, *CDK5RAP2 functions in centrosome to spindle pole attachment and DNA damage response*. *The Journal of Cell Biology*, 2010. **189**(1): p. 23-39.
34. Ohta, S., et al., *CENP-32 is required to maintain centrosomal dominance in bipolar spindle assembly*. *Molecular Biology of the Cell*, 2015. **26**(7): p. 1225-1237.
35. Bogoyevitch, M.A., et al., *WD40-repeat protein 62 is a JNK-phosphorylated spindle pole protein required for spindle maintenance and timely mitotic progression*. *Journal of Cell Science*, 2012. **125**(21): p. 5096-5109.
36. Chavali, Pavithra L., I. Peset, and F. Gergely, *Centrosomes and mitotic spindle poles: a recent liaison?* *Biochemical Society Transactions*, 2015. **43**(1): p. 13-18.
37. Wang, W.-J., et al., *The conversion of centrioles to centrosomes: essential coupling of duplication with segregation*. *The Journal of Cell Biology*, 2011. **193**(4): p. 727-739.
38. Debec, A., W. Sullivan, and M. Bettencourt-Dias, *Centrioles: active players or passengers during mitosis?* *Cellular and Molecular Life Sciences*, 2010. **67**(13): p. 2173-2194.
39. Walsh, C.J., *The Structure of the Mitotic Spindle and Nucleolus during Mitosis in the Amebo-Flagellate Naegleria*. *PLOS ONE*, 2012. **7**(4): p. e34763.
40. Gillott, M.A. and R.E. Triemer, *The ultrastructure of cell division in Euglena gracilis*. *Journal of Cell Science*, 1978. **31**(1): p. 25-35.
41. Feldman, J.L., S. Geimer, and W.F. Marshall, *The Mother Centriole Plays an Instructive Role in Defining Cell Geometry*. *PLOS Biology*, 2007. **5**(6): p. e149.
42. Beisson, J. and T.M. Sonneborn, *Cytoplasmic Inheritance of the Organization of the Cell Cortex in Paramecium Aurelia*. *Proceedings of the National Academy of Sciences*, 1965. **53**(2): p. 275-282.
43. Moreira-Leite, F.F., et al., *A Trypanosome Structure Involved in Transmitting Cytoplasmic Information During Cell Division*. *Science*, 2001. **294**(5542): p. 610-612.
44. Sonneborn, T.M., *The Differentiation of Cells*. *Proceedings of the National Academy of Sciences*, 1964. **51**(5): p. 915-929.

45. Tollenaere, M.A.X., N. Mailand, and S. Bekker-Jensen, *Centriolar satellites: key mediators of centrosome functions*. Cellular and Molecular Life Sciences, 2015. **72**(1): p. 11-23.
46. Basto, R., et al., *Flies without Centrioles*. Cell. **125**(7): p. 1375-1386.
47. Bazzi, H. and K.V. Anderson, *Acentriolar mitosis activates a p53-dependent apoptosis pathway in the mouse embryo*. Proceedings of the National Academy of Sciences, 2014. **111**(15): p. E1491-E1500.
48. Meitinger, F., et al., *53BP1 and USP28 mediate p53 activation and G1 arrest after centrosome loss or extended mitotic duration*. The Journal of Cell Biology, 2016. **214**(2): p. 155-166.
49. Fong, C.S., et al., *53BP1 and USP28 mediate p53-dependent cell cycle arrest in response to centrosome loss and prolonged mitosis*. eLife, 2016. **5**: p. e16270.
50. SZOLLOSI, D., P. CALARCO, and R.P. DONAHUE, *Absence of Centrioles in the First and Second Meiotic Spindles of Mouse Oocytes*. Journal of Cell Science, 1972. **11**(2): p. 521-541.
51. Calarco-Gillam, P.D., et al., *Centrosome development in early mouse embryos as defined by an autoantibody against pericentriolar material*. Cell, 1983. **35**(3): p. 621-629.
52. Coelho, Paula A., et al., *Spindle Formation in the Mouse Embryo Requires Plk4 in the Absence of Centrioles*. Developmental Cell, 2013. **27**(5): p. 586-597.
53. Azimzadeh, J., et al., *Centrosome Loss in the Evolution of Planarians*. Science, 2012. **335**(6067): p. 461-463.
54. Hodges, M.E., et al., *The evolution of land plant cilia*. New Phytologist, 2012. **195**(3): p. 526-540.
55. Ogden, A., P.C.G. Rida, and R. Aneja, *Heading off with the herd: how cancer cells might maneuver supernumerary centrosomes for directional migration*. Cancer and Metastasis Reviews, 2012. **32**(1-2): p. 269-287.
56. Bornens, M., *Organelle positioning and cell polarity*. Nat Rev Mol Cell Biol, 2008. **9**(11): p. 874-886.
57. Pannu, V., et al., *Centrosome-declustering drugs mediate a two-pronged attack on interphase and mitosis in supercentrosomal cancer cells*. Cell Death & Disease, 2014. **5**(11): p. e1538.
58. Holy, T.E., et al., *Assembly and positioning of microtubule asters in microfabricated chambers*. Proceedings of the National Academy of Sciences, 1997. **94**(12): p. 6228-6231.
59. Burakov, A., et al., *Centrosome positioning in interphase cells*. The Journal of Cell Biology, 2003. **162**(6): p. 963-969.

60. Buendia, B., et al., *Cytoskeletal control of centrioles movement during the establishment of polarity in Madin-Darby canine kidney cells*. The Journal of Cell Biology, 1990. **110**(4): p. 1123-1135.
61. Nguyen, M.M., M.C. Stone, and M.M. Rolls, *Microtubules are organized independently of the centrosome in Drosophila neurons*. Neural Development, 2011. **6**: p. 38-38.
62. Bettencourt-Dias, M., *Q&A: Who needs a centrosome?* BMC Biology, 2013. **11**(1): p. 28.
63. Rogers, G.C., et al., *A Multicomponent Assembly Pathway Contributes to the Formation of Acentrosomal Microtubule Arrays in Interphase Drosophila Cells*. Molecular Biology of the Cell, 2008. **19**(7): p. 3163-3178.
64. Ahmad, F.J., et al., *An Essential Role for Katanin in Severing Microtubules in the Neuron*. The Journal of Cell Biology, 1999. **145**(2): p. 305-315.
65. De Brabander, M., et al., *Nucleated assembly of mitotic microtubules in living PTK2 cells after release from nocodazole treatment*. Cell Motil, 1981. **1**(4): p. 469-83.
66. McNally, F.J., et al., *Katanin, the microtubule-severing ATPase, is concentrated at centrosomes*. Journal of Cell Science, 1996. **109**(3): p. 561-567.
67. Svenson, I.K., et al., *Subcellular localization of spastin: implications for the pathogenesis of hereditary spastic paraplegia*. Neurogenetics, 2005. **6**(3): p. 135-141.
68. Piel, M., et al., *The Respective Contributions of the Mother and Daughter Centrioles to Centrosome Activity and Behavior in Vertebrate Cells*. The Journal of Cell Biology, 2000. **149**(2): p. 317-330.
69. Gorgidze, L.A. and I.A. Vorobjev, *Centrosome and microtubules behavior in the cytoplasts*. J Submicrosc Cytol Pathol, 1995. **27**(3): p. 381-9.
70. Dammermann, A. and A. Merdes, *Assembly of centrosomal proteins and microtubule organization depends on PCM-1*. The Journal of Cell Biology, 2002. **159**(2): p. 255-266.
71. Hori, A., et al., *Msd1/SSX2IP - dependent microtubule anchorage ensures spindle orientation and primary cilia formation*. EMBO reports, 2014. **15**(2): p. 175-184.
72. Delgehyr, N., J. Sillibourne, and M. Bornens, *Microtubule nucleation and anchoring at the centrosome are independent processes linked by ninein function*. Journal of Cell Science, 2005. **118**(8): p. 1565-1575.
73. Yan, X., R. Habedanck, and E.A. Nigg, *A Complex of Two Centrosomal Proteins, CAP350 and FOP, Cooperates with EB1 in Microtubule Anchoring*. Molecular Biology of the Cell, 2006. **17**(2): p. 634-644.

74. Clark, I.B. and D.I. Meyer, *Overexpression of normal and mutant Arp1alpha (centractin) differentially affects microtubule organization during mitosis and interphase*. Journal of Cell Science, 1999. **112**(20): p. 3507-3518.
75. Askham, J.M., et al., *Evidence That an Interaction between EB1 and p150(Glued) Is Required for the Formation and Maintenance of a Radial Microtubule Array Anchored at the Centrosome*. Molecular Biology of the Cell, 2002. **13**(10): p. 3627-3645.
76. Bartolini, F. and G.G. Gundersen, *Generation of noncentrosomal microtubule arrays*. Journal of Cell Science, 2006. **119**(20): p. 4155-4163.
77. Mogensen, M.M., et al., *Microtubule minus-end anchorage at centrosomal and non-centrosomal sites: the role of ninein*. Journal of Cell Science, 2000. **113**(17): p. 3013-3023.
78. Miller, P.M., et al., *Golgi-derived CLASP-dependent microtubules control Golgi organization and polarized trafficking in motile cells*. Nature, 2009. **11**(9): p. 1069-1080.
79. Schmidt, K.N., et al., *Cep164 mediates vesicular docking to the mother centriole during early steps of ciliogenesis*. The Journal of Cell Biology, 2012. **199**(7): p. 1083-1101.
80. Tanos, B.E., et al., *Centriole distal appendages promote membrane docking, leading to cilia initiation*. Genes & Development, 2013. **27**(2): p. 163-168.
81. Joo, K., et al., *CCDC41 is required for ciliary vesicle docking to the mother centriole*. Proceedings of the National Academy of Sciences, 2013. **110**(15): p. 5987-5992.
82. Sillibourne, J.E., et al., *Primary ciliogenesis requires the distal appendage component Cep123*. Biol Open, 2013. **2**(6): p. 535-45.
83. Failler, M., et al., *Mutations of CEP83 Cause Infantile Nephronophthisis and Intellectual Disability*. The American Journal of Human Genetics, 2014. **94**(6): p. 905-914.
84. Garcia, G. and J.F. Reiter, *A primer on the mouse basal body*. Cilia, 2016. **5**: p. 17.
85. Clare, D.K., et al., *Basal foot MTOC organizes pillar MTs required for coordination of beating cilia*. Nature Communications, 2014. **5**: p. 4888.
86. Doolin, P.F. and W.J. Birge, *Ultrastructural Organization of Cilia and Basal Bodies of the Epithelium of the Choroid Plexus In the Chick Embryo*. The Journal of Cell Biology, 1966. **29**(2): p. 333-345.
87. Vorobjev, I.A. and Chentsov YuS, *Centrioles in the cell cycle. I. Epithelial cells*. The Journal of Cell Biology, 1982. **93**(3): p. 938-949.
88. Chang, P., et al., *[epsiv]-Tubulin is required for centriole duplication and microtubule organization*. Nat Cell Biol, 2003. **5**(1): p. 71-76.

89. Mazo, G., et al., *Spatial Control of Primary Ciliogenesis by Subdistal Appendages Alters Sensation-Associated Properties of Cilia*. *Developmental Cell*, 2016. **39**(4): p. 424-437.
90. Hung, H.-F., H. Hehnlly, and S. Doxsey, *The Mother Centriole Appendage Protein Cenexin Modulates Lumen Formation through Spindle Orientation*. *Current Biology*, 2016. **26**(6): p. 793-801.
91. Kodani, A., et al., *Kif3a interacts with Dynactin subunit p150Glued to organize centriole subdistal appendages*. *The EMBO Journal*, 2013. **32**(4): p. 597-607.
92. Srivatsa, S., et al., *Sip1 downstream Effector ninein controls neocortical axonal growth, ipsilateral branching, and microtubule growth and stability*. *Neuron*, 2015. **85**(5): p. 998-1012.
93. Shinohara, H., et al., *Ninein is essential for the maintenance of the cortical progenitor character by anchoring the centrosome to microtubules*. *Biology Open*, 2013. **2**(7): p. 739-749.
94. Graser, S., et al., *Cep164, a novel centriole appendage protein required for primary cilium formation*. *The Journal of Cell Biology*, 2007. **179**(2): p. 321-330.
95. Soung, N.-K., et al., *Plk1-Dependent and -Independent Roles of an ODF2 Splice Variant, hCenexin1, at the Centrosome of Somatic Cells*. *Developmental Cell*, 2009. **16**(4): p. 539-550.
96. Matsumoto, T., et al., *Ninein Is Expressed in the Cytoplasm of Angiogenic Tip-Cells and Regulates Tubular Morphogenesis of Endothelial Cells*. *Arteriosclerosis, Thrombosis, and Vascular Biology*, 2008. **28**(12): p. 2123-2130.
97. Keryer, G., et al., *Part of Ran Is Associated with AKAP450 at the Centrosome: Involvement in Microtubule-organizing Activity*. *Molecular Biology of the Cell*, 2003. **14**(10): p. 4260-4271.
98. Zhang, L., et al., *Pre-spermiogenic initiation of flagellar growth and correlative ultrastructural observations on nuage, nuclear and mitochondrial developmental morphology in the zebrafish *Danio rerio**. *Micron*, 2014. **66**: p. 1-8.
99. Klotz, C., et al., *Parthenogenesis in *Xenopus* eggs requires centrosomal integrity*. *The Journal of Cell Biology*, 1990. **110**(2): p. 405-415.
100. Bornens, M., *Centrosome composition and microtubule anchoring mechanisms*. *Current Opinion in Cell Biology*, 2002. **14**(1): p. 25-34.
101. Gottardo, M., G. Callaini, and M.G. Riparbelli, *The *Drosophila* centriole – conversion of doublets into triplets within the stem cell niche*. *Journal of Cell Science*, 2015. **128**(14): p. 2437-2442.
102. Callaini, G., W.G.F. Whitfield, and M.G. Riparbelli, *Centriole and Centrosome Dynamics during the Embryonic Cell Cycles That Follow the Formation of the Cellular Blastoderm in *Drosophila**. *Experimental Cell Research*, 1997. **234**(1): p. 183-190.



103. Hagan, I.M. and R.E. Palazzo, *Warming up at the poles*. Workshop on Centrosomes and Spindle Pole Bodies, 2006. **7**(4): p. 364-371.
104. Zheng, Y., et al., *The Seckel syndrome and centrosomal protein Ninein localizes asymmetrically to stem cell centrosomes, but is not required for normal development, behavior, or DNA damage response in Drosophila*. *Molecular Biology of the Cell*, 2016.
105. Allen, R.D., *The morphogenesis of basal bodies and accessory structures of the cortex of the ciliated protozoan Tetrahymena pyriformis*. *The Journal of Cell Biology*, 1969. **40**(3): p. 716-733.
106. Piccinni, E. and M. Mammi, *Motor Apparatus of Euglena Gracilis: Ultrastructure of the Basal Portion of the Flagellum and the Paraflagellar Body*. *Bolletino di zoologia*, 1978. **45**(4): p. 405-414.
107. Geimer, S., *The ultrastructure of the Chlamydomonas reinhardtii basal apparatus: identification of an early marker of radial asymmetry inherent in the basal body*. *Journal of Cell Science*, 2004. **117**(13): p. 2663-2674.
108. Karpov, S.A., *Flagellar apparatus structure of choanoflagellates*. *Cilia*, 2016. **5**(1): p. 1-5.
109. Karpov, S.A. and B.S.C. Leadbeater, *Cell and nuclear division in a freshwater choanoflagellate, Monosiga ovata Kent*. *European Journal of Protistology*, 1997. **33**(3): p. 323-334.
110. Hibberd, D.J., *Observations on the ultrastructure of the choanoflagellate Codosiga botrytis (Ehr.) Saviile-Kent with special reference to the flagellar apparatus*. *Journal of Cell Science*, 1975. **17**(1): p. 191-219.
111. Bouckson-Castaing, V., et al., *Molecular characterisation of ninein, a new coiled-coil protein of the centrosome*. *Journal of Cell Science*, 1996. **109**(1): p. 179.
112. Ou, Y.Y., et al., *CEP110 and ninein are located in a specific domain of the centrosome associated with centrosome maturation*. *Journal of Cell Science*, 2002. **115**(9): p. 1825-1835.
113. Stillwell, E.E., J. Zhou, and H.C. Joshi, *Human ninein is a centrosomal autoantigen recognized by CREST patient sera and plays a regulatory role in microtubule nucleation*. *Cell cycle (Georgetown, Tex)*, 2004. **3**(7): p. 923-930.
114. Lin, C.-C., et al., *Characterization and functional aspects of human ninein isoforms that regulated by centrosomal targeting signals and evidence for docking sites to direct gamma-tubulin*. *Cell Cycle*, 2006. **5**(21): p. 2517-2527.
115. Delgehyr, N., *Microtubule nucleation and anchoring at the centrosome are independent processes linked by ninein function*. *Journal of Cell Science*, 2005. **118**(8): p. 1565-1575.
116. Abal, M., et al., *Microtubule release from the centrosome in migrating cells*. *The Journal of Cell Biology*, 2002. **159**(5): p. 731-737.

117. Mogensen, M.M., et al., *Microtubule minus-end anchorage at centrosomal and non-centrosomal sites: the role of ninein*. 2000: p. 1-11.
118. Moss, D.K., et al., *Ninein is released from the centrosome and moves bidirectionally along microtubules*. *Journal of Cell Science*, 2007. **120**(17): p. 3064-3074.
119. Ohama, Y. and K. Hayashi, *Relocalization of a microtubule-anchoring protein, ninein, from the centrosome to dendrites during differentiation of mouse neurons*. *Histochemistry and Cell Biology*, 2009. **132**(5): p. 515-524.
120. Veleri, S., et al., *Ciliopathy-associated gene Cc2d2a promotes assembly of subdistal appendages on the mother centriole during cilia biogenesis*. *Nature Communications*, 2014. **5**: p. 1-12.
121. Cheng, T.-S., et al., *SUMO-1 modification of centrosomal protein hNinein promotes hNinein nuclear localization*. *Life sciences*, 2006. **78**(10): p. 1114-1120.
122. Srivatsa, S., et al., *Sip1 Downstream Effector ninein Controls Neocortical Axonal Growth, Ipsilateral Branching, and Microtubule Growth and Stability*. *Neuron*, 2015. **85**(5): p. 998-1012.
123. Rao, A.N., et al., *Sliding of centrosome-unattached microtubules defines key features of neuronal phenotype*. *The Journal of Cell Biology*, 2016. **213**(3): p. 329-341.
124. Wang, X., et al., *Asymmetric centrosome inheritance maintains neural progenitors in the neocortex*. *Nature*, 2009. **461**(7266): p. 947-955.
125. Dauber, A., et al., *Novel Microcephalic Primordial Dwarfism Disorder Associated with Variants in the Centrosomal Protein Ninein*. *The Journal of Clinical Endocrinology and Metabolism*, 2012. **97**(11): p. E2140-E2151.
126. Grosch, M., et al., *Identification of a Ninein (NIN) mutation in a family with spondyloepimetaphyseal dysplasia with joint laxity (leptodactylic type)-like phenotype*. *Matrix Biology*, 2013. **32**(7-8): p. 387-392.
127. Brohmann, H., S. Pinnecke, and S. Hoyer-Fender, *Identification and Characterization of New cDNAs Encoding Outer Dense Fiber Proteins of Rat Sperm*. *Journal of Biological Chemistry*, 1997. **272**(15): p. 10327-10332.
128. Tarnasky, H., et al., *Gene trap mutation of murine Outer dense fiber protein-2 gene can result in sperm tail abnormalities in mice with high percentage chimaerism*. *BMC Developmental Biology*, 2010. **10**(1): p. 1-11.
129. Nakagawa, Y., et al., *Outer dense fiber 2 is a widespread centrosome scaffold component preferentially associated with mother centrioles: its identification from isolated centrosomes*. *Molecular Biology of the Cell*, 2001. **12**(6): p. 1687-1697.
130. Hüber, D., et al., *Molecular dissection of ODF2/Cenexin revealed a short stretch of amino acids necessary for targeting to the centrosome and the primary cilium*. *European Journal of Cell Biology*, 2008. **87**(3): p. 137-146.

131. Hüber, D. and S. Hoyer-Fender, *Alternative splicing of exon 3b gives rise to ODF2 and Cenexin*. Cytogenetic and Genome Research, 2007. **119**(1-2): p. 68-73.
132. Hehnly, H., H.F. Hung, and S. Doxsey, *One among many: ODF2 isoform 9, a.k.a. Cenexin-1, is required for ciliogenesis*. Cell Cycle, 2013. **12**(7): p. 1021.
133. Chang, J., et al., *Essential role of Cenexin1, but not Odf2, in ciliogenesis*. Cell Cycle, 2013. **12**(4): p. 655-662.
134. Soung, N.-K., et al., *Requirement of hCenexin for Proper Mitotic Functions of Polo-Like Kinase 1 at the Centrosomes*. Molecular and Cellular Biology, 2006. **26**(22): p. 8316-8335.
135. Salmon, N.A., R.A. Reijo Pera, and E.Y. Xu, *A gene trap knockout of the abundant sperm tail protein, outer dense fiber 2, results in preimplantation lethality*. genesis, 2006. **44**(11): p. 515-522.
136. Kunimoto, K., et al., *Coordinated Ciliary Beating Requires *Odf2*-Mediated Polarization of Basal Bodies via Basal Feet*. Cell. **148**(1): p. 189-200.
137. Gromley, A., et al., *A novel human protein of the maternal centriole is required for the final stages of cytokinesis and entry into S phase*. The Journal of Cell Biology, 2003. **161**(3): p. 535-545.
138. Hehnly, H., et al., *The centrosome regulates the Rab11- dependent recycling endosome pathway at appendages of the mother centriole*. Current Biology, 2012. **22**(20): p. 1944-1950.
139. Gromley, A., et al., *Centriolin Anchoring of Exocyst and SNARE Complexes at the Midbody Is Required for Secretory-Vesicle-Mediated Abscission*. Cell, 2005. **123**(1): p. 75-87.
140. Rannou, Y., et al., *MNK1 kinase activity is required for abscission*. Journal of Cell Science, 2012. **125**(12): p. 2844-2852.
141. Ganem, N.J., *The KinI kinesin Kif2a is required for bipolar spindle assembly through a functional relationship with MCAK*. The Journal of Cell Biology, 2004. **166**(4): p. 473-478.
142. Jang, C.Y., et al., *Plk1 and Aurora A regulate the depolymerase activity and the cellular localization of Kif2a*. Journal of Cell Science, 2009. **122**(9): p. 1334-1341.
143. Manning, A.L., et al., *The kinesin-13 proteins Kif2a, Kif2b, and Kif2c/MCAK have distinct roles during mitosis in human cells*. Molecular Biology of the Cell, 2007. **18**(8): p. 2970-2979.
144. Desai, A., et al., *Kin I kinesins are microtubule-destabilizing enzymes*. Cell, 1999. **96**(1): p. 69-78.
145. Tan, D., et al., *Kinesin-13s form rings around microtubules*. The Journal of Cell Biology, 2006. **175**(1): p. 25-31.

146. Miyamoto, T., et al., *The Microtubule-Depolymerizing Activity of a Mitotic Kinesin Protein KIF2A Drives Primary Cilia Disassembly Coupled with Cell Proliferation*. Cell Reports, 2015. **10**(5): p. 664-673.
147. Guarguaglini, G., et al., *The Forkhead-associated Domain Protein Cep170 Interacts with Polo-like Kinase 1 and Serves as a Marker for Mature Centrioles*. Molecular Biology of the Cell, 2005. **16**(3): p. 1095-1107.
148. Welburn, J.P.I. and I.M. Cheeseman, *The microtubule-binding protein Cep170 promotes the targeting of the kinesin-13 depolymerase Kif2b to the mitotic spindle*. Molecular Biology of the Cell, 2012. **23**(24): p. 4786-4795.
149. Maliga, Z., et al., *A genomic toolkit to investigate kinesin and myosin motor function in cells*. Nat Cell Biol, 2013. **15**(3): p. 325-334.
150. Eckley, D.M., et al., *Analysis of Dynactin Subcomplexes Reveals a Novel Actin-Related Protein Associated with the Arp1 Minifilament Pointed End*. The Journal of Cell Biology, 1999. **147**(2): p. 307-320.
151. Gill, S.R., et al., *Dynactin, a conserved, ubiquitously expressed component of an activator of vesicle motility mediated by cytoplasmic dynein*. The Journal of Cell Biology, 1991. **115**(6): p. 1639-1650.
152. Cianfrocco, M.A., et al., *Mechanism and regulation of cytoplasmic dynein*. Annu Rev Cell Dev Biol, 2015. **31**: p. 83-108.
153. Kim, H., et al., *Microtubule binding by dynactin is required for microtubule organization but not cargo transport*. The Journal of Cell Biology, 2007. **176**(5): p. 641-651.
154. Quintyne, N.J. and T.A. Schroer, *Distinct cell cycle-dependent roles for dynactin and dynein at centrosomes*. The Journal of Cell Biology, 2002. **159**(2): p. 245-254.
155. Quintyne, N.J., et al., *Dynactin Is Required for Microtubule Anchoring at Centrosomes*. The Journal of Cell Biology, 1999. **147**(2): p. 321-334.
156. Chen, J.V., et al., *Rootletin organizes the ciliary rootlet to achieve neuron sensory function in Drosophila*. The Journal of Cell Biology, 2015. **211**(2): p. 435-453.
157. Yang, J., et al., *Rootletin, a novel coiled-coil protein, is a structural component of the ciliary rootlet*. The Journal of Cell Biology, 2002. **159**(3): p. 431-440.
158. Yang, J., et al., *The Ciliary Rootlet Maintains Long-Term Stability of Sensory Cilia*. Molecular and Cellular Biology, 2005. **25**(10): p. 4129-4137.
159. Yang, J., M. Adamian, and T. Li, *Rootletin interacts with C-Nap1 and may function as a physical linker between the pair of centrioles/basal bodies in cells*. Molecular Biology of the Cell, 2006. **17**(2): p. 1033-1040.
160. Bahe, S., et al., *Rootletin forms centriole-associated filaments and functions in centrosome cohesion*. The Journal of Cell Biology, 2005. **171**(1): p. 27-33.

161. Faragher, A.J. and A.M. Fry, *Nek2A kinase stimulates centrosome disjunction and is required for formation of bipolar mitotic spindles*. *Molecular Biology of the Cell*, 2003. **14**(7): p. 2876-2889.
162. Fry, A.M., et al., *C-Nap1, a novel centrosomal coiled-coil protein and candidate substrate of the cell cycle-regulated protein kinase Nek2*. *The Journal of Cell Biology*, 1998. **141**(7): p. 1563-1574.
163. Mayor, T., et al., *The centrosomal protein C-Nap1 is required for cell cycle-regulated centrosome cohesion*. *The Journal of Cell Biology*, 2000. **151**(4): p. 837-846.
164. He, R., et al., *LRRC45 Is a Centrosome Linker Component Required for Centrosome Cohesion*. *Cell Reports*, 2013. **4**(6): p. 1100-1107.
165. Fang, G., et al., *Centlein mediates an interaction between C-Nap1 and Cep68 to maintain centrosome cohesion*. *Journal of Cell Science*, 2014. **127**(8): p. 1631-1639.
166. Bahmanyar, S., et al., *-Catenin is a Nek2 substrate involved in centrosome separation*. *Genes & Development*, 2008. **22**(1): p. 91-105.
167. Mayor, T., et al., *The mechanism regulating the dissociation of the centrosomal protein C-Nap1 from mitotic spindle poles*. *Journal of Cell Science*, 2002. **115**(16): p. 3275-3284.
168. Mi, J., et al., *Protein Phosphatase-1 $\alpha$  Regulates Centrosome Splitting through Nek2*. *Cancer Research*, 2007. **67**(3): p. 1082-1089.
169. Meraldi, P. and E.A. Nigg, *Centrosome cohesion is regulated by a balance of kinase and phosphatase activities*. *Journal of Cell Science*, 2001. **114**(20): p. 3749-3757.
170. Helps, N.R., et al., *NIMA-related kinase 2 (Nek2), a cell-cycle-regulated protein kinase localized to centrosomes, is complexed to protein phosphatase 1*. *Biochemical Journal*, 2000. **349**(2): p. 509-518.
171. Pagan, J.K., et al., *Degradation of Cep68 and PCNT cleavage mediate Cep215 removal from the PCM to allow centriole separation, disengagement and licensing*. *Nat Cell Biol*, 2015. **17**(1): p. 31-43.
172. Euteneuer, U. and M. Schliwa, *Evidence for an involvement of actin in the positioning and motility of centrosomes*. *The Journal of Cell Biology*, 1985. **101**(1): p. 96.
173. Euteneuer, U. and M. Schliwa, *Mechanism of centrosome positioning during the wound response in BSC-1 cells*. *The Journal of Cell Biology*, 1992. **116**(5): p. 1157-1166.
174. Jean, C., et al., *The mammalian interphase centrosome: two independent units maintained together by the dynamics of the microtubule cytoskeleton*. *European Journal of Cell Biology*, 1999. **78**(8): p. 549-560.

175. Panic, M., et al., *The Centrosomal Linker and Microtubules Provide Dual Levels of Spatial Coordination of Centrosomes*. PLoS genetics, 2015. **11**(5): p. e1005243.
176. Matsuo, K., et al., *Kendrin Is a Novel Substrate for Separase Involved in the Licensing of Centriole Duplication*. Current Biology, 2012. **22**(10): p. 915-921.
177. Mardin, B.R., et al., *Components of the Hippo pathway cooperate with Nek2 kinase to regulate centrosome disjunction*. Nat Cell Biol, 2010. **12**(12): p. 1166-1176.
178. Hadjihannas, M.V., M. Brückner, and J. Behrens, *Conductin/axin2 and Wnt signalling regulates centrosome cohesion*. EMBO reports, 2010. **11**(4): p. 317-324.
179. Bahmanyar, S., et al., *beta-Catenin is a Nek2 substrate involved in centrosome separation*. Genes Dev, 2008. **22**(1): p. 91-105.
180. Conroy, P.C., et al., *C-NAP1 and rootletin restrain DNA damage-induced centriole splitting and facilitate ciliogenesis*. Cell cycle (Georgetown, Tex), 2012. **11**(20): p. 3769-3778.
181. Hori, A. and T. Toda, *Regulation of centriolar satellite integrity and its physiology*. Cellular and Molecular Life Sciences, 2017. **74**(2): p. 213-229.
182. Nigg, E.A. and T. Stearns, *The centrosome cycle: Centriole biogenesis, duplication and inherent asymmetries*. Nat Cell Biol, 2011. **13**(10): p. 1154-1160.
183. Tsou, M.-F.B. and T. Stearns, *Mechanism limiting centrosome duplication to once per cell cycle*. Nature, 2006. **442**(7105): p. 947-951.
184. Dujardin, D.L., et al., *A role for cytoplasmic dynein and LIS1 in directed cell movement*. The Journal of Cell Biology, 2003. **163**(6): p. 1205-1211.
185. Kim, Mun J. and I.V. Maly, *Deterministic Mechanical Model of T-Killer Cell Polarization Reproduces the Wandering of Aim between Simultaneously Engaged Targets*. PLOS Computational Biology, 2009. **5**(1): p. e1000260.
186. Gomes, E.R., S. Jani, and G.G. Gundersen, *Nuclear Movement Regulated by Cdc42, MRCK, Myosin, and Actin Flow Establishes MTOC Polarization in Migrating Cells*. Cell. **121**(3): p. 451-463.
187. Wu, J., et al., *Effects of dynein on microtubule mechanics and centrosome positioning*. Molecular Biology of the Cell, 2011. **22**(24): p. 4834-4841.
188. Burute, M., et al., *Polarity Reversal by Centrosome Repositioning Primes Cell Scattering during Epithelial-to-Mesenchymal Transition*. Developmental Cell. **40**(2): p. 168-184.
189. Schmoranzer, J., et al., *Par3 and dynein associate to regulate local microtubule dynamics and centrosome orientation in migrating cells*. Current biology : CB, 2009. **19**(13): p. 1065-1074.

190. Palazzo, A.F., et al., *Cdc42, dynein, and dynactin regulate MTOC reorientation independent of Rho-regulated microtubule stabilization*. *Current Biology*. **11**(19): p. 1536-1541.
191. Westlake, C.J., et al., *Primary cilia membrane assembly is initiated by Rab11 and transport protein particle II (TRAPP II) complex-dependent trafficking of Rabin8 to the centrosome*, in *Proceedings of the National Academy of Sciences*. 2011. p. 2759-2764.
192. Follit, J.A., et al., *The Golgin GMAP210/TRIP11 Anchors IFT20 to the Golgi Complex*. *PLoS genetics*, 2008. **4**(12): p. e1000315.
193. Sutterlin, C. and A. Colanzi, *The Golgi and the centrosome: building a functional partnership*. *The Journal of Cell Biology*, 2010. **188**(5): p. 621-628.
194. Vinogradova, T., et al., *Concerted effort of centrosomal and Golgi-derived microtubules is required for proper Golgi complex assembly but not for maintenance*. *Molecular Biology of the Cell*, 2012. **23**(5): p. 820-833.
195. Hurtado, L., et al., *Disconnecting the Golgi ribbon from the centrosome prevents directional cell migration and ciliogenesis*. *The Journal of Cell Biology*, 2011. **193**(5): p. 917-933.
196. Nishita, M., et al., *Ror2 signaling regulates Golgi structure and transport through IFT20 for tumor invasiveness*. *Scientific Reports*, 2017. **7**(1): p. 1.
197. Gundersen, G.G. and J.C. Bulinski, *Selective stabilization of microtubules oriented toward the direction of cell migration*. *Proceedings of the National Academy of Sciences*, 1988. **85**(16): p. 5946-5950.
198. Wakida, N.M., et al., *An Intact Centrosome Is Required for the Maintenance of Polarization during Directional Cell Migration*. *PLOS ONE*, 2010. **5**(12): p. e15462.
199. Tang, N. and W.F. Marshall, *Centrosome positioning in vertebrate development*. *Journal of Cell Science*, 2012. **125**(21): p. 4951-4961.
200. de Anda, F.C., et al., *Centrosome localization determines neuronal polarity*. *Nature*, 2005. **436**(7051): p. 704-708.
201. Ghossoub, R., et al., *The ciliary pocket: a once-forgotten membrane domain at the base of cilia*. *Biol Cell*, 2011. **103**(3): p. 131-44.
202. Rohatgi, R. and W.J. Snell, *The ciliary membrane*. *Current Opinion in Cell Biology*, 2010. **22**(4): p. 541-546.
203. Rattner, J.B., et al., *Primary cilia in fibroblast-like type B synoviocytes lie within a cilium pit: a site of endocytosis*. *Histol Histopathol*, 2010. **25**(7): p. 865-75.
204. Molla-Herman, A., et al., *The ciliary pocket: an endocytic membrane domain at the base of primary and motile cilia*. *Journal of Cell Science*, 2010. **123**(10): p. 1785-1795.

205. Nonaka, S., et al., *Randomization of Left–Right Asymmetry due to Loss of Nodal Cilia Generating Leftward Flow of Extraembryonic Fluid in Mice Lacking KIF3B Motor Protein*. *Cell*, 1998. **95**(6): p. 829-837.
206. Sotelo, J.R. and O. Trujillo-Cenóz, *Electron microscope study on the development of ciliary components of the neural epithelium of the chick embryo*. *Zeitschrift für Zellforschung und Mikroskopische Anatomie*, 1958. **49**(1): p. 1-12.
207. Liem, K.F., et al., *The IFT-A complex regulates Shh signaling through cilia structure and membrane protein trafficking*. *The Journal of Cell Biology*, 2012. **197**(6): p. 789-800.
208. Barnes, B.G., *Ciliated secretory cells in the pars distalis of the mouse hypophysis*. *J Ultrastruct Res*, 1961. **5**: p. 453-67.
209. Sorokin, S., *Centrioles And The Formation Of Rudimentary Cilia By Fibroblasts And Smooth Muscle Cells*. *The Journal of Cell Biology*, 1962. **15**(2): p. 363-377.
210. Fisher, S.K. and R.H. Steinberg, *Origin and organization of pigment epithelial apical projections to cones in cat retina*. *The Journal of Comparative Neurology*, 1982. **206**(2): p. 131-145.
211. Allen, R.A., *Isolated cilia in inner retinal neurons and in retinal pigment epithelium*. *Journal of Ultrastructure Research*, 1965. **12**(5): p. 730-747.
212. Fonte, V.G., R.L. Searls, and S.R. Hilfer, *The relationship of cilia with cell division and differentiation*. *J Cell Biol*, 1971. **49**(1): p. 226-9.
213. Arrighi, S., *Primary cilia in the basal cells of equine epididymis: A serendipitous finding*. *Tissue and Cell*, 2013. **45**(2): p. 140-144.
214. Wilsch-Bräuninger, M., et al., *Basolateral rather than apical primary cilia on neuroepithelial cells committed to delamination*. *Development*, 2012. **139**(1): p. 95-105.
215. Whitfield, J.F., *The neuronal primary cilium—an extrasynaptic signaling device*. *Cellular Signalling*, 2004. **16**(7): p. 763-767.
216. Lim, Y.S., C.E.L. Chua, and B.L. Tang, *Rabs and other small GTPases in ciliary transport*. *Biology of the Cell*, 2011. **103**(5): p. 209-221.
217. Nachury, M.V., E.S. Seeley, and H. Jin, *Trafficking to the ciliary membrane: how to get across the periciliary diffusion barrier?* *Annu Rev Cell Dev Biol*, 2010. **26**: p. 59-87.
218. Hu, Q., et al., *A Septin Diffusion Barrier at the Base of the Primary Cilium Maintains Ciliary Membrane Protein Distribution*. *Science*, 2010. **329**(5990): p. 436-439.
219. Pedersen, L.B., J.B. Mogensen, and S.T. Christensen, *Endocytic Control of Cellular Signaling at the Primary Cilium*. *Trends in Biochemical Sciences*. **41**(9): p. 784-797.



220. Garcia-Gonzalo, F.R. and J.F. Reiter, *Scoring a backstage pass: Mechanisms of ciliogenesis and ciliary access*. The Journal of Cell Biology, 2012. **197**(6): p. 697-709.
221. Lu, Q., et al., *Early steps in primary cilium assembly require EHD1/EHD3-dependent ciliary vesicle formation*. Nat Cell Biol, 2015. **17**(3): p. 228-240.
222. Vieira, O.V., et al., *FAPP2, cilium formation, and compartmentalization of the apical membrane in polarized Madin–Darby canine kidney (MDCK) cells*. Proceedings of the National Academy of Sciences, 2006. **103**(49): p. 18556-18561.
223. Stoops, E.H., et al., *The periciliary ring in polarized epithelial cells is a hot spot for delivery of the apical protein gp135*. The Journal of Cell Biology, 2015. **211**(2): p. 287-294.
224. Milenkovic, L., M.P. Scott, and R. Rohatgi, *Lateral transport of Smoothed from the plasma membrane to the membrane of the cilium*. The Journal of Cell Biology, 2009. **187**(3): p. 365-374.
225. Maerker, T., et al., *A novel Usher protein network at the periciliary reloading point between molecular transport machineries in vertebrate photoreceptor cells*. Human Molecular Genetics, 2007. **17**(1): p. 71-86.
226. Yang, J., et al., *Ablation of Whirlin Long Isoform Disrupts the USH2 Protein Complex and Causes Vision and Hearing Loss*. PLOS Genetics, 2010. **6**(5): p. e1000955.
227. Bauß, K., et al., *Phosphorylation of the Usher syndrome 1G protein SANS controls Magi2-mediated endocytosis*. Human Molecular Genetics, 2014. **23**(15): p. 3923-3942.
228. Koemeter-Cox, A.I., et al., *Primary cilia enhance kisspeptin receptor signaling on gonadotropin-releasing hormone neurons*. Proceedings of the National Academy of Sciences, 2014. **111**(28): p. 10335-10340.
229. Falk, N., et al., *Specialized Cilia in Mammalian Sensory Systems*. Cells, 2015. **4**(3): p. 500-519.
230. Clement, Christian A., et al., *TGF- $\beta$  Signaling Is Associated with Endocytosis at the Pocket Region of the Primary Cilium*. Cell Reports, 2013. **3**(6): p. 1806-1814.
231. Corbit, K.C., et al., *Kif3a constrains [beta]-catenin-dependent Wnt signalling through dual ciliary and non-ciliary mechanisms*. Nat Cell Biol, 2008. **10**(1): p. 70-76.
232. Schneider, L., et al., *PDGFR $\alpha$  Signaling Is Regulated through the Primary Cilium in Fibroblasts*. Current Biology, 2005. **15**(20): p. 1861-1866.
233. Domire, J.S., et al., *Dopamine receptor 1 localizes to neuronal cilia in a dynamic process that requires the Bardet-Biedl syndrome proteins*. Cellular and Molecular Life Sciences, 2011. **68**(17): p. 2951-2960.

234. Green, J.A., et al., *Recruitment of  $\beta$ -Arrestin into Neuronal Cilia Modulates Somatostatin Receptor Subtype 3 Ciliary Localization*. *Molecular and Cellular Biology*, 2016. **36**(1): p. 223-235.
235. Berbari, N.F., et al., *Identification of Ciliary Localization Sequences within the Third Intracellular Loop of G Protein-coupled Receptors*. *Molecular Biology of the Cell*, 2008. **19**(4): p. 1540-1547.
236. Kim, J., et al., *The role of ciliary trafficking in Hedgehog receptor signaling*. *Science signaling*, 2015. **8**(379): p. ra55-ra55.
237. McEwen, D.P., et al., *Hypomorphic CEP290/NPHP6 mutations result in anosmia caused by the selective loss of G proteins in cilia of olfactory sensory neurons*. *Proceedings of the National Academy of Sciences*, 2007. **104**(40): p. 15917-15922.
238. Loktev, Alexander V. and Peter K. Jackson, *Neuropeptide Y Family Receptors Traffic via the Bardet-Biedl Syndrome Pathway to Signal in Neuronal Primary Cilia*. *Cell Reports*, 2013. **5**(5): p. 1316-1329.
239. Rohatgi, R., L. Milenkovic, and M.P. Scott, *Patched1 Regulates Hedgehog Signaling at the Primary Cilium*. *Science*, 2007. **317**(5836): p. 372-376.
240. Pal, K., et al., *Smoothed determines  $\beta$ -arrestin-mediated removal of the G protein-coupled receptor Gpr161 from the primary cilium*. *The Journal of Cell Biology*, 2016. **212**(7): p. 861-875.
241. Jin, H., et al., *The Conserved Bardet-Biedl Syndrome Proteins Assemble a Coat that Traffics Membrane Proteins to Cilia*. *Cell*, 2010. **141**(7): p. 1208-1219.
242. Marley, A. and M. von Zastrow, *DISC1 Regulates Primary Cilia That Display Specific Dopamine Receptors*. *PLOS ONE*, 2010. **5**(5): p. e10902.
243. Nachury, M.V., *How do cilia organize signalling cascades?* *Philosophical Transactions of the Royal Society B: Biological Sciences*, 2014. **369**(1650): p. 20130465.
244. Pennekamp, P., et al., *Situs inversus and ciliary abnormalities: 20 years later, what is the connection?* *Cilia*, 2015. **4**(1): p. 1.
245. Huangfu, D., et al., *Hedgehog signalling in the mouse requires intraflagellar transport proteins*. *Nature*, 2003. **426**(6962): p. 83-87.
246. Huangfu, D. and K.V. Anderson, *Cilia and Hedgehog responsiveness in the mouse*. *Proceedings of the National Academy of Sciences*, 2005. **102**(32): p. 11325-11330.
247. Tuson, M., M. He, and K.V. Anderson, *Protein kinase A acts at the basal body of the primary cilium to prevent Gli2 activation and ventralization of the mouse neural tube*. *Development*, 2011. **138**(22): p. 4921-4930.
248. Mukhopadhyay, S., et al., *The Ciliary G-Protein-Coupled Receptor Gpr161 Negatively Regulates the Sonic Hedgehog Pathway via cAMP Signaling*. *Cell*, 2013. **152**(1-2): p. 210-223.

249. Gorojankina, T., *Hedgehog signaling pathway: a novel model and molecular mechanisms of signal transduction*. Cellular and Molecular Life Sciences, 2016. **73**(7): p. 1317-1332.
250. Niewiadomski, P., et al., *Gli Protein Activity Is Controlled by Multisite Phosphorylation in Vertebrate Hedgehog Signaling*. Cell Reports. **6**(1): p. 168-181.
251. Tukachinsky, H., L.V. Lopez, and A. Salic, *A mechanism for vertebrate Hedgehog signaling: recruitment to cilia and dissociation of SuFu–Gli protein complexes*. The Journal of Cell Biology, 2010. **191**(2): p. 415-428.
252. Chen, Y., et al., *Sonic Hedgehog Dependent Phosphorylation by CK1 $\alpha$  and GRK2 Is Required for Ciliary Accumulation and Activation of Smoothed*. PLOS Biology, 2011. **9**(6): p. e1001083.
253. Moore, B.S., et al., *Cilia have high cAMP levels that are inhibited by Sonic Hedgehog-regulated calcium dynamics*. Proceedings of the National Academy of Sciences, 2016. **113**(46): p. 13069-13074.
254. Nigg, E.A., *Centrosome aberrations: cause or consequence of cancer progression?* Nat Rev Cancer, 2002. **2**(11): p. 815-825.
255. Adon, A.M., et al., *Cdk2 and Cdk4 Regulate the Centrosome Cycle and Are Critical Mediators of Centrosome Amplification in p53-Null Cells*. Molecular and Cellular Biology, 2010. **30**(3): p. 694-710.
256. Hanashiro, K., et al., *Roles of cyclins A and E in induction of centrosome amplification in p53-compromised cells*. Oncogene, 2008. **27**(40): p. 5288-5302.
257. Mahathre, M.M., P.C. Rida, and R. Aneja, *The more the messier: centrosome amplification as a novel biomarker for personalized treatment of colorectal cancers*. J Biomed Res, 2016. **30**(6): p. 441-451.
258. Dementyeva, E., et al., *Centrosome amplification as a possible marker of mitotic disruptions and cellular carcinogenesis in multiple myeloma*. Leuk Res, 2010. **34**(8): p. 1007-11.
259. Chng, W.J., et al., *The centrosome index is a powerful prognostic marker in myeloma and identifies a cohort of patients that might benefit from aurora kinase inhibition*. Blood, 2008. **111**(3): p. 1603-1609.
260. Ganem, N.J., S.A. Godinho, and D. Pellman, *A mechanism linking extra centrosomes to chromosomal instability*. Nature, 2009. **460**(7252): p. 278-282.
261. Mitchison, H.M. and E.M. Valente, *Motile and non-motile cilia in human pathology: from function to phenotypes*. The Journal of Pathology, 2017. **241**(2): p. 294-309.
262. Davenport, J.R., et al., *Disruption of intraflagellar transport in adult mice leads to obesity and slow-onset cystic kidney disease*. Curr Biol, 2007. **17**(18): p. 1586-94.
263. Wong, S.Y., et al., *Primary cilia can both mediate and suppress Hedgehog pathway-dependent tumorigenesis*. Nat Med, 2009. **15**(9): p. 1055-1061.

264. Xie, J., et al., *Activating Smoothed mutations in sporadic basal-cell carcinoma*. Nature, 1998. **391**(6662): p. 90-92.
265. Gupta, S., N. Takebe, and P. LoRusso, *Targeting the Hedgehog pathway in cancer*. Therapeutic Advances in Medical Oncology, 2010. **2**(4): p. 237-250.
266. Tostar, U., et al., *Deregulation of the hedgehog signalling pathway: a possible role for the PTCH and SUFU genes in human rhabdomyoma and rhabdomyosarcoma development*. The Journal of Pathology, 2006. **208**(1): p. 17-25.
267. Hoang-Minh, L.B., et al., *Disruption of KIF3A in patient-derived glioblastoma cells: effects on ciliogenesis, hedgehog sensitivity, and tumorigenesis*. Oncotarget, 2016. **7**(6).
268. Barakat, M.T., E.W. Humke, and M.P. Scott, *Kif3a is necessary for initiation and maintenance of medulloblastoma*. Carcinogenesis, 2013. **34**(6): p. 1382-1392.
269. Pitaval, A., et al., *Cell shape and contractility regulate ciliogenesis in cell cycle-arrested cells*. The Journal of Cell Biology, 2010. **191**(2): p. 303-312.
270. Gottardo, M., G. Callaini, and M.G. Riparbelli, *The *Drosophila* centriole – conversion of doublets into triplets within the stem cell niche*. Journal of Cell Science, 2015. **128**(14): p. 2437-2442.
271. Hagan, I.M. and R.E. Palazzo, *Warming up at the poles*. EMBO Reports, 2006. **7**(4): p. 364-371.
272. Hodges, M.E., et al., *Reconstructing the evolutionary history of the centriole from protein components*. Journal of Cell Science, 2010. **123**(9): p. 1407-1413.
273. Wang, W.-J., et al., *CEP162 is an axoneme-recognition protein promoting ciliary transition zone assembly at the cilia base*. Nature, 2013. **15**(6): p. 591-601.
274. Mali, P., et al., *RNA-Guided Human Genome Engineering via Cas9*. Science, 2013. **339**(6121): p. 823-826.
275. Kellogg, D.R., M. Moritz, and B.M. Alberts, *The centrosome and cellular organization*. Annual review of biochemistry, 1994. **63**: p. 639-674.
276. Westlake, C.J., et al., *Primary cilia membrane assembly is initiated by Rab11 and transport protein particle II (TRAPP II) complex-dependent trafficking of Rabin8 to the centrosome*. Proceedings of the National Academy of Sciences, 2011. **108**(7): p. 2759-2764.
277. Rivero, S., et al., *Microtubule nucleation at the cis-side of the Golgi apparatus requires AKAP450 and GM130*. The EMBO Journal, 2009. **28**(8): p. 1016-1028.
278. Mahjoub, M.R. and T. Stearns, *Supernumerary Centrosomes Nucleate Extra Cilia and Compromise Primary Cilium Signaling*. Current Biology, 2012. **22**(17): p. 1628-1634.

279. Mahjoub, M.R. and T. Stearns, *Supernumerary centrosomes nucleate extra cilia and compromise primary cilium signaling*. *Curr Biol*, 2012. **22**.
280. Taipale, J., et al., *Effects of oncogenic mutations in Smoothed and Patched can be reversed by cyclopamine*. *Nature*, 2000. **406**(6799): p. 1005-1009.
281. Cole, N.B., et al., *Diffusional mobility of Golgi proteins in membranes of living cells*. *Science (New York, NY)*, 1996. **273**(5276): p. 797-801.
282. Izquierdo, D., et al., *Stabilization of Cartwheel-less Centrioles for Duplication Requires CEP295-Mediated Centriole-to-Centrosome Conversion*. *Cell Reports*, 2014. **8**(4): p. 957-965.
283. Honga, Y.R., et al., *Cloning and characterization of a novel human ninein protein that interacts with the glycogen synthase kinase 3beta1*. *Biochimica et Biophysica Acta (BBA)/Gene Structure and Expression*, 2000. **1492**(2): p. 513-516.
284. Ibi, M., et al., *Trichoplein controls microtubule anchoring at the centrosome by binding to Odf2 and ninein*. *Journal of Cell Science*, 2011. **124**(6): p. 857-864.
285. Grishchuk, E.L., et al., *Force production by disassembling microtubules*. *Nature*, 2005. **438**(7066): p. 384-388.
286. McIntosh, J.R., et al., *Tubulin depolymerization may be an ancient biological motor*. *Journal of Cell Science*, 2010. **123**(20): p. 3425-3434.
287. Yang, J. and T. Li, *The ciliary rootlet interacts with kinesin light chains and may provide a scaffold for kinesin-1 vesicular cargos*. *Experimental Cell Research*, 2005. **309**(2): p. 379-389.
288. Floriot, S., et al., *C-Nap1 mutation affects centriole cohesion and is associated with a Seckel-like syndrome in cattle*. *Nature Communications*, 2015. **6**: p. 6894.
289. Bachmann, V.A., et al., *Gpr161 anchoring of PKA consolidates GPCR and cAMP signaling*. *Proceedings of the National Academy of Sciences*, 2016. **113**(28): p. 7786-7791.
290. Mick, David U., et al., *Proteomics of Primary Cilia by Proximity Labeling*. *Developmental Cell*. **35**(4): p. 497-512.
291. Witczak, O., et al., *Cloning and characterization of a cDNA encoding an A-kinase anchoring protein located in the centrosome, AKAP450*. *The EMBO Journal*, 1999. **18**(7): p. 1858-1868.
292. Chen, C.-H., et al., *Molecular characterization of human ninein protein: two distinct subdomains required for centrosomal targeting and regulating signals in cell cycle*. *Biochemical and Biophysical Research Communications*, 2003. **308**(4): p. 975-983.